

國立臺灣大學理學院物理學研究所
博士論文

Department of Physics
College of Science
National Taiwan University
Doctoral Dissertation

標準模型之外的粒子現象學
Particle Phenomenology beyond Standard Model



蔡律行
Lu-Hsing Tsai

指導教授：何小剛 博士
Advisor: Xiao-Gang He, Ph.D.

中華民國 101 年 6 月
June, 2012



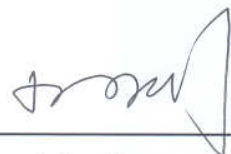
國立臺灣大學博士學位論文
口試委員會審定書

標準模型之外的粒子現象學

Particle Phenomenology beyond Standard Model

本論文係蔡律行君(學號 d98222002)在國立臺灣大學物理學系、
所完成之博士學位論文，於民國 101 年 6 月 22 日承下列考試委員審
查通過及口試及格，特此證明

口試委員：

55  (簽名)
(指導教授)

張寶棟

陳東宏

耿朝陽

楊桂周

張嘉泓



摘 要

以強作用力, 弱作用力, 電磁作用力相關的規範群 $SU(3)_c \times SU(2)_L \times U(1)_Y$ 所描述的標準模型, 解釋了自然界大部分的現象. 然而, 仍然有部分問題無法以標準模型解釋, 像是 CP 破缺的源頭, 重子數不對稱, 弱作用尺度與蒲朗克尺度的階級差異, 強作用 CP 破缺, 微中子的輕質量, 費米子家族代的數目. 在這篇論文我將集中在其中三個問題中, 如下所列.

1. 有關 CP 破缺來源的主題. 為了解釋 CP 破缺的來源我們引進了具有自發性 CP 破缺相角的多希格斯模型, 並且使這個相角在大小上等同於夸克混合矩陣的相角, 作為 CP 破缺的來源. 這個假設將得到比較簡單的湯川耦合矩陣. 我們也應用這個點子到輕子的部分. 賈斯科不變量在 PMNS 矩陣可以被預測, 這可以用來區分我們所取的不同模型.

2. 有關輕微中子質量與在翹翹板模型中希格斯衰變的主題. 與極重右手馬由拉那微中子相關的翹翹板機制, 成功的解釋輕微中子質量. 但是極重的重微中子與這個重微中子和其他粒子極微小的藕荷, 造

成驗證翹翹板理論的困難。我們檢視在某些具有大的重輕微中子混合矩陣的翹翹板模型中的希格斯粒子衰變，能夠有超過標準模型 20% 的增量。接連的四體衰變也與標準模型的預測不同。

3. 有關四代費米子標準模型中的輕子味破壞的主題。超過三代費米子的標準模型，例如包含四代，也是一個可能的人選。我們研究輕子味破壞的過程，像是原子中的 μ -e 轉換在四代費米子標準模型。我們發現目前實驗的上界在金原子中的 μ -e 轉換，能夠最緊迫地限制相關的藕和常數。在未來鈦原子中的 μ -e 轉換實驗將會得到最緊迫的限制。

關鍵字：標準模型，自發性 CP 破缺，CKM 矩陣，PMNS 矩陣，翹翹板機制，希格斯衰變，四代的標準模型

Abstract

The standard model (SM), which describes the gauge group $SU(3)_C \times SU(2)_L \times U(1)_Y$ related to strong interaction, weak theory and electromagnetic interaction, explains most of the phenomena in the nature. However, there remain some problems which can not be explained by the SM, such as the the origin of CP violation, the baryon asymmetry of the universe, the hierarchy problem related to the weak scale and Plank scale, the strong CP problem, the light neutrino mass, and the number of fermion generations. In this thesis I will focus on three of these problems, which are listed as follows.

1. The topic related to the source of CP violation. In order to explain the source of CP violation we introduced a multi-Higgs model with nonzero spontaneous CP violating phase, and regarded the phase, which is assumed to be identical in magnitude to the phases in quark mixing matrices, as the source of CP violation. This assumption will lead to some simpler Yukawa coupling matrices. We also applied the idea to the lepton sector. The Jarlskog invariant in PMNS matrix can be predicted, which can be used to distinguish different models we take.
2. The topic related to the light neutrino mass and Higgs decay in seesaw models. The seesaw mechanism, involving right-handed neutrinos with very large Majorana mass, explains the light neutrino masses successfully. But the too huge mass of the heavy neutrino and the too tiny coupling with this heavy neutrino the other particles cause the difficulty in verifying the seesaw mechanism. We investigated the effect on Higgs decay in some seesaw models with large heavy-light mixing, which can increase more than 20% than that in the SM. The subsequent four body decays are also different from the prediction in SM.

3. The topic related to the lepton flavor violation in SM with four fermion generations. The SM with more than three generations, *e.g.*, with four generations, is also a possible candidate. We studied the lepton flavor violating process such as $\mu - e$ conversion in atoms in the SM with sequential four generations. We found that the current experimental bound on $\mu - e$ conversion with Au constrains the relevant coupling constant most stringently. The experiment on $\mu - e$ conversion in Ti will lead to the most stringent constraint in the future.

Keywords: standard model, spontaneous CP violation, CKM matrix, PMNS matrix, seesaw mechanism, Higgs decay, four generation standard model



Contents

1	Introduction	1
2	Standard Model	5
2.1	Electroweak Theory	5
2.1.1	The Full Lagrangian	5
2.1.2	Spontaneous Symmetry Breaking	7
2.1.3	Electroweak Parameters	8
2.2	Quark Mixing Matrix	10
2.2.1	CP violation and Complex Elements	11
2.2.2	CKM Matrix Elements and CP Violation	12
2.3	Lepton Mixing Matrix	16
2.3.1	Neutrino Oscillation and Mixing Angles	16
3	Spontaneous CP Violation and Fermion Mixing Matrix Phases	21
3.1	Spontaneous CP Violation	21
3.1.1	Two Higgs Doublet Model	22
3.1.2	Three Higgs Doublet Model	23
3.1.3	Peccei-Quinn Symmetry	25
3.2	SCPV and CKM matrix	27
3.2.1	Identifying CKM matrix phase with SCPV matrix phase . . .	27
3.2.2	Higgs potential and mass matrices	30
3.2.3	Some Implication	33
3.3	SCPV and PMNS matrix	39

3.3.1	Identifying PMNS matrix phase with SCPV phase	40
3.3.2	Effect on Charged Lepton Flavor Violating Processes	45
4	Higgs Decay in Large Heavy-Light Mixing Seesaw Model	49
4.1	Higgs Decay	49
4.2	Type-I Seesaw	51
4.2.1	Introduction	51
4.2.2	Heavy-Light Large Mixing	53
4.2.3	$h \rightarrow \nu N$	54
4.2.4	Three-Body Decays of N and Four-Body Decays of Higgs . . .	58
4.3	Type-III Seesaw	61
4.3.1	Introduction	61
4.3.2	$h \rightarrow \nu N$ and $h \rightarrow \ell E$	62
5	Lepton Flavor Violation in Standard Model with Four Generations	65
5.1	Charged Lepton Flavor Changing Processes	67
5.2	$\mu - e$ Conversion	69
5.3	Comparison with $\mu \rightarrow e\gamma$ and $\mu \rightarrow 3e$	71
6	Conclusion	75
A	Higgs Mass Matrices	79
B	Light Neutrino Mass in Seesaw Mechanism	85
C	Large Mixing Matrix	87
D	Overlapped functions in Nucleon	89

List of Figures

2.1	The electroweak test constrains m_h in $m_W - m_t$ plane. Figure is captured from Ref. [6].	9
2.2	The experimental fit for the $\bar{\rho}$ and $\bar{\eta}$. Figure is captured from Ref. [6].	15
2.3	The neutrino oscillation experiment results, shown by the allowed area in $\Delta m^2 - \tan^2 \theta$ plane. Figure is captured from Ref. [7, 37]. . . .	18
3.1	Comparison of Model (a-M) and Model (a-KM) by $\langle m_{\beta\beta} \rangle$ as a function of light neutrino mass m_{ν_1}	44
3.2	The allowed range in $v_{1,2}$ plane constrained by $\mu \rightarrow e\bar{e}e$ and $\tau \rightarrow l_1\bar{l}_2l_3$, where M- and KM- indicate the modified standard parametrization and KM parametrization, respectively.	47
4.1	The left panel is the mainly branching ratios of the Higgs decay channels as a function of m_h , and the right panel is the total decay rate of Higgs as a function of m_h . The numerical results is calculated by the package HDECAY [81].	51
4.2	The ratio of decay width of $h \rightarrow \nu N$ to total Higgs decay width in SM as a function of m_h , for $m_N = 70, 80, 90, 100\text{GeV}$ as marked in the figures, with (a) $U_{\nu N} = U_0^a$, and (b) $U_{\nu N} = U_0^e$. The numerical result of the SM Higgs decay width is calculated by the package HDECAY [81].	56

4.3	(a,b,c) Decay widths of the channels $h \rightarrow \nu N \rightarrow \nu f f' f''$ versus m_h with $m_N = 80, 90, 100 \text{ GeV}$, respectively, with heavy-light mixing $U_{\nu N} = U_0^e$. (d) The branching ratios of four body decay channels in SM. The numerical result of SM total and partial decay rates in these figures is calculated by package HDECAY [81].	61
4.4	The ratios of decay width including the channels $h \rightarrow \nu N$ and $h \rightarrow l^- E^+$ to total SM Higgs decay width, as the functions of m_h , with $m_N = 100, 110 \text{ GeV}$ for (a) $U_{\nu N} = U_0^e$; for (b) $U_{\nu N} = U_0^f$. The numerical result for the SM Higgs total decay width is calculated by package HDECAY [81].	64
5.1	The upper bounds of the coupling $ \lambda_{\mu e} $ from experimental constraints on $\mu - e$ conversion in Au, S, Ti, Pb, $\mu \rightarrow e\gamma$, and $\mu \rightarrow 3e$, as the functions of m_{ν_4}	72
5.2	The ratios of $\mu - e$ conversion in Au, S, Ti, Pb, Al, and $\mu \rightarrow 3e$ to $\mu \rightarrow e\gamma$, respectively, as the functions of m_{ν_4}	73
5.3	The upper bounds of $ \lambda_{\mu e} $, constrained by projected sensitivities of future experiments for $\mu \rightarrow e\gamma$ [114], $\mu \rightarrow 3e$ [115], and $\mu - e$ conversion on Al [117] and Ti [118], as functions of m_{ν_4}	73

List of Tables

4.1	Cross section for different center-mass energy \sqrt{s} with different m_N , which is compared with experiment result. The values in last column are taken from Ref. [92]. All cross-section numbers are in pb.	58
4.2	Decay rates of three body decay modes for different m_N	60
5.1	The overlapped functions D , $V^{(p)}$, and $V^{(n)}$ related to $\mu-e$ conversion on different atomic nuclei [111]. The numbers in last column is the values of $R_{\mu \rightarrow e}^0$	71



Chapter 1

Introduction

The standard model (SM) has been proved and verified in the past forty years. Glashow, Weinberg and Salam succeeded to unify the electromagnetic interaction and the nuclear weak interaction together in 1967 [10]. In 1973 Kobayashi and Maskawa [14] extended the SM to three generations fermions which elegantly explains the CP violation in several hadronic processes. From the discovery of neutrino oscillation, it is confirmed that more than one neutrino are massive, which conflicts with the structure of SM, under which neutrinos should be massless exactly. Besides the massive neutrinos, there are still several theoretical predictions and experimental observations which cannot be explained solely by the SM.

The source of CP violation is an interesting research topic. In the SM the CP violation is arisen from the complex Yukawa couplings. However, the source of the complex couplings has not been understood yet. A good way to explain the source of CP violation is by the two Higgs doublet model (2HDM), in which CP violation is generated from the relative phase of vacuum expectation values (VEVs) between Higgs doublets. The three Higgs doublet model (3HDM) with appropriate discrete symmetry can generate a flavor conserved neutral current with the existence of spontaneous CP violation. We proposed an idea that the CKM matrix phase as well as the PMNS matrix phase come from and are identified with the spontaneous CP violating phase in magnitude [1, 2]. To realize this idea with Peccei–Quinn

symmetry simultaneously three Higgs doublets and one Higgs singlet are imposed into this model, where Yukawa couplings for quark and lepton sectors are only functions of fermion masses and mixing angles.

The seesaw mechanism is usually applied by introducing a very heavy fermion called heavy neutrino to generate very light active neutrinos. The generic feature of such models is that there is some mixing between the heavy and light neutrinos, and the scale of the mixing strength is approximately proportional to the inverse of the square root of heavy neutrino mass. One way to enlarge such heavy-light mixing is to build it as an approximately rank-1 matrix, which is shown in details in Ref. [85]. Such a model will enhance the Higgs decay rate significantly if the Higgs is heavier than the heavy neutrino masses [4]. This model is expected to be verified at the Large Hadronic Collider (LHC) in the future.

The SM with three generations have been shown to possess good agreement with experiments. However, the existence of the fourth generation is still not precluded, although there are stringent bounds on corresponding fermion masses and couplings. One of the possible approaches to search for the existence of the fourth generation is by the lepton flavor violating processes, such like $\mu \rightarrow e\gamma$, $\mu \rightarrow ee\bar{e}$ and $\mu - e$ conversion with the nucleus in the atoms, which might be affected significantly by the fourth generation neutrino in the loop diagram. It is worth to compare these processes in order to find which one could provide the tightest constraint on the fourth generation coupling constants, with the heavy neutrino mass in different range [5].

In this thesis, I will describe these topics and their corresponding implications in details. In Chapter 2, the structure of the SM, especially in electroweak part, the CKM matrix together with CP violation, and some of the extension by adding the right-handed neutrinos will be introduced. In Chapter 3, with brief introduction to spontaneous CP violation, I will describe how to identify the spontaneous CP violating phase with the phases in quark and lepton mixing matrices [1, 2, 3]. In Chapter 4, I will describe about some of the seesaw models, and the effect of large

heavy-light mixing on Higgs decay and other relevant processes [4]. In Chapter 5, I will show the comparison between $\mu \rightarrow e\gamma$, $\mu - e$ conversion in nucleus and $\mu \rightarrow ee\bar{e}$ in the sequential four generations model [5]. In the last chapter, the Chapter 6, I will conclude these topics.





Chapter 2

Standard Model

The standard model (SM) is built on quantum chromodynamics and electroweak theory. The former is related to the $SU(3)$ gauge symmetry, and the later is the unification of electrodynamics and weak interaction into the $SU(2) \times U(1)$ gauge group, which is performed by Glashow, Weinberg, and Salam (GWS) [10]. Another important contribution to SM is the three generations of fermions, which is proposed by Kobayashi and Maskawa (KM) [14]. The SM has been well verified by electroweak precision test, and many of the processes such as hadronic and semileptonic decays of hadrons, flavor changing neutral current processes, and CP violation for meson mixing and decaying [6]. In this chapter I will briefly introduce the GWS electroweak theory followed by the KM theory. Neutrino mixing and neutrino mass will also be introduced in the end of this chapter.

2.1 Electroweak Theory

2.1.1 The Full Lagrangian

The SM is built on the gauge symmetry of the group $SU(3)_C \times SU(2)_L \times U(1)_Y$. A set of numbers are assigned to describe the transformation of a particle under some gauge group. For example, in the SM gauge group, the first two numbers in the set are shown the dimensions of representation for $SU(3)_C$ and $SU(2)_L$, respectively,

and the last number is related to the charge for $U(1)_Y$. In the following we list the SM particles with the corresponding gauge group representation

$$\begin{aligned} Q_{Li} &= \begin{pmatrix} u_{Li} \\ d_{Li} \end{pmatrix} : (3, 2, \frac{1}{6}), \quad U_{Ri} : (3, 1, \frac{2}{3}), \quad D_{Ri} : (3, 1, -\frac{1}{3}), \\ L_{Li} &= \begin{pmatrix} \nu_{Li} \\ l_{Li} \end{pmatrix} : (1, 2, -\frac{1}{2}), \quad l_{Ri} : (1, 1, -1), \quad H : (1, 2, \frac{1}{2}), \end{aligned} \quad (2.1)$$

where i means that there might include several generations for fermions. H is a spin-0 scalar, which will be discussed later. Under the SM gauge group the covariant derivative is define as

$$D_\mu = \partial_\mu + ig_1 Y B_\mu + ig_2 T^a W_\mu^a + ig_3 T^b G_\mu^b, \quad (2.2)$$

with Y the hypercharge operator, T^a the $SU(2)$ generators for $a = 1, 2, 3$, and T^b the $SU(3)$ generators for $b = 1, 2, \dots, 8$. The B_μ , W_μ , and G_μ are the spin-1 gauge bosons with the gauge group representation given by

$$B_\mu : (1, 1, 0), \quad W_\mu : (1, 3, 0), \quad G_\mu : (8, 1, 0), \quad (2.3)$$

where the numbers for these gauge bosons indicates the adjoint representation dimension of the gauge group. With the information of gauge representation of SM particles, the full Lagrangian for SM is written as follows

$$\begin{aligned} \mathcal{L} &= -\frac{1}{4} G_{\mu\nu}^b G^{b\mu\nu} - \frac{1}{4} W_{\mu\nu}^a W^{a\mu\nu} - \frac{1}{4} B_{\mu\nu} B^{\mu\nu} + (D_\mu H)^\dagger (D^\mu H) - V(H) \\ &\quad + \overline{Q_{Li}} i \not{D} Q_{Li} + \overline{U_{Ri}} i \not{D} U_{Ri} + \overline{D_{Ri}} i \not{D} D_{Ri} + \overline{L_{Li}} i \not{D} L_{Li} + \overline{l_{Ri}} i \not{D} l_{Ri} \\ &\quad + (\overline{Q_{Li}} Y_u^{ij} \tilde{H} U_{Rj} + \overline{Q_{Li}} Y_d^{ij} H D_{Rj} + \overline{L_{Li}} Y_l^{ij} H l_{Rj} + \text{h.c.}), \end{aligned} \quad (2.4)$$

where $B_{\mu\nu}$, $W_{\mu\nu}^a$, and $G_{\mu\nu}^b$ are defined as follows

$$\begin{aligned} B_{\mu\nu} &= \partial_\mu B_\nu - \partial_\nu B_\mu, \\ W_{\mu\nu}^a &= \partial_\mu W_\nu^a - \partial_\nu W_\mu^a - g_2 \epsilon^{akl} W_\mu^k W_\nu^l, \\ G_{\mu\nu}^b &= \partial_\mu G_\nu^b - \partial_\nu G_\mu^b - g_3 f^{bmn} G_\mu^m G_\nu^n, \end{aligned} \quad (2.5)$$

with ϵ^{akl} and f^{bmn} are the structure constants for SU(2) and SU(3), respectively. $\tilde{H} = i\sigma_2 H^*$ is also SU(2) doublet with hypercharge opposite to H . $V(H)$ is the Higgs potential given by

$$V(H) = -\mu^2(H^\dagger H) + \lambda(H^\dagger H)^2, \quad (2.6)$$

with μ^2 and λ are real couplings in general.

2.1.2 Spontaneous Symmetry Breaking

In the following we will focus on the GWS theorem, which is, to break electroweak gauge group $SU(2)_L \times U(1)_Y$ into the electromagnetic gauge group $U(1)_{EM}$. There are massless photon A and massive spin-1 bosons W^\pm and Z in our world, governed by the electromagnetic gauge symmetry $U(1)_{EM}$. From gauge theory the existence of massive gauge bosons implies some breaking of a bigger gauge group in the underlying theory. The spontaneous symmetry breaking is manifested by minimizing the Higgs potential $V(H)$. First we take a look at the Higgs potential $V(H)$. Assuming there is a scale of temperature, below which the parameter μ^2 is positive. At this situation H acquires a vacuum expectation value (VEV) in order to stabilize the ground state and to obtain the physical state of H . That is, $\langle H \rangle = (0, v/\sqrt{2})^T$, where v is the VEV, and it makes us to expand H as follows

$$H = \begin{pmatrix} h^+ \\ \frac{1}{\sqrt{2}}(v + h + ia) \end{pmatrix}, \quad (2.7)$$

where h and a are the scalar and pseudoscalar particles, respectively, and h^+ is the charged component, whose hermitian conjugate is h^- . By definition, v is chosen to minimize the Higgs potential with respect to all of the components h^+ , h and a vanishing. This minimal condition leads to the relation

$$v = \sqrt{\frac{\mu^2}{\lambda}}. \quad (2.8)$$

Substituting the above relation into Eq. (2.7) and Eq. (2.6), the Higgs mass can be obtained from the quadratic terms in Higgs potential, which are given by

$$m_h^2 = 2\lambda v^2, \quad m_a^2 = m_{h^+}^2 = m_{h^-}^2 = 0. \quad (2.9)$$

Only the neutral scalar Higgs component acquires mass, whereas neutral pseudoscalar and charged component are massless, which are just the well-known Nambu–Goldstone bosons [11]. In the following context, we will express μ^2 and λ in terms of v and m_h .

The gauge boson masses can be extracted from the Higgs kinetic term, which gives

$$|(\frac{g_1}{2}B_\mu + \frac{\tau^a}{2}g_2W_\mu^a)\langle H \rangle|^2 = \frac{v^2}{4}g_2^2W_\mu^+W^{\mu-} + \frac{v^2}{8}(g_1B_\mu - g_2W_\mu^3)^2, \quad (2.10)$$

where W^\pm is defined as $W^\pm = (W^1 \mp W^2)/\sqrt{2}$, which are eigenstates of the electric charge operator. It is straightforward to obtain the mass eigenstates of neutral component by the rotation

$$\begin{pmatrix} W_\mu^3 \\ B_\mu \end{pmatrix} = \begin{pmatrix} \cos \theta_W & \sin \theta_W \\ -\sin \theta_W & \cos \theta_W \end{pmatrix} \begin{pmatrix} Z_\mu^0 \\ A_\mu \end{pmatrix}, \text{ with } \sin \theta = \frac{g_1}{\sqrt{g_1^2 + g_2^2}}. \quad (2.11)$$

The masses for gauge bosons are given by

$$m_W^2 = \frac{1}{4}g_2^2v^2, \quad m_Z^2 = \frac{1}{4}(g_1^2 + g_2^2)v^2, \quad m_A^2 = 0. \quad (2.12)$$

The tree level m_W and m_Z satisfy the relation $(m_W/m_Z) = \cos \theta_W$. The W^\pm and Z^0 acquired masses from the Goldstone Boson, which is the famous Higgs mechanism [12]. The original gauge group $SU(2)_L \times U(1)_Y$ has been broken, which is easily known from the massive gauge boson W^\pm and Z^0 . The massless photon field A^μ corresponds to the unbroken gauge group $U(1)_{EM}$.

2.1.3 Electroweak Parameters

There are thousands of processes which are governed by the electroweak interaction. Physicist defined some of the parameters which are useful and can be directly measured by experiments. We will briefly mention some of the important parameters as follows.

The electromagnetic fine-structure constant $\alpha_e \equiv (e^2/4\pi)$ can be obtained precisely from the electron anomalous magnetic dipole moment at higher order loop correction, which gives $1/\alpha_e = 137.035999084(51)$ [15]. The Fermi constant $G_F \equiv (\sqrt{2}g_2^2/8m_W^2)$ is related to the order of four fermion electroweak interaction. The

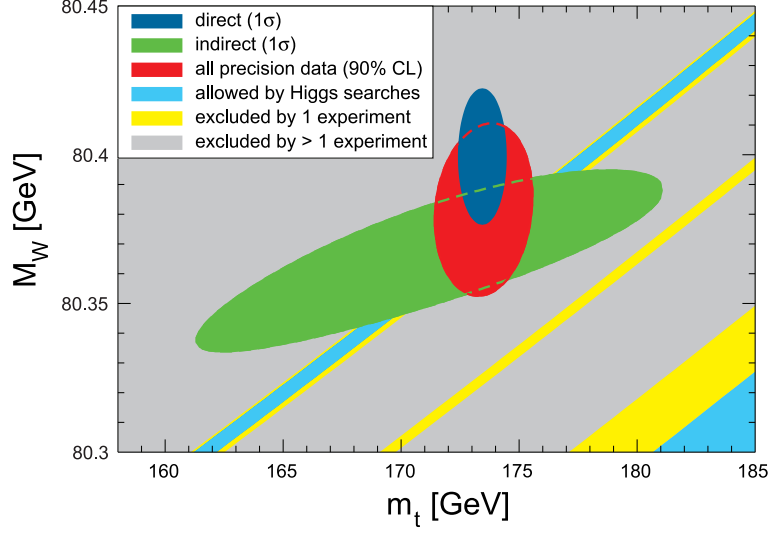


Figure 2.1: The electroweak test constrains m_h in $m_W - m_t$ plane. Figure is captured from Ref. [6].

measurement of muon life time provides $G_F = 1.16637(1) \times 10^{-5} \text{GeV}^{-2}$ [7]. $\sin \theta_W$ is also a sensitive quantity to test the electroweak theory. From Ref. [7], this quantity is $\sin \theta_W = 0.23116(13)$.

The gauge boson Z^0 and W^\pm have also been measured precisely. The most famous process involving W boson exchange is the β decay of neutron. Its mass is $m_W = 80.367 \pm 0.026 \text{GeV}$ [16], from the measurement of $W \rightarrow e\nu$. Z boson mass is measured very precisely at LEP experiment [18], which give $m_Z = 91.1876 \pm 0.0021 \text{GeV}$. The final SM particle which has still not been found is the Higgs boson, whose mass has been constrained by theoretical and experimental limits [17]. The electroweak precision test provides a sensitive search for m_h with the results for m_W and m_t , shown in Fig. 2.1 from Ref. [6]. Recently LHC result [19, 20] has ruled out much of the Higgs mass range. In CMS result $110 < m_h < 112.5 \text{GeV}$ and $127 < m_h < 600 \text{GeV}$ at 95% C.L., and a excess observed around $m_h \simeq 125 \text{GeV}$, with five statistical significant deviation from the background [20]. We will discuss more about the Higgs decay in Section 4.1.

One part of the SM, the electroweak theory has been measured very precisely. There is still another important topic that needs to be understood. This topic is the

number of fermion generations for SM, which can be related to the CP violation of the particle physics. We will discuss it in next section.

2.2 Quark Mixing Matrix

After the symmetry breaking, quarks and leptons acquired their masses from the Yukawa coupling. In the SM with n generations of fermions the charged current interaction and mass matrices for fermions are given by [13, 14]

$$\begin{aligned}\mathcal{L}_{\text{CC+mass}} = & -\frac{g_2}{\sqrt{2}}(\overline{U}_L\gamma_\mu D_L W^{\mu+} + \overline{\ell}_L\gamma_\mu \nu_L W^{\mu-}) \\ & -(\overline{U}_L M_u U_R + \overline{D}_L M_d D_R + \overline{l}_L M_l l_R + \text{h.c.}) .\end{aligned}\quad (2.13)$$

In this formula we omit the index i, j and regard Q_L, U_R, \dots as n -plet objects which can be multiplied by matrix such as M_u, M_d and M_l . At this stage, the quarks and leptons in the above formula are the so-called weak eigenstates, under which the charged current interaction is diagonal. In other words, there is no mixing between different generations of fermions in the electroweak gauge interaction. By contrast, the mass matrices are not diagonal in general.

We need to diagonalize the mass matrices M_u, M_d , and M_l by transforming Q_L, U_R, D_R, L_L and l_R field operators

$$\begin{aligned}U_L &\rightarrow V_L^{u\dagger} U_L, \quad U_R \rightarrow V_R^{u\dagger} U_R, \quad D_L \rightarrow V_L^{d\dagger} D_L, \quad D_R \rightarrow V_R^{d\dagger} D_R, \\ \nu_L &\rightarrow V_L^{\nu\dagger} \nu_L, \quad l_L \rightarrow V_L^{l\dagger} l_L, \quad l_R \rightarrow V_R^{l\dagger} l_R,\end{aligned}\quad (2.14)$$

where the above V 's are the corresponding transformation matrices for each types of fermions. Note that V_L^ν can be taken arbitrary since there is no neutrino mass matrix in SM. After applying the above transformation the charged current interaction and mass terms are given by

$$\begin{aligned}\mathcal{L}_{\text{CC+mass}} = & -\frac{g_2}{\sqrt{2}}[\overline{U}_L(V_L^u V_L^{d\dagger})\gamma_\mu D_L W^{\mu+} + \overline{\ell}_L(V_L^l V_L^{\nu\dagger})\gamma_\mu \nu_L W^{\mu-}] \\ & -(\overline{U}_L \hat{M}_u U_R + \overline{D}_L \hat{M}_d D_R + \overline{l}_L \hat{M}_l l_R + \text{h.c.}) .\end{aligned}\quad (2.15)$$

In the charged current interaction there is mixing between different generations. For quark mixing matrix $V_L^u V_L^{d\dagger}$ is usually denoted as the V_{CKM} , the so-called Cabibbo-Kobayashi-Maskawa mixing matrix [13, 14]. For the lepton sector the mixing matrix $V_L^l V_L^{\nu\dagger}$ is just taken to be identity since we can take $V_L^\nu = V_L^l$ to achieve it. If the neutrino eigenstates are fixed by other mechanism, then the mixing matrix for lepton sector would exist, which is named as the Pontecorvo-Maki-Nakagawa-Sakata (PMNS) matrix [29, 30].

2.2.1 CP violation and Complex Elements

In this section, we will show briefly how the relation between charged current weak interaction and CP violation is. First of all, recall that the parity transformation and charged conjugation for spin-1/2 particle ψ and spin-1 particle A_μ are given by

$$\begin{aligned}\psi^{\text{P}} &= \gamma_0 \psi, \quad \psi^{\text{C}} = C \bar{\psi}^T, \quad \text{with } C = i\gamma_0 \gamma_2, \\ A_\mu^{\text{P}} &= A_\mu, \quad A_\mu^{\text{C}} = -A_\mu.\end{aligned}\tag{2.16}$$

The charged current weak interaction for quark is

$$\mathcal{L}_{\text{CC}}^{(q)} = -\frac{g_2}{\sqrt{2}} [\overline{U_{Li}} (V_{\text{CKM}})_{ij} \gamma_\mu D_{Lj} W^{\mu+} - \overline{D_{Lj}} (V_{\text{CKM}}^*)_{ij} \gamma_\mu U_{Li} W^{\mu-}]. \tag{2.17}$$

Under the parity transformation, we have

$$\mathcal{L}_{\text{CC}}^{(q)\text{P}} = -\frac{g_2}{\sqrt{2}} [\overline{U_{Ri}} (V_{\text{CKM}})_{ij} \gamma_\mu D_{Rj} W^{\mu+} + \overline{D_{Rj}} (V_{\text{CKM}}^*)_{ij} \gamma_\mu U_{Ri} W^{\mu-}]. \tag{2.18}$$

Then following by the charge conjugation, we get the CP transformation of the Lagrangian

$$\mathcal{L}_{\text{CC}}^{(q)\text{CP}} = -\frac{g_2}{\sqrt{2}} [\overline{U_{Li}} (V_{\text{CKM}}^*)_{ij} \gamma_\mu D_{Lj} W^{\mu+} + \overline{D_{Lj}} (V_{\text{CKM}})_{ij} \gamma_\mu U_{Li} W^{\mu-}]. \tag{2.19}$$

From the above results, it is straightforward to show that the action is invariant under CP transformation when V_{CKM} is real.

Now we focus on the structure of V_{CKM} , which is in general a $n \times n$ unitary matrix for n generations. There are n^2 free parameters including rotating angles

and complex phases for an $n \times n$ unitary matrix. The number of angles is equal to that of the corresponding orthogonal matrices, which has $C_2^n = n(n-1)/2$ angles. So the number of complex phase should be $n(n+1)/2$, which can be reduced to a less number by the redefinition of quark fields. We can absorb n phases from one side, and $n-1$ phases from the other side of V_{CKM} . Finally there are only $(n-1)(n-2)/2$ irreducible phases in V_{CKM} . Therefore, the minimal number of generations to have CP violation in charge current of quark sector is three. This is the so-called Kobayashi-Maskawa theory [14].

2.2.2 CKM Matrix Elements and CP Violation

The CKM matrix is related to the mixing between quarks of different generations in the charged current, which is denoted by

$$V_{\text{CKM}} = \begin{pmatrix} V_{ud} & V_{us} & V_{ub} \\ V_{cd} & V_{cs} & V_{cb} \\ V_{td} & V_{ts} & V_{tb} \end{pmatrix}, \quad (2.20)$$

where V_{ij} 's denote the coupling of $q_i - q_j - W$ interaction. We parametrize the CKM matrix by the standard parametrization in which the four parameters θ_{12} , θ_{23} , θ_{13} , and δ_{13} are involved in the form [21]

$$V_S = \begin{pmatrix} c_{12}c_{13} & s_{12}c_{13} & s_{13}e^{-i\delta_{13}} \\ -s_{12}c_{23} - c_{12}s_{23}s_{13}e^{i\delta_{13}} & c_{12}c_{23} - s_{12}s_{23}s_{13}e^{i\delta_{13}} & s_{23}c_{13} \\ s_{12}s_{23} - c_{12}c_{23}s_{13}e^{i\delta_{13}} & -c_{12}s_{23} - s_{12}c_{23}s_{13}e^{i\delta_{13}} & c_{23}c_{13} \end{pmatrix}. \quad (2.21)$$

where $s_{12} = \sin \theta_{12}$, $c_{12} = \cos \theta_{12}$, ... and so on. The δ_{13} characterizes the CP violation of the charged current interaction. It is also useful to write down the above CKM matrix parametrization in terms of the Wolfenstein parameters λ , A , ρ , and η as follows [22]

$$V_S = \begin{pmatrix} 1 - \lambda^2/2 & \lambda & A\lambda^3(\rho - i\eta) \\ -\lambda & 1 - \lambda^2/2 & A\lambda^2 \\ A\lambda^3(1 - \rho - i\eta) & -A\lambda^2 & 1 \end{pmatrix} + \mathcal{O}(\lambda^4). \quad (2.22)$$

In the above formula V_S is expressed as the expansion of λ up to third order.

Now we discuss some of the experimental evidence of CP violation. There are three types of CP violation in the meson system. One of these comes from decay of meson purely, which is also called the direct CP violation. The source of such CP violation is the difference in magnitudes between a decay amplitude and its CP counterpart. Another type of CP violation is originated from the mixing of neutral meson in which the CP eigenstates do not coincide with the mass eigenstates. We also name this type of CP violation as the indirect CP violation. The last type of CP violation is the interference between the meson decay and meson mixing. Obviously it only occurs on neutral mesons. We take the kaon system as an example to explain the above three types of CP violation.

The neutral kaon system is usually described by a 2×2 matrix with K^0 and \overline{K}^0 as the basis. The CP eigenstates are just the maximal mixing of these kaon states, $K_{1,2} = (K^0 \mp \overline{K}^0)/\sqrt{2}$, where K_1 and K_2 are CP even and odd eigenstates, respectively. The mass eigenstates of neutral kaon system is obtained by solving the corresponding 2×2 Hamiltonian, which is non-Hermitian since the kaon might decay into other lighter states. If the mass eigenstates coincide with the CP eigenstates, then the neutral kaon system is CP conserving. On the other hand, if there are small deviation between the CP eigenstates and mass eigenstates, for example,

$$K_S = \frac{1}{\sqrt{1+|\tilde{\epsilon}|^2}}(K_1 - \tilde{\epsilon}K_2); K_L = \frac{1}{\sqrt{1+|\tilde{\epsilon}|^2}}(K_2 + \tilde{\epsilon}K_1), \quad (2.23)$$

where $\tilde{\epsilon}$ is a small quantity, then CP symmetry is violated. It will leads to the oscillation between two CP eigenstates K_1 and K_2 . Such effect was first discovered in 1964 [23], which is also the first evidence of CP violation, from the study of $K^0 \rightarrow \pi\pi$. They found that the CP even eigenstate $\pi\pi$ comes not only from K_S but also slightly from K_L . It has been verified that there is indeed a small mixing of CP even component K_1 in K_L , with $|\tilde{\epsilon}| = (2.44 \pm 0.04) \times 10^{-3}$ [24].

The CP violation from meson decay comes from the amplitudes of loop correction. The complex loop function with complex coupling constants leads to the difference between the amplitudes for a process and those of its CP transformation.

The dominant contribution to $K^0 \rightarrow \pi\pi$ is from the tree level diagram with W boson exchange, and the penguin diagrams. We need to extract the direct CP asymmetry from the total CP asymmetry results. It is convenient to define the quantities ϵ and ϵ' as follows

$$\frac{\mathcal{A}(K_L \rightarrow \pi^0\pi^0)}{\mathcal{A}(K_S \rightarrow \pi^0\pi^0)} = \epsilon - 2\epsilon', \quad \frac{\mathcal{A}(K_L \rightarrow \pi^+\pi^-)}{\mathcal{A}(K_S \rightarrow \pi^+\pi^-)} = \epsilon + \epsilon', \quad (2.24)$$

where ϵ and ϵ' correspond to the indirect and direct CP violation contribution, respectively. Finally, the imaginary part of ϵ represents the CP violation caused by interference between meson decay with and without mixing. The present numerical results are given by [7, 25]

$$\text{Re}(\epsilon') = (2.5 \pm 0.4) \times 10^{-6}, \quad \begin{cases} \text{Re}(\epsilon) = (1.66 \pm 0.02) \times 10^{-3}, \\ \text{Im}(\epsilon) = (1.57 \pm 0.02) \times 10^{-3}. \end{cases} \quad (2.25)$$

From the unitarity condition of CKM matrix we have one of the relation, $V_{ud}V_{ub}^* + V_{cd}V_{cb}^* + V_{td}V_{tb}^* = 0$, which is associated with a triangle in the complex plane, with three angles defined as follows

$$\beta \equiv \arg\left(-\frac{V_{cd}V_{cb}^*}{V_{td}V_{tb}^*}\right), \quad \alpha \equiv \arg\left(-\frac{V_{td}V_{tb}^*}{V_{ud}V_{ub}^*}\right), \quad \gamma \equiv \arg\left(-\frac{V_{ud}V_{ub}^*}{V_{cd}V_{cb}^*}\right). \quad (2.26)$$

Note that the area of this triangle is also an important quantity, twice of which is the Jarlskog invariant J . It is also worthwhile to understand that J , α , β , and γ are independent of the phase redefinition of quarks.

The three angles can be found by the experiments at B factory. We will follow the discussion in Ref. [7]. The time dependent asymmetry of the process $B \rightarrow J/\psi K$ can help to get β . HFAG shows the average as $\sin 2\beta = 0.673 \pm 0.023$ [26]. The α angle is extracted by the combination of the three process $B \rightarrow \pi\pi$, $B \rightarrow \rho\rho$, and $B \rightarrow \pi\rho$, which are related to the quark level process $b \rightarrow d\bar{u}u$. Also note that the CKM structure makes the tree level and one loop diagrams of the same order. The result is $\alpha = (89.0_{-4.2}^{+4.4})^\circ$ [27]. The γ angle can be obtained from the interference between $B^- \rightarrow D^0 K^-$ and $B^- \rightarrow \bar{D}^0 K^-$, which is the tree level dominated process. The final result is $\gamma = (73_{-25}^{+22})^\circ$ [27].

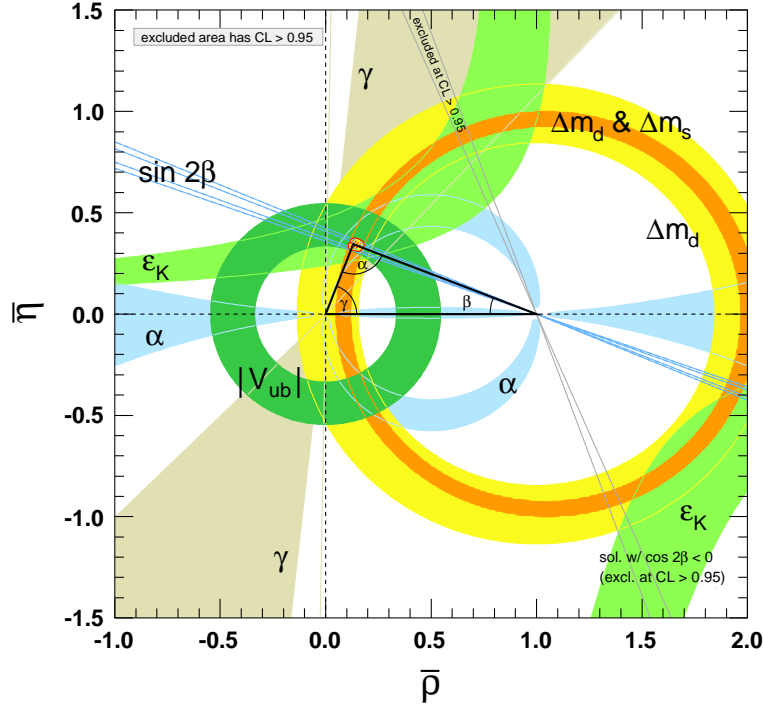


Figure 2.2: The experimental fit for the $\bar{\rho}$ and $\bar{\eta}$. Figure is captured from Ref. [6].

Combining all kinds of experiments related to CKM element magnitudes and angles provides the global fitting of CKM matrix parameters. The CKMfitter summarized the result in Fig. 2.2 which is excerpted from Ref. [6], also with the fitting values of Wolfenstein parameters which are given by [6]

$$\begin{aligned}\lambda &= 0.22535 \pm 0.00065 ; A = 0.811^{+0.022}_{-0.012} ; \\ \bar{\rho} &= 0.131^{+0.026}_{-0.013} ; \bar{\eta} = 0.345^{+0.013}_{-0.014} .\end{aligned}\tag{2.27}$$

These fitting values lead to the value of Jarlskog invariant J as $J = (2.96^{+0.20}_{-0.16}) \times 10^{-5}$ [6], and other kinds of parameters can also be obtained directly.

The CKM matrix is well consistent with almost every experiments involving hadronic process. The CP violation in meson decay have been detected and explained elegantly by the CKM matrix. In the following we will discuss the matrix in the charged current interaction with leptons, which plays the analogous role as CKM matrix.

2.3 Lepton Mixing Matrix

2.3.1 Neutrino Oscillation and Mixing Angles

From Eq. (2.15) we know that the $V_{\text{PMNS}} = V_L^e V_L^{\nu\dagger}$ is the mixing matrix of mass eigenstates of charged lepton and that of neutrino, which is also the mixing matrix between the neutrino flavor eigenstates and the mass eigenstates. The 3×3 V_{PMNS} is expressed as [29, 30]

$$V_{\text{PMNS}} = \begin{pmatrix} V_{e1} & V_{e2} & V_{e3} \\ V_{\mu 1} & V_{\mu 2} & V_{\mu 3} \\ V_{\tau 1} & V_{\tau 2} & V_{\tau 3} \end{pmatrix}. \quad (2.28)$$

The common parametrization of three generations V_{PMNS} is the same as Eq. (2.21). To distinguish from quark mixing parameters we will add the superscript “ ℓ ” to the mixing angles and phases. If the active neutrinos are Majorana, the phase of neutrino fields can not be transformed freely. In this case, the general form of V_{PMNS} should be matrix in Eq. (2.21) multiplying a phase matrix $\text{diag}(\exp(i\alpha_1), \exp(i\alpha_2), 1)$ to the right-handed side. The phases $\alpha_{1,2}$ are called the Majorana phases, which cannot be absorbed into neutrino fields.

If there is deviation between flavor eigenstates and mass eigenstates, neutrino oscillation would appear. To measure the oscillation, experimentalist detected the flavors of the neutrinos both near and far away from the detector. Roughly speaking, the amplitude of initial state ν_a propagating to the final state ν_b is given by [7]

$$\begin{aligned} \mathcal{M}(\nu_a \rightarrow \nu_b) &= \sum_k V_{ak}^* V_{bk} \exp[-i(E_k t - |\mathbf{p}_k|L)] \\ &\simeq \sum_k V_{ak}^* V_{bk} \exp(-i \frac{L}{2.48\text{m}} \frac{\Delta m_{kj}^2}{E}) \exp(-i(E_j t - |\mathbf{p}_j|L)), \end{aligned} \quad (2.29)$$

where we have use the approximation in the last step, with E and $\Delta m_{kj}^2 = m_k^2 - m_j^2$ the numbers for the energy of the propagating neutrinos and the mass square difference of neutrino eigenstates in MeV and eV^2 , respectively. L is the length of

propagation for neutrinos, and $|\mathbf{p}|$ is the momentum of the travelling neutrinos. The corresponding probability is then given by [7]

$$P(\nu_a(\bar{\nu}_a) \rightarrow \nu_b(\bar{\nu}_b)) = \sum_j |V_{aj}|^2 |V_{bj}|^2 + 2 \sum_{j>k} |V_{bj} V_{aj}^* V_{ak} V_{bk}^*| \cos\left(\frac{\Delta m_{jk}^2 L}{2E} \mp \arg(V_{bj} V_{aj}^* V_{ak} V_{bk}^*)\right), \quad (2.30)$$

where the “−” is for neutrino and “+” for antineutrino. From the obtained probability of $\nu_i \rightarrow \nu_j$, the mixing angles and the mass square differences of neutrino mass eigenstates can be extracted.

Up to now, there are three mixing angles observed in experiments. One is the solar neutrino angle, which comes from the electron neutrino produced from sun. SNO collaboration utilized heavy water as the target to detect the ratio of flux of electron neutrino to that of other types of neutrinos, where the mixing angle is $\sin^2 2\theta_{12}^\ell = 0.861_{-0.022}^{+0.026}$ [33], and the corresponding mass square difference is $\Delta m_{21}^2 = (7.59_{-0.21}^{+0.20}) \times 10^{-5} \text{eV}^2$ [31]. Another mixing angle is the so-called atmospheric neutrino mixing angle, which is related to the disappearance of muon neutrino from the cosmic ray. The corresponding mixing angle is given by $\sin^2 2\theta_{23}^\ell > 0.92$ [34]. The mass square difference magnitude is $|\Delta m_{32}^2| = (2.43 \pm 0.13) \times 10^{-3} \text{eV}^2$ [32], although the sign of it remains unknown. The sign of Δm_{32}^2 leads to two different scenario of neutrino mass spectrum. The normal hierarchy is the spectrum $m_1 < m_2 < m_3$; the inverted hierarchy is for $m_3 < m_1 < m_2$. T2K collaboration proposed the first direct result showing that the θ_{13}^ℓ is non-zero [35]. Recently Daya Bay collaboration announced a more accurate result for θ_{13}^ℓ , which is $\sin^2 2\theta_{13}^\ell = 0.092 \pm 0.016(\text{stat}) \pm 0.005(\text{sys})$ [36]. The above data of mixing angles and phases are obtained from individual experiment results. Fig. 2.3 from Ref. [7, 37] shows the current experimental results about possible ranges of mixing angles and mass square difference.

The standard model, including electroweak theory and Kobayashi-Maskawa theory, can explain most of the phenomena in our world. Almost every CP violating processes known in the present can be explained. However, for the evolution of the

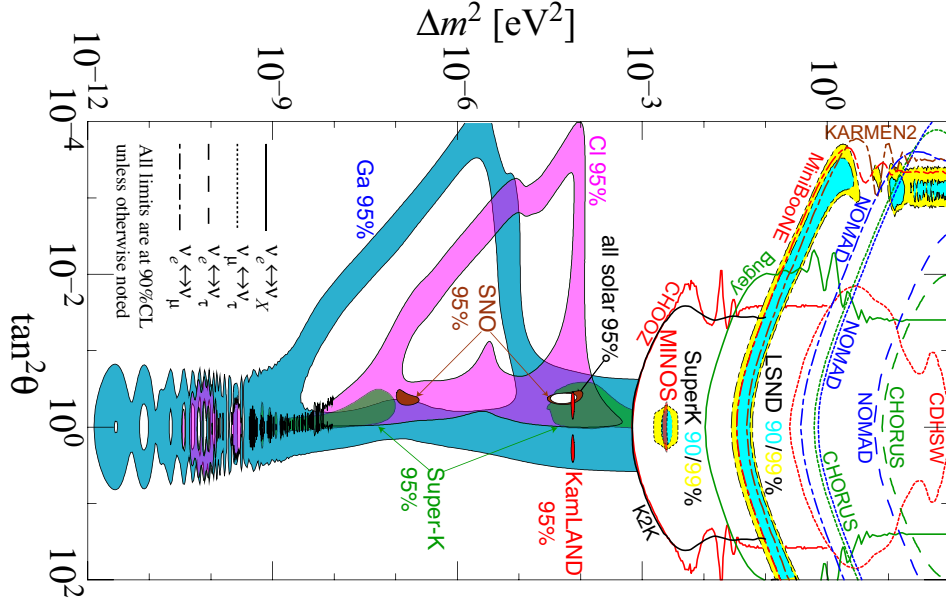


Figure 2.3: The neutrino oscillation experiment results, shown by the allowed area in $\Delta m^2 - \tan^2 \theta$ plane. Figure is captured from Ref. [7, 37].

universe, we can not explain why the number of baryons is so much larger than that of antibaryons, which is also called the baryon asymmetry. From the observation we know that the ratio of the baryon number density n_B to the photon number density n_γ , is about $n_B/n_\gamma \approx 10^{-8}$ [39]. For theoretical calculation we need the CP violation to saturate the experimental results. However, the Kobayashi-Maskawa theory can only provide $n_B/n_\gamma \approx 10^{-20}$ [38], with very high temperature. This implies that the phase in CKM matrix might not be the only source of CP violation. It is well known that the phase of the CKM matrix comes from the complex Yukawa couplings, but it remains an open question on the explanation of the origin of the complex numbers. The SM doesn't tell us the origin of these complex numbers, and it could be solved in an elegant way in the next chapter.

Another one is the explanation of light neutrino mass. One way to obtain the massive neutrino is to add one or more right-handed neutrinos to the SM. The Yukawa couplings with neutrinos should be very tiny, if the Majorana mass terms are not allowed. But it is necessary to explain why the scale of Yukawa couplings for charged leptons ($\lesssim 10^{-3}$) and neutrinos ($\lesssim 10^{-11}$) are so different. It turns out

that seesaw mechanism can solve this problem, and we will focus on some specific seesaw models which can be tested in the LHC.

It is also worthwhile to study the possibility of existence of the fourth generation, although many of the corresponding coupling constants are constrained by many experiments, both in CKM and PMNS matrices.





Chapter 3

Spontaneous CP Violation and Fermion Mixing Matrix Phases

In this chapter we will focus on a type of models, in which more than one Higgs doublet is introduced. Each Higgs can have its own VEV. The main idea is that there might be a relative phase between the VEVs of Higgs. Such an irreducible phase can cause the CP violation. We call such a mechanism spontaneous CP violation (SCPV), since it happens due to the spontaneous symmetry breaking. We will briefly introduce the background of these models, and then proceed to the most important topic in this chapter, which is to understand how to connect spontaneous CP violating phase to CKM and PMNS matrices phases.

3.1 Spontaneous CP Violation

We discuss several models in this section. The simplest extension beyond SM to include the spontaneous CP violation is the two Higgs doublet model. Another one is the model built to exclude the flavor change neutral current and keep the spontaneous CP violation, three Higgs doublet model. The last one is about the multi-Higgs models with some global symmetry, to solve the strong CP problem.

3.1.1 Two Higgs Doublet Model

The model with two Higgs doublets (2HDM) was first proposed by T. D. Lee in 1973 [40]. One of the special features of this model is that there could be a phase different between the two Higgs doublets. Generally, we can write down the two Higgs doublets with SM gauge group $(1, 2, -1/2)$ as

$$\phi_i = e^{i\theta_i} H_i = e^{i\theta_i} \begin{pmatrix} \frac{1}{\sqrt{2}}(v_i + R_i + iA_i) \\ h_i^- \end{pmatrix}, \quad i = 1, 2, \quad (3.1)$$

where $R_{1,2}$ and $A_{1,2}$ are real scalars. $v_{1,2}$ and $\theta_{1,2}$ are the magnitudes and phases for VEVs of $\phi_{1,2}$, respectively. The Higgs potential is then given by

$$\begin{aligned} V(H_1, H_2) = & -m_1^2 H_1^\dagger H_1 - m_2^2 H_2^\dagger H_2 + \lambda_1 (H_1^\dagger H_1)^2 + \lambda_2 (H_2^\dagger H_2)^2 \\ & + \lambda_s (H_1^\dagger H_1)(H_2^\dagger H_2) + \lambda_t (H_1^\dagger H_2)(H_2^\dagger H_1) + \frac{1}{2} [\tilde{\lambda}_{12} (H_1^\dagger H_2)(H_1^\dagger H_2) e^{i2\delta} \\ & + \tilde{\lambda}_{11} (H_1^\dagger H_2)(H_1^\dagger H_1) e^{i\delta} + \tilde{\lambda}_{22} (H_1^\dagger H_2)(H_2^\dagger H_2) e^{i\delta} + \text{h.c.}], \end{aligned} \quad (3.2)$$

where $\delta = \theta_2 - \theta_1$ is the only phase appear in the Higgs potential. $m_1^2, m_2^2, \lambda_{1,2,s,t}$ are automatically real, and we assign $\tilde{\lambda}_{12,11,22}$ to be real, since we hope to construct this model to be CP conserving at the beginning. Also note that the term $H_1^\dagger H_2 e^{i\delta}$ and its hermitian conjugate can be eliminated by appropriate rotation between ϕ_1 and ϕ_2 . The values of $v_{1,2}$ and δ should make the ground state achieve the minimal values in the potential. One of the condition required is to differentiate the potential with respect to δ at the ground state, which leads to

$$\sin \delta \left(\cos \delta + \frac{\tilde{\lambda}_{11} v_1^2 + \tilde{\lambda}_{22} v_2^2}{4 \tilde{\lambda}_{12} v_1 v_2} \right) = 0. \quad (3.3)$$

For general choices of λ 's, the minimal can occur at $\cos \delta \neq \pm 1$, which means that δ is nonzero. After symmetry breaking δ will appear in the potential, which violates the CP symmetry. Such mechanism is called the spontaneous CP violation.

The 2HDM is more complicated than SM, since there are five physical Higgs existing under spontaneous symmetry breaking, with other three components eaten

by gauge bosons W^\pm and Z^0 . The general form of Yukawa coupling is given by

$$\begin{aligned}\mathcal{L} = & \overline{Q}_L(Y_{u1}\phi_1 + Y_{u2}\phi_2)U_R + \overline{Q}_L(Y_{d1}\tilde{\phi}_1 + Y_{d2}\tilde{\phi}_2)D_R \\ & + \overline{L}_L(Y_{l1}\tilde{\phi}_1 + Y_{l2}\tilde{\phi}_2)l_R + \text{h.c.},\end{aligned}\tag{3.4}$$

where $Y_{u1,2}$, $Y_{d1,2}$, and $Y_{l1,2}$ are real coupling matrices in the beginning. After symmetry breaking, the complex phase δ will appear in the Yukawa coupling, and the complex CKM matrix can be obtained. Also, the two coupling matrices coupled to the same chiral fermion can not be diagonalized simultaneously in general. The tree level flavor changing neutral current (FCNC) would appear for quarks and leptons sectors, which is difficult to be determined, and also constrained stringently by a lot of experiments.

The common methods to simplify the Yukawa coupling is to introduce a discrete symmetry on Higgs and chiral fermions. For example, The model is presumed to be invariant under the transformation $H_1 \rightarrow H_1$, $H_2 \rightarrow -H_2$. With some choice of such transformation on fermions, it would prohibit the Yukawa coupling in which two Higgs doublets are coupled to the same chiral fermion. Therefore, FCNC vanishes successfully in the model, which is also regarded as the natural flavor conservation. However, imposing this discrete symmetry will sacrifice the spontaneous CP violation of this model. The reason is that the discrete symmetry prohibits the terms proportional to $\tilde{\lambda}_{11}$ and $\tilde{\lambda}_{22}$ in Eq. (3.2), and the phases $\theta_{1,2}$ in Yukawa coupling can be also absorbed by chiral fermions. Then 2δ is the only phase appearing in the Higgs potential, but the minimal condition in Eq. (3.3) will result in $\sin 2\delta = 0$. Finally the CP is conserved in the model. In summary, if one hope to build a model with both spontaneous CP violation and natural flavor conservation, a model with more than two Higgs doublets is required.

3.1.2 Three Higgs Doublet Model

The three Higgs doublet model (3HDM) was first proposed by Weinberg in 1976 [41] in order to generate a natural flavor conserving model with also the sponta-

neous CP violation. The three Higgs doublets with the gauge group representation $(1, 2, -1/2)$ are given by

$$\phi_k = e^{i\theta_k} H_k = e^{i\theta_k} \begin{pmatrix} \frac{1}{\sqrt{2}}(v_k + R_k + iA_k) \\ H_k^- \end{pmatrix}, \quad k = 1, 2, 3, \quad (3.5)$$

where all variables in the above formula are the same as that in 2HDM discussed previously, except for the three copies of Higgs particles and VEVs. Ref. [42] shows that for arbitrary numbers of quarks it is possible to build a natural flavor conserved model by imposing a discrete symmetry, which is given by

$$\begin{aligned} D_1 : & \quad \phi_1 \rightarrow \phi_1; \phi_2 \rightarrow -\phi_2; \phi_3 \rightarrow \phi_3; Q_L \rightarrow Q_L; D_R \rightarrow -D_R; U_R \rightarrow U_R, \\ D_2 : & \quad \phi_1 \rightarrow \phi_1; \phi_2 \rightarrow \phi_2; \phi_3 \rightarrow -\phi_3; Q_L \rightarrow Q_L; D_R \rightarrow D_R; U_R \rightarrow U_R. \end{aligned} \quad (3.6)$$

The Higgs potential satisfying the discrete symmetry given above is written as [43]

$$\begin{aligned} V = & \quad -m_1^2 H_1^\dagger H_1 - m_2^2 H_2^\dagger H_2 - m_3^2 H_3^\dagger H_3 + \lambda_1 (H_1^\dagger H_1)^2 + \lambda_2 (H_2^\dagger H_2)^2 + \lambda_3 (H_3^\dagger H_3)^2 \\ & + \lambda_{12}^s (H_1^\dagger H_1)(H_2^\dagger H_2) + \lambda_{23}^s (H_2^\dagger H_2)(H_3^\dagger H_3) + \lambda_{31}^s (H_3^\dagger H_3)(H_1^\dagger H_1) \\ & + \lambda_{12}^t (H_1^\dagger H_2)(H_2^\dagger H_1) + \lambda_{23}^t (H_2^\dagger H_3)(H_3^\dagger H_2) + \lambda_{31}^t (H_3^\dagger H_1)(H_1^\dagger H_3) \\ & + \frac{1}{2} [\tilde{\lambda}_{12} (H_1^\dagger H_2)^2 e^{i2\delta_{12}} + \tilde{\lambda}_{23} (H_2^\dagger H_3)^2 e^{i2\delta_{23}} + \tilde{\lambda}_{31} (H_3^\dagger H_1)^2 e^{i2(\delta_{12} + \delta_{23})} + \text{h.c.}], \end{aligned} \quad (3.7)$$

where all the coupling constants are real in the model. $\delta_{12} \equiv \theta_2 - \theta_1$ and $\delta_{23} \equiv \theta_3 - \theta_2$ are regarded as the two independent phases in the potential. Differentiating V with respect to δ_{12} and δ_{23} , we have [43]

$$\frac{\tilde{\lambda}_{12}}{v_3^2} \sin 2\delta_{12} = \frac{\tilde{\lambda}_{23}}{v_1^2} \sin 2\delta_{23} = -\frac{\tilde{\lambda}_{13}}{v_2^2} \sin 2(\delta_{12} + \delta_{23}). \quad (3.8)$$

Because nonzero δ_{12} and δ_{23} are allowed, the spontaneous CP violation exists and comes from the mixing of neutral and charged Higgs mass matrices [43].

Another important feature of this model is the natural flavor conservation in Yukawa couplings, which is due to the imposing of the discrete symmetry. The Yukawa coupling in this model is given by

$$\mathcal{L}_Y = \overline{Q}_L Y_u \phi_1 U_R + \overline{Q}_L Y_d \tilde{\phi}_2 D_R + \overline{L}_L Y_l \tilde{\phi}_3 E_R + \text{h.c.}, \quad (3.9)$$

where Y_u , Y_d , and Y_l are real matrices. The phases of VEVs can be absorbed into chiral components of fermions, and so the coupling matrices keep real, which will lead to a real CKM matrix. The Yukawa coupling is then given as

$$\begin{aligned}\mathcal{L} = & -\frac{1}{v_1}\overline{U_L}\hat{M}_uU_R(R_1^0 + iA_1) - \frac{1}{v_2}\overline{D_L}\hat{M}_dD_R(R_2^0 + iA_2) - \frac{1}{v_2}\overline{L_L}\hat{M}_l l_R(R_3^0 + iA_3) \\ & - \frac{\sqrt{2}}{v_1}\overline{D_L}V_{\text{CKM}}^\dagger\hat{M}_uU_RH_1^- + \frac{\sqrt{2}}{v_2}\overline{U_L}V_{\text{CKM}}\hat{M}_dD_RH_2^+ + \frac{\sqrt{2}}{v_3}\overline{L_L}V_{\text{CKM}}\hat{M}_l l_RH_3^+ + \text{h.c.},\end{aligned}\tag{3.10}$$

There is no FCNC in the above formula.

As we know the CP violation relevant to CKM matrix has been well confirmed by the present experiments, as given in Section 2.2.2. The Weinberg model predicts $|\sin 2\beta| < 0.05$ [44, 45], with $\sin 2\beta$ being the analogous quantity to that in CKM matrix when discussing $B \rightarrow J/\psi K$. This quantity has been ruled out by experimental data $\sin \beta$ shown previously. The present experiment result also provides an upper bound on neutron electric dipole moment (nEDM) $|d_n| < 0.29 \times 10^{-25} e \text{ cm}$ [47]. This result has ruled out the 3HDM as the source of CP violation, which predicts $|d_n| \approx 10^{-23} e \text{ cm}$ [46]. Other evidences to rule out this model were proposed by Ref. [44, 45].

3.1.3 Peccei-Quinn Symmetry

The SM Lagrangian has been shown in Eq. (2.4). Besides these terms, however, a surface term with the non-abelian gauge bosons involving, $(\theta g_3^2/32\pi^2)G^{a\mu\nu}\tilde{G}_{\mu\nu}^a$, with $\tilde{G}_{\mu\nu}^a = \frac{1}{2}\epsilon_{\mu\nu\rho\sigma}G^{a\rho\sigma}$ and θ as a free parameter, should also be considered. This term violates P and CP symmetries, thus one often names it as strong CP violating term. If one apply an axial U(1) transformation to a quark q , the corresponding axial current is $j^{5\mu} = \bar{q}\gamma_\mu\gamma_5q$, which is not conserved due to $\partial_\mu j^{5\mu} = 2m_q i\bar{q}\gamma_5q$, with the quark mass m_q . The famous Adler-Bell-Jackiw anomaly [54] implies that this situation still holds even if quarks are massless, which reads

$$\partial_\mu j^{5\mu} = \frac{g_3^2}{16\pi^2}G_{\mu\nu}^a\tilde{G}^{\mu\nu a}.\tag{3.11}$$

This will modify the strong CP violating term in the SM to be

$$\mathcal{L}_{\text{strong}} = \bar{\theta} \frac{g_3^2}{16\pi^2} G_{\mu\nu}^a \tilde{G}^{\mu\nu a}, \quad \text{with } \bar{\theta} = \theta - \arg(\det(M_u)) - \arg(\det(M_d)). \quad (3.12)$$

Thus the strength of the strong CP interaction is characterized by $\bar{\theta}$. The interaction should contribute to neutron electric dipole moment (nEDM). The current experimental result gives an upper bound which is still larger in several order than the contribution from complex CKM elements about $|d_n| \lesssim 10^{-31} e \text{ cm}$ [50, 51, 52]. It will result in a very stringent constraint on $\bar{\theta}$ with $|\bar{\theta}| \lesssim 10^{-10}$ [9], which is a very tiny and unnatural coupling. This is the strong CP problem. The $\bar{\theta}$ terms can also be induced at loop diagram related to complex quark mass, in SM the contribution is very small [53]. However, in multi-Higgs models the mixing between Higgs bosons would generate a very large correction to $\bar{\theta}$, of order 10^{-3} [49, 48]. Thus it is required to impose some other mechanism in order to solve the problem.

There is a elegant way to solve the problem, which is first proposed by Peccei and Quinn [55]. Take the two Higgs model as an example. By imposing a global axial symmetry $U(1)_{\text{PQ}}$ to the 2HDM, The $U(1)_{\text{PQ}}$ transformation is given as follows

$$\begin{aligned} Q_L &\rightarrow e^{-i\alpha} Q_L, \quad U_R \rightarrow e^{i\alpha} U_R, \quad D_R \rightarrow e^{i\alpha} D_R, \\ H_1 &\rightarrow e^{i2\alpha} H_1, \quad H_2 \rightarrow e^{-i2\alpha} H_2, \end{aligned} \quad (3.13)$$

which corresponds to the chiral transformation for quarks. It turns out that a natural flavor conserving 2HDM satisfies this $U(1)_{\text{PQ}}$ symmetry, except for the strong CP violating term. It means that we can always reduce the strong CP terms with the form of other terms kept in the Lagrangian. In other words, the change from chiral transformation of quarks can be absorbed into Higgs sector. Indeed 2HDM is also the minimal extension of SM to have the $U(1)_{\text{PQ}}$ symmetry. After spontaneous symmetry breaking, $U(1)_{\text{PQ}}$ is broken. A Goldstone boson with very light mass arises, which is the Peccei-Quinn-Weinberg-Wilczek (PQWW) axion a [55, 68]. From the detection of $a \rightarrow \gamma\gamma$, $a \rightarrow e^+e^-$ and other detection from the universe, the visible axion has been ruled out [69]. Ref. [57] proposed that in order to build a model with invisible axion, the original PQ model needs to be extended.

3.2 SCPV and CKM matrix

In Section 3.1 we have briefly introduced the spontaneous CP violation in several multi-Higgs models. But in general these models can not explain the CP violation and FCNC processes very well, which have been established by experiments. In the following we will build some models in which the phase of CKM matrix is connected from spontaneous CP violating phase.

3.2.1 Identifying CKM matrix phase with SCPV matrix phase

We consider a sort of models in which flavor changing neutral current appears in Yukawa coupling with U_R or D_R involving. At least two Higgs doublets are required in order to construct such Yukawa coupling. We list two type of models as below

$$\text{Model}(a) : \mathcal{L}_Y = \overline{Q_L}(Y_{u1}\phi_1 + Y_{u2}\phi_2)U_R + \overline{Q_L}Y_{d3}\tilde{\phi}_3D_R + \text{h.c.} , \quad (3.14)$$

$$\text{Model}(b) : \mathcal{L}_Y = \overline{Q_L}Y_{u3}\phi_3U_R + \overline{Q_L}(Y_{d1}\tilde{\phi}_1 + Y_{d2}\tilde{\phi}_2)D_R + \text{h.c.} , \quad (3.15)$$

where ϕ 's are Higgs doublets

$$\phi_k = e^{i\theta_k} \begin{pmatrix} \frac{1}{\sqrt{2}}(v_k + R_k + iA_k) \\ h_k^- \end{pmatrix}, \text{ for } k = 1, 2, \dots, \quad (3.16)$$

and Y 's are real 3×3 coupling matrices. In Model (a), two Higgs are coupled to U_R and the other one is coupled to D_R . The situation is opposite for Model (b), in which two Higgs coupling to D_R , and only one couple to U_R .

After spontaneous symmetry breaking the quark mass matrices arise, which are given in the form

$$\begin{aligned} \text{Model}(a) : \mathcal{L}_m &= -\overline{U_L}(M_{u1}e^{i\theta_1} + M_{u2}e^{i\theta_2})U_R - \overline{D_L}M_{d3}e^{-i\theta_3}D_R + \text{h.c.} , \\ \text{Model}(b) : \mathcal{L}_m &= -\overline{U_L}M_{u3}e^{i\theta_3}U_R - \overline{D_L}(M_{d1}e^{-i\theta_1} + M_{d2}e^{-i\theta_2})D_R + \text{h.c.} \end{aligned} \quad (3.17)$$

where $M_{ui} = v_i Y_{ui} / \sqrt{2}$. In Model (a), we can absorb the phase θ_1 to U_R and $-\theta_3$ to D_R . Similarly, in Model (b) the phases $-\theta_1$ and θ_3 can be absorbed to D_R and U_R ,

respectively. Then Eq. (3.17) can be expressed as

$$\begin{aligned}\mathcal{L}_m &= -\overline{U}_L M_u U_R - \overline{D}_L M_d D_R + \text{h.c.}, \text{ where for} \\ \text{Model(a)} &: M_u = M_{u1} + M_{u2}e^{i\delta}, M_d = M_{d3}; \\ \text{Model(b)} &: M_u = M_{u3}, M_d = M_{d1} + M_{d2}e^{-i\delta}.\end{aligned}$$

The mass matrix M_d in Model (a) and M_u in Model (b) can be diagonalized directly by the following transformation

$$\begin{aligned}\text{Model(a)} &: D_L \rightarrow V_L^{d\dagger} D_L; D_R \rightarrow V_R^{d\dagger} D_R, \\ \text{Model(b)} &: U_L \rightarrow V_L^{u\dagger} U_L; U_R \rightarrow V_R^{u\dagger} U_R,\end{aligned}\tag{3.18}$$

with also $U_L \rightarrow V_L^{d\dagger} U_L$ in Model (a) and $D_L \rightarrow V_L^{u\dagger} D_L$ in Model (b). We can regard this type of quark states as the flavor eigenstates, with the charged current weak interaction in quark sector in diagonal form. The mass matrix of the flavor eigenstates can be diagonalized by the relations

$$\begin{aligned}\text{Model (a)} &: \hat{M}_u = (V_L^u V_L^{d\dagger}) M'_u V_R^{u\dagger}, \text{ with } M'_u = V_L^d M_u; \\ \text{Model (b)} &: \hat{M}_d = (V_L^d V_L^{u\dagger}) M'_d V_R^{d\dagger}, \text{ with } M'_d = V_L^u M_d.\end{aligned}$$

We will focus on the special cases that V_R^u in Model (a) and V_R^d in Model (b) are real. Also note that $V_L^u V_L^{d\dagger}$ is just the CKM matrix, up to the phases redefinition in both sides of it. We will substitute $V_L^u V_L^{d\dagger}$ by different CKM matrix parametrizations, and they will lead to completely different models in the following.

At first we introduce the modified standard parametrization (M-parametrization) matrix V_M , which is given by

$$\begin{aligned}V_M &= \text{diag}(e^{-i\delta_{13}}, 1, 1) V_S \\ &= \begin{pmatrix} c_{12}c_{13}e^{i\delta_{13}} & s_{12}c_{13}e^{i\delta_{13}} & s_{13} \\ -s_{12}c_{23} - c_{12}s_{23}s_{13}e^{i\delta_{13}} & c_{12}c_{23} - s_{12}s_{23}s_{13}e^{i\delta_{13}} & s_{23}c_{13} \\ s_{12}s_{23} - c_{12}c_{23}s_{13}e^{i\delta_{13}} & -c_{12}s_{23} - s_{12}c_{23}s_{13}e^{i\delta_{13}} & c_{23}c_{13} \end{pmatrix},\end{aligned}\tag{3.19}$$

where V_S is the standard parametrization shown in Eq. (2.21). The above parametriza-

tion can be expanded by two real matrices V_M^r and V_M^p as follows

$$V_M^r = \begin{pmatrix} 0 & 0 & s_{13} \\ -s_{12}c_{23} & c_{12}c_{23} & s_{23}c_{13} \\ s_{12}s_{23} & -c_{12}s_{23} & c_{23}c_{13} \end{pmatrix}, \quad V_M^p = \begin{pmatrix} c_{12}c_{13} & s_{12}c_{13} & 0 \\ -c_{12}s_{23}s_{13} & -s_{12}s_{23}s_{13} & 0 \\ -c_{12}c_{23}s_{13} & -s_{12}c_{23}s_{13} & 0 \end{pmatrix};$$

$$V_M = V_M^r + V_M^p e^{i\delta_{13}}, \text{ and } V_M^r V_M^{p\dagger} = V_M^{r\dagger} V_M^p = 0. \quad (3.20)$$

If we take $V_L^u V_L^{d\dagger} = V_M$, then we get

$$\text{Model (a)} : M'_u V_R^{u\dagger} = V_M^\dagger \hat{M}_u; \quad (3.21)$$

$$\text{Model (b)} : M'_d V_R^{d\dagger} = V_M \hat{M}_d. \quad (3.22)$$

At this step we will introduce a crucial assumption to connect the identification of spontaneous CP violating phase δ and CKM matrix phase δ_{13} , which means $\delta = -\delta_{13}$ for both Model(a) and (b), with $\delta_{13} = (69 \pm 4)^\circ$ from CKM parameters fitting result [6]. The mass matrices for flavor basis $M'_{u(1,2)} = V_L^d M_{u(1,2)}$ is then obtained by

$$\begin{aligned} \text{Model(a)} : M'_{u1} V_R^{u\dagger} &= V_M^{r\dagger} \hat{M}_u, \quad M'_{u2} V_R^{u\dagger} = V_M^{p\dagger} \hat{M}_u, \\ \text{Model(b)} : M'_{d1} V_R^{d\dagger} &= V_M^r \hat{M}_d, \quad M'_{d2} V_R^{d\dagger} = V_M^p \hat{M}_d. \end{aligned} \quad (3.23)$$

The mass matrices under mass basis are given by

$$\begin{aligned} \text{Model(a)} : M''_{u1} &= V_M M'_{u1} V_R^{u\dagger} = V_M^r V_M^{r\dagger} \hat{M}_u, \\ M''_{u2} e^{i\delta} &= V_M M'_{u2} V_R^{u\dagger} = V_M^p V_M^{p\dagger} \hat{M}_u, \\ \text{Model(b)} : M''_{d1} &= V_M^\dagger M'_{d1} V_R^{d\dagger} = V_M^{r\dagger} V_M^r \hat{M}_d, \\ M''_{d2} e^{-i\delta} &= V_M^\dagger M'_{d2} V_R^{d\dagger} = V_M^{p\dagger} V_M^p \hat{M}_d. \end{aligned} \quad (3.24)$$

Also note that the combinations $V_M^r V_M^{r\dagger}$ and $V_M^p V_M^{p\dagger}$ are given by

$$V_M^p V_M^{p\dagger} = \begin{pmatrix} c_{13}^2 & -c_{13}s_{23}s_{13} & -c_{13}c_{23}s_{13} \\ -c_{13}s_{23}s_{13} & s_{23}^2 s_{13}^2 & s_{23}c_{23}s_{13}^2 \\ -c_{13}c_{23}s_{13} & s_{23}c_{23}s_{13}^2 & c_{23}^2 s_{13}^2 \end{pmatrix}, \quad V_M^r V_M^{r\dagger} = 1 - V_M^p V_M^{p\dagger}, \quad (3.25)$$

$$V_M^{p\dagger} V_M^p = \begin{pmatrix} c_{12}^2 & c_{12}s_{12} & 0 \\ c_{12}s_{12} & s_{12}^2 & 0 \\ 0 & 0 & 0 \end{pmatrix}, \quad V_M^{r\dagger} V_M^r = 1 - V_M^{p\dagger} V_M^p, \quad (3.26)$$

which depend only on the mixing angles in CKM matrix.

This kind of model is parametrization dependent. Different parametrization of $V_L^u V_L^{d\dagger}$ will lead to different model. We can also take the original Kobayashi–Maskawa parametrization as the choice, which is given by [14],

$$V_{\text{KM}} = \begin{pmatrix} c_1 & -s_1 c_3 & -s_1 s_3 \\ s_1 c_2 & c_1 c_2 c_3 - s_2 s_3 e^{i\delta_{\text{KM}}} & c_1 c_2 s_3 + s_2 c_3 e^{i\delta_{\text{KM}}} \\ s_1 s_2 & c_1 s_2 c_3 + c_2 s_3 e^{i\delta_{\text{KM}}} & c_1 s_2 s_3 - c_2 c_3 e^{i\delta_{\text{KM}}} \end{pmatrix}, \quad (3.27)$$

where $s_1 = \sin \theta_1$, $c_1 = \cos \theta_1$, ..., and so on. Following the same steps which we have done for modified standard parametrization V_{M} , also the identification $\delta = -\delta_{\text{KM}}$, with $\delta_{\text{KM}} = (91 \pm 4)^\circ$ [6], the final mass matrices in the mass basis is obtained in terms of V_{KM}^r and V_{KM}^p , which are the analogy of V_{KM}^r and V_{M}^p in V_{M} parametrization. The explicit form is given by

$$V_{\text{KM}}^p V_{\text{KM}}^{p\dagger} = \begin{pmatrix} 0 & 0 & 0 \\ 0 & s_2^2 & -s_2 c_2 \\ 0 & -s_2 c_2 & c_2^2 \end{pmatrix}, \quad V_{\text{KM}}^r V_{\text{KM}}^{r\dagger} = 1 - V_{\text{KM}}^p V_{\text{KM}}^{p\dagger}. \quad (3.28)$$

$$V_{\text{KM}}^{p\dagger} V_{\text{KM}}^p = \begin{pmatrix} 0 & 0 & 0 \\ 0 & s_3^2 & -s_3 c_3 \\ 0 & -s_3 c_3 & c_3^2 \end{pmatrix}, \quad V_{\text{KM}}^{r\dagger} V_{\text{KM}}^r = 1 - V_{\text{KM}}^{p\dagger} V_{\text{KM}}^p. \quad (3.29)$$

We have show that it is possible to make the spontaneous CP violating phase be identified with CKM matrix phase. In the next section, we will build a specific model to realize the idea.

3.2.2 Higgs potential and mass matrices

In section 3.1.3 we have understood that the loop correction in multi-Higgs models will enlarge the θ in general. The model with spontaneous CP violation as the sole source of CP violation would be ruled out if there is no mechanism to suppress θ . The supplementing of the PQ symmetry will solve the problem. In two Higgs doublet model, however, the PQ symmetry will exclude some of the crucial terms

in Higgs potential, which will lead to the vanishing of spontaneous CP violating phase. So the model with more than two Higgs doublets is required [56]. To realize our idea in previous section, we need at least three Higgs doublets. Also note that, the present experimental results only allow the possibility of invisible axion, corresponding with a singlet with very large VEV [57]. In summary, we will take the three Higgs doublets and one Higgs singlet to build our model.

In our model, three Higgs doublets $\phi_k : (1, 2, -1/2)$ with $k = 1 \sim 3$ and one Higgs singlet $\tilde{S} : (1, 1, 0)$ are given by

$$\begin{aligned}\phi_k &= e^{i\theta_k} H_k = e^{i\theta_k} \begin{pmatrix} \frac{1}{\sqrt{2}}(v_k + R_k + iA_k) \\ h_k^- \end{pmatrix}, \\ \tilde{S} &= e^{i\theta_s} S = e^{i\theta_s} \frac{1}{\sqrt{2}}(v_s + R_s + iA_s).\end{aligned}\tag{3.30}$$

where the definition for three Higgs doublets is the same as that in Section 3.1.2. For the Higgs singlet, v_s and θ_s are the magnitude and phase of the VEV, and R_s and A_s are real scalars. Note that as mentioned in the Section 3.1.3, to get an invisible axion a very large v_s is required. Since we would like to build a model with PQ symmetry, assigning the PQ charge for each particle is required. The PQ charges for the Higgs doublets and singlet are given by

$$\phi_1 : +1, \phi_2 : +1, \phi_3 : -1, \tilde{S} : +2.\tag{3.31}$$

The above assignment ensures that ϕ_1 and ϕ_2 coupling to the same chiral fermions in the Yukawa coupling. The assignment is different for Model (a) and Model (b), which is given by

$$\text{Model (a): } Q_L : 0, U_R : -1, D_R : -1,\tag{3.32}$$

$$\text{Model (b): } Q_L : 0, U_R : +1, D_R : +1.\tag{3.33}$$

The Higgs potential under PQ symmetry is then written as

$$\begin{aligned}
V = & - m_1^2 H_1^\dagger H_1 - m_2^2 H_2^\dagger H_2 - m_3^2 H_3^\dagger H_3 - m_{12}^2 (H_1^\dagger H_2 e^{i\delta} + \text{h.c.}) \\
& - m_s^2 S^\dagger S + \lambda_1 (H_1^\dagger H_1)^2 + \lambda_2 (H_2^\dagger H_2)^2 + \lambda_t (H_3^\dagger H_3)^2 + \lambda_s (S^\dagger S)^2 \\
& + \lambda_3 (H_1^\dagger H_1) (H_2^\dagger H_2) + \lambda'_3 (H_1^\dagger H_1) (H_3^\dagger H_3) + \lambda''_3 (H_2^\dagger H_2) (H_3^\dagger H_3) \\
& + \lambda_4 (H_1^\dagger H_2) (H_2^\dagger H_1) + \lambda'_4 (H_1^\dagger H_3) (H_3^\dagger H_1) + \lambda''_4 (H_2^\dagger H_3) (H_3^\dagger H_2) \\
& + \frac{1}{2} \lambda_5 ((H_1^\dagger H_2)^2 e^{i2\delta} + \text{h.c.}) + \lambda_6 (H_1^\dagger H_1) (H_1^\dagger H_2 e^{i\delta} + \text{h.c.}) \\
& + \lambda_7 (H_2^\dagger H_2) (H_1^\dagger H_2 e^{i\delta} + \text{h.c.}) + \lambda_8 (H_3^\dagger H_3) (H_1^\dagger H_2 e^{i\delta} + \text{h.c.}) \\
& + d_{12} (H_1^\dagger H_2 e^{i\delta} + \text{h.c.}) S^\dagger S + \lambda'_8 ((H_1^\dagger H_3) (H_3^\dagger H_2) e^{i\delta} + \text{h.c.}) \\
& + f_1 (H_1^\dagger H_1) S^\dagger S + f_2 (H_2^\dagger H_2) S^\dagger S + f_3 (H_3^\dagger H_3) S^\dagger S \\
& + f_{13} (H_1^\dagger H_3 S e^{i(\delta_s + \delta)} + \text{h.c.}) + f_{23} (H_1^\dagger H_3 S e^{i\delta_s} + \text{h.c.}) , \tag{3.34}
\end{aligned}$$

where the phases appearing in Higgs potential are δ , which is same as given in Section 3.2.1, and $\delta_s \equiv \theta_3 + \theta_s - \theta_2$. All of the coupling constants in Higgs potential are real to reveal the fact that our model is CP conserving before spontaneous CP violation. We will investigate the allowed values of these phases. By differentiating with respect to δ_s for minimization of the potential, we get the relation

$$f_{13} v_1 v_3 v_s \sin(\delta_s + \delta) + f_{23} v_2 v_3 v_s \sin \delta_s = 0 . \tag{3.35}$$

In the above formula the nonzero δ and δ_s are allowed, and δ is the only source to generate CP violation in the model. Note that since a large separation for the magnitudes of VEVs between Higgs doublets and Higgs singlet, the fine tuning for parameters of Higgs potential is required in the model and other invisible axion models.

The next step is to extract the Goldstone boson modes related to gauge boson W^\pm , Z^0 and the PQ symmetry breaking. These Goldstone states are given by

$$\begin{aligned}
h_w^- &= \frac{1}{v} (v_1 h_1^- + v_2 h_2^- + v_3 h_3^-) , \\
h_z &= \frac{1}{v} (v_1 A_1 + v_2 A_2 + v_3 A_3) , \\
a &= (-v_1 v_3^2 A_1 - v_2 v_3^2 A_2 + v_{12}^2 v_3 A_3 - v^2 v_s A_s) / N_a , \tag{3.36}
\end{aligned}$$

where $v^2 = v_1^2 + v_2^2 + v_3^2$. h_w, h_z are the Goldstone bosons eaten by W^\pm and Z^0 , respectively. a is the axion, with $N_a = v\sqrt{v_{12}^2 v_3^2 + v^2 v_s^2}$ the normalization factor, in which $v_{12}^2 = v_1^2 + v_2^2$. To extract the Goldstone boson modes and to transfer the FCNC coupling to only one Higgs boson, the transformation matrices for pseudoscalar and charged components are shown as

$$\begin{pmatrix} A_1 \\ A_2 \\ A_3 \\ A_s \end{pmatrix} = \begin{pmatrix} v_2/v_{12} & -v_1 v_3 v_s / N_A & v_1/v & -v_1 v_3^2 / N_a \\ -v_1/v_{12} & -v_2 v_3 v_s / N_A & v_2/v & -v_2 v_3^2 / N_a \\ 0 & v_{12}^2 v_s / N_A & v_3/v & v_{12}^2 v_3 / N_a \\ 0 & v_{12}^2 v_3 / N_A & 0 & -v^2 v_s / N_a \end{pmatrix} \begin{pmatrix} a_1 \\ a_2 \\ h_z \\ a \end{pmatrix},$$

$$\begin{pmatrix} h_1^- \\ h_2^- \\ h_3^- \end{pmatrix} = \begin{pmatrix} v_2/v_{12} & v_1 v_3 / v v_{12} & v_1/v \\ -v_1/v_{12} & v_2 v_3 / v v_{12} & v_2/v \\ 0 & -v_{12}/v & v_3/v \end{pmatrix} \begin{pmatrix} H_1^- \\ H_2^- \\ h_w^- \end{pmatrix}, \quad (3.37)$$

with $N_A = \sqrt{v_{12}^2(v_{12}^2 v_3^2 + v_s^2 v^2)}$ the normalization constant of second column in pseudoscalar transformation matrix. In the limit $v_s \gg v_{1,2,3}$ we have a good approximation $N_a = v^2 v_s$ and $N_A = v_{12} v v_s$. For the neutral scalar components $(R_1, R_2, R_3, R_s)^T$, we simply implement the same transformation as that in pseudoscalar transformation matrix to get a simpler form in Yukawa coupling, with the neutral scalar state $(H_1^0, H_2^0, H_3^0, H_4^0)^T$ taken. Note that we don't mix the scalar and pseudoscalar components to get the mass eigenstates, so that when we study some realistic problem we need to consider the mixing between different neutral components.

3.2.3 Some Implication

Since the mass matrices for Higgs sector in our model is already known in the rotated basis given in last section, The Yukawa interaction can be derived directly,

which is given by

$$\begin{aligned}
\mathcal{L}_Y^{(a)} &= \overline{U}_L \left[\frac{v_1}{v_{12}v_2} - V^r V^{r\dagger} \frac{v_{12}}{v_1v_2} \right] \hat{M}_u U_R (H_1^0 + ia_1) \\
&\quad + \overline{U}_L \hat{M}_u U_R \left[\frac{v_3}{v_{12}v} (H_2^0 + ia_2) - \frac{1}{v} H_3^0 + \frac{v_3^2}{v^2 v_s} (H_4^0 + ia) \right] \\
&\quad - \overline{D}_L \hat{M}_u D_R \left[\frac{v_{12}}{v_3v} (H_2^0 - ia_2) + \frac{1}{v} H_3^0 + \frac{v_{12}^2}{v^2 v_s} (H_4^0 - ia) \right] \\
&\quad + \sqrt{2} \overline{D}_L V_{\text{CKM}}^\dagger \left[\frac{v_1}{v_2v_{12}} - V^r V^{r\dagger} \frac{v_{12}}{v_1v_2} \right] \hat{M}_u U_R H_1^- \\
&\quad - \sqrt{2} \frac{v_3}{v_{12}v} \overline{D}_L V_{\text{CKM}}^\dagger \hat{M}_u U_R H_2^- - \sqrt{2} \frac{v_{12}}{vv_3} \overline{U}_L V_{\text{CKM}} \hat{M}_d D_R H_2^+ + \text{h.c.}, \\
\mathcal{L}_Y^{(b)} &= \overline{D}_L \left[\frac{v_1}{v_{12}v_2} - V^{r\dagger} V^r \frac{v_{12}}{v_1v_2} \right] \hat{M}_d D_R (H_1^0 - ia_1) \\
&\quad + \overline{D}_L \hat{M}_d D_R \left[\frac{v_3}{v_{12}v} (H_2^0 - ia_2) - \frac{1}{v} H_3^0 + \frac{v_3^2}{v^2 v_s} (H_4^0 - ia) \right] \\
&\quad - \overline{U}_L \hat{M}_u U_R \left[\frac{v_{12}}{v_3v} (H_2^0 + ia_2) + \frac{1}{v} H_3^0 + \frac{v_{12}^2}{v^2 v_s} (H_4^0 + ia) \right] \\
&\quad - \sqrt{2} \overline{U}_L V_{\text{CKM}} \left[\frac{v_1}{v_2v_{12}} - V^{r\dagger} V^r \frac{v_{12}}{v_1v_2} \right] \hat{M}_d D_R H_1^+ \\
&\quad + \sqrt{2} \frac{v_3}{v_{12}v} \overline{U}_L V_{\text{CKM}} \hat{M}_d D_R H_2^+ + \sqrt{2} \frac{v_{12}}{vv_3} \overline{D}_L V_{\text{CKM}}^\dagger \hat{M}_u U_R H_2^- + \text{h.c.}, \quad (3.38)
\end{aligned}$$

where V^r can be V_M^r or V_{KM}^r , depends on which parametrization of CKM matrix we take. The couplings of H_4^0 and a are suppressed by $1/v_s$. In both model only H_1^0 and a_1 have tree level FCNC coupling due to our choice of Higgs states. The FCNC couplings are associated with $V^r V^{r\dagger}$ in Model (a) and $V^{r\dagger} V^r$ in Model (b).

Neutral meson mixing has been observed in $K^0 - \bar{K}^0$, $B_{d,s}^0 - \bar{B}_{d,s}^0$, and $D^0 - \bar{D}^0$ system [7]. In the SM the neutral meson mixing is generated by box diagrams with W boson exchange. In this model tree level FCNC with H_1^0 exchange, a_1 exchange, and the mixing of H_1^0 and a_1 in the propagator should be also taken into account. The Yukawa coupling with H_1^0 and a_1 related to the neutral meson mixing is given in the form

$$\mathcal{L} = -\bar{q}_i (a_{ij} + b_{ij} \gamma_5) q_j H_1^0 + i\bar{q}_i (b_{ij} + a_{ij} \gamma_5) q_j a_1, \quad (3.39)$$

where the tree level FCNC couplings a_{ij} and b_{ij} are related to what we show in Eq. (3.38). With the equation of motion $\bar{q}_i \gamma_5 q_j = (p_i - p_j)^\mu \bar{q}_i \gamma_\mu \gamma_5 q_j / (m_i + m_j)$, the

mixing element of mass matrix of neutral meson system is given by

$$\begin{aligned}
M_{12} = & \frac{1}{m_{H_1^0}^2} [(b_{ij}^2 - \frac{1}{12}(a_{ij}^2 + b_{ij}^2)) \frac{f_P^2 m_P^3}{(m_i + m_j)^2} + \frac{1}{12}(b_{ij}^2 - a_{ij}^2) f_P^2 m_P] \\
& - \frac{1}{m_{a_1}^2} [(a_{ij}^2 - \frac{1}{12}(a_{ij}^2 + b_{ij}^2)) \frac{f_P^2 m_P^3}{(m_i + m_j)^2} + \frac{1}{12}(a_{ij}^2 - b_{ij}^2) f_P^2 m_P] \\
& + \frac{i 2 m_{H_1^0 a_1}^2}{m_{H_1^0}^2 m_{a_1}^2} \frac{5 a_{ij} b_{ij}}{6} \frac{f_P^2 m_P^3}{(m_i + m_j)^2}, \tag{3.40}
\end{aligned}$$

where f_P is the meson decay constant defined from $\langle 0 | \bar{q}_i \gamma^\mu \gamma_5 q_j | P \rangle = i f_P p_P^\mu$. The vacuum saturation approximation is also applied to Eq. (3.40). The meson decay can provide some information about the mass of H_1^0 . For the numerical analysis, we use the CKM mixing angles $s_{12} = 0.2254$, $s_{23} = 0.041$, $s_{13} = 0.0035$, $\sin \delta_{13} = 0.94$ in M-parametrization (equivalently $s_1 = 0.2254$, $s_2 = 0.039$, $s_3 = 0.0156$, $\sin \delta_{\text{KM}} = 0.9999$ in KM-parametrization), which are obtained from central values of Wolfenstein parameters given in Eq. (2.27). We take the values of decay constants $f_K = 156$ MeV, $f_D = 201$ MeV, and $f_{B_s} = 260$ MeV from Ref. [59]. The light quark masses $m_u(1 \text{ GeV}) = 3.1$ MeV, $m_d(1 \text{ GeV}) = 6.5$ MeV, $m_s(1 \text{ GeV}) = 129$ MeV and the heavy quark masses $m_c(m_c) = 1.275$ GeV, $m_b(m_b) = 4.18$ GeV, $m_t = 173.5$ GeV are given in Ref. [6].

The structure of flavor changing coupling for different CKM matrix parametrization are very different. For example, in Model (a-M), the modified standard parametrization in Model (a), there is tree level $D^0 - \bar{D}^0$ mixing, but no contribution to K^0 , B_d^0 , and B_s^0 mixing. We will discuss the numerical analysis of neutral meson mixing for M- and KM- parametrization in Model (a) and Model (b) as follows.

Model (a-M): It can contribute to $D^0 - \bar{D}^0$ mixing. The experiments by BaBar and Belle [60] provide that $x = \Delta m_D / \Gamma_D = (5.5 \pm 2.2) \times 10^{-3}$ at 68% C.L. [61], which can be used to compare with the new contribution

$$x = 5.7 \times 10^{-5} \frac{f_D^2 m_D^3}{(\sin 2\beta)^2 v_1^2 \Gamma_D} \left(\frac{1}{m_{H_1^0}^2} - \frac{1}{m_{a_1}^2} \right), \tag{3.41}$$

with $\tan \beta \equiv (v_1/v_2)$. New physics may contribute significantly [61]. If one hope the Higgs mass of order hundred GeV, with the assumption that one of v_1 and v_2 is large, around 240 GeV, then $\sin \beta \sim 0.05$, which indicates that the magnitudes of

v_1 and v_2 are different by forty times. In contrast, the tree level contribution with all VEVs of the same order of magnitudes does not produce enough x to saturate the measured value.

Model (b-M) The only nonzero flavor change neutral current comes from $s - d - H_1^0(a_1)$ interaction, which contributes to the neutral K meson mixing. The related mass difference from tree level interaction is given by

$$\frac{\Delta m_K}{m_K} = 4.4 \times 10^{-12} \frac{1}{\sin^2 2\beta v_{12}^2} \left(\frac{1}{m_{H_1^0}^2} - \frac{1}{m_{a_1}^2} \right) (100\text{GeV})^4. \quad (3.42)$$

The current experimental result gives $\Delta m_K/m_K = 7.000 \times 10^{-15}$ [7]. It constrains the mass of Higgs stringently. The scale of lightest Higgs mass between H_1^0 or a_1 should be larger than TeV scale.

Model (b-KM) In this model the FCNC only occurs in $b - s - H_1^0(a_1)$ interaction. It leads to the $B_s - \overline{B}_s$ mixing which is shown as

$$\frac{\Delta m_{B_s}}{m_{B_s}} = 7.4 \times 10^{-12} \frac{1}{\sin^2 2\beta v_{12}^2} \left(\frac{1}{m_{H_1^0}^2} - \frac{1}{m_{a_1}^2} \right) (100\text{GeV})^4. \quad (3.43)$$

Comparing with the experimental result $\Delta m_{B_s}/m_{B_s} = 2.2 \times 10^{-12}$ for $\Delta m_{B_s} = 17.77\text{ps}^{-1}$ [62], with the knowledge that only 10% of the experimental result can comes from contribution beyond the SM [63], the lightest one between H_1^0 and a_1 should be larger than 300GeV if we take $v_1 = v_2 = v_3$.

In the next step we study the neutron EDM (nEDM) in our model after imposing the constraints from meson and anti-meson mixing discussed in the above. It has been known that the prediction of nEDM in the SM is very small when comparing with presented experimental upper bound. The one loop contribution for quark EDM is usually proportional to light quarks masses to the third power for a diagram in which the internal quark is the same as the external quark. For heavy quark in the loop, its coupling is too small in the model. In our model the related operators for quark EDM are given by [64, 65]

$$\begin{aligned} O_q^\gamma &= -\frac{d_q}{2} i \bar{q} \sigma_{\mu\nu} \gamma_5 F^{\mu\nu} q, \quad O_q^C = -\frac{f_q}{2} i g_s \bar{q} \sigma_{\mu\nu} \gamma_5 G^{\mu\nu} q, \\ O_g^C &= -\frac{1}{6} C f_{abc} G_{\mu\nu}^a G_{\mu\alpha}^b \tilde{G}_{\nu\alpha}^c, \end{aligned} \quad (3.44)$$

where d_q , f_q and C come from two loop contribution dominantly in most of the multi-Higgs models [64, 65]. They are usually given [64, 65]

$$d_q = \frac{e\alpha_{\text{em}}Q_q}{24\pi^3}m_q G(q), \quad f_q = \frac{\alpha_s}{64\pi^3}m_q G(q), \quad C = \frac{1}{8\pi}H(g), \quad (3.45)$$

where the function $G(q)$ and $H(q)$ are given by

$$\begin{aligned} G(q) &= \left[\left(f\left(\frac{m_t^2}{m_{H_l^0}^2}\right) - f\left(\frac{m_t^2}{m_{a_k}^2}\right) \right) \text{Im}Z_{tq}^{lk} + \left(g\left(\frac{m_t^2}{m_{H_l^0}^2}\right) - g\left(\frac{m_t^2}{m_{a_k}^2}\right) \right) \text{Im}Z_{qt}^{lk} \right]; \\ H(g) &= \left(h\left(\frac{m_t^2}{m_{H_l^0}^2}\right) - h\left(\frac{m_t^2}{m_{a_k}^2}\right) \right) \text{Im}Z_{tt}^{lk}, \end{aligned} \quad (3.46)$$

where $\text{Im}Z_{ij}^{lk} = 2a_{ii}^l a_{jj}^k \lambda_{lk} / m_i m_j$, and $\lambda_{lk} = m_{H_l^0}^2 / (m_{H_l^0}^2 - m_{a_k}^2)$ is the mixing factor in the loop. The functions f , g , and h defined as

$$\begin{aligned} f(z) &= \frac{z}{2} \int_0^1 dx \frac{1-2x(1-x)}{x(1-x)-z} \ln \frac{x(1-x)}{z}, \\ g(z) &= \frac{z}{2} \int_0^1 dx \frac{1}{x(1-x)-z} \ln \frac{x(1-x)}{z}, \\ h(z) &= \frac{z^2}{2} \int_0^1 dx \int_0^1 du \frac{u^3 x^3 (1-x)}{[zx(1-ux) + (1-u)(1-x)]^2}. \end{aligned} \quad (3.47)$$

The valence quark model is usually used to associate the neutron EDM with quark EDM. It provides that [50, 51, 52]

$$d_n^\gamma = \eta_d \left[\frac{4}{3}d_d - \frac{1}{3}d_u \right]_\Lambda, \quad d_n^C = e\eta_f \left[\frac{4}{9}f_d + \frac{2}{9}f_u \right]_\Lambda, \quad d_n \approx \frac{eM}{4\pi}\xi C, \quad (3.48)$$

where Λ is the scale for the hadrons; d_n contributed from gluon color EDM is estimated by naive dimensional analysis (NDA). $M = 1190\text{MeV}$ is the chiral breaking scale and η_d , η_f , and ξ are the factor coming from the renormalization group evolution [66, 67]

$$\begin{aligned} \eta_d &= \left(\frac{\alpha_s(m_Z)}{\alpha_s(m_b)} \right)^{16/23} \left(\frac{\alpha_s(m_b)}{\alpha_s(m_c)} \right)^{16/25} \left(\frac{\alpha_s(m_c)}{\alpha_s(\Lambda)} \right)^{16/27} \approx 0.167, \\ \eta_f &= \left(\frac{\alpha_s(m_Z)}{\alpha_s(m_b)} \right)^{14/23} \left(\frac{\alpha_s(m_b)}{\alpha_s(m_c)} \right)^{14/25} \left(\frac{\alpha_s(m_c)}{\alpha_s(\Lambda)} \right)^{14/27} \frac{\alpha_s(m_Z)}{\alpha_s(\Lambda)} \approx 0.0118, \\ \xi &= \left(\frac{g(\Lambda)}{4\pi} \right)^3 \left(\frac{\alpha_s(m_b)}{\alpha_s(m_t)} \right)^{-54/23} \left(\frac{\alpha_s(m_c)}{\alpha_s(m_b)} \right)^{-54/25} \left(\frac{\alpha_s(\Lambda)}{\alpha_s(m_c)} \right)^{-54/27} \approx 1.3 \times 10^{-4}. \end{aligned} \quad (3.49)$$

Model (a-M): the two loop contribution to nEDM due to the Higgs bosons exchange in the loop are proportional to the mixing factor $\lambda_{lk}(f, g, h)$. These factor

will be taken to be approximately equal to estimate the contribution from different Higgs exchanges.

In this model we will take the parameters $\tan\beta = 40$, $v_{12} = 240\text{GeV}$, which has been used in $D^0 - \overline{D}^0$ mixing previously. Then the dominant contribution to neutron EDM comes from the mixing of H_3^0 and a_1 , which is given by

$$d_n \approx -2 \times 10^{-25} \frac{m_{H_3^0 a_1}^2}{m_{H_3^0}^2 - m_{a_1}^2} e \text{ cm} . \quad (3.50)$$

For another case with $v_1 = v_2 = v_3$, and $m_{a_1} \approx 100\text{GeV}$. If $H_3^0 - a_1$ mixing is larger than other mixing, then we have

$$d_n \approx 9 \times 10^{-26} \frac{m_{H_3^0 a_1}^2}{m_{H_3^0}^2 - m_{a_1}^2} e \text{ cm} . \quad (3.51)$$

For both cases the d_n can be close to the current upper bound.

Model (b-M): in this case H_1^0 and a_1 do not couple to $\bar{t}t$, so the two loop contribution to the quark EDM and the quark and gluon color EDM from the H_1^0 and a_1 are small. The contributions to the neutron EDM are about the same from the H_1^0 , a_2 , and $H_{2,3}^0$, a_1 exchange, with different mixing factors. Explicitly as an example, for the case H_1^0 and a_2 exchange, we take the Higgs mass $m_{H_1^0}$ to be around 1TeV , which is obtained from $K^0 - \overline{K}^0$ mixing terms. It leads to

$$d_n \approx -8 \times 10^{-27} \frac{m_{H_1^0 a_2}^2}{m_{H_1^0}^2 - m_{a_2}^2} e \text{ cm} . \quad (3.52)$$

If $m_{H_1^0 a_2}^2$ is not too much smaller than $m_{H_2^0 a_1}^2$ and $m_{H_3^0 a_1}^2$, the neutron EDM can be close to the experimental upper bound.

Model (a-KM): We just take $v_1 = v_2 = v_3$ in this model, and for Higgs mass it can be around 100GeV since there is no constraint on it from meson mixing. The nEDM contribution coming from $H_1^0 - a_2$ mixing is given by

$$d_n \approx 7 \times 10^{-26} \frac{m_{H_1^0 a_2}^2}{m_{H_1^0}^2 - m_{a_2}^2} e \text{ cm} . \quad (3.53)$$

Model (b-KM): As in the M-parametrization case, the contributions from the H_1^0 and a_1 exchange are small. With the parameters $v_1 = v_2 = v_3$ and $m_{H_1^0} \approx 100\text{GeV}$

from $B_s - \overline{B}_s$ mixing, the nEDM contribution coming from $H_1^0 - a_2$ mixing is given by

$$d_n \approx 6 \times 10^{-26} \frac{m_{H_1^0 a_2}^2}{m_{H_1^0}^2 - m_{a_2}^2} e \text{ cm} . \quad (3.54)$$

All the results for neutron EDM given in the above are close to the experimental upper bound in the present.

In summary, with the fixed Yukawa couplings in our model, we can constrain the Higgs mass $m_{H_1^0}$ or m_{a_1} from different type of neutral meson mixing. The neutron EDM in our model can also be close to the current experiment upper bounds, with the Higgs mass constrained from the neutral meson mixing.

We have proposed a model that the CP violating phase in the CKM mixing matrix be the same as that causing spontaneous CP violation in the Higgs potential. Specific multi-Higgs doublet models have been constructed to realize this idea. In our previous discussions, we have not considered Yukawa coupling for the lepton sector. An analogous study will be carried out in the next section.

3.3 SCPV and PMNS matrix

In this section, we will apply the idea in the previous section for quark sector to the lepton sector. Also in order to have non-zero neutrino masses in the model, we need to introduce the right-handed neutrinos. The main different feature for the lepton sector is that the Majorana mass term of the right-handed neutrino is allowed. It will make the progress more difficult since we need to apply the seesaw mechanism to relate the Dirac mass with heavy and light neutrino masses. We will take the models built for quark sector in the last section, and extend them to the lepton sector, for both Model (a) and Model (b).

3.3.1 Identifying PMNS matrix phase with SCPV phase

First of all, we assign the PQ charges of leptons in two types of model for quarks discussed previously as follows

$$\begin{aligned} \text{Model (a): } & L_L(0), l_R(-1), N_R(-1), \\ \text{Model (b): } & L_L(0), l_R(+1), N_R(+1). \end{aligned} \quad (3.55)$$

The Yukawa couplings satisfying the above PQ symmetry are given by

$$\begin{aligned} \text{Model(a): } \mathcal{L} &= \overline{L}_L(Y_1 H_1 + Y_2 H_2 e^{i\delta}) N_R + \overline{L}_L Y_3 \tilde{H}_3 l_R + \overline{(N_R)^c} Y_s S N_R + \text{h.c.}; \\ \text{Model(b): } \mathcal{L} &= \overline{L}_L Y_3 \tilde{H}_3 N_R + \overline{L}_L(Y_1 \tilde{H}_1 + Y_2 \tilde{H}_2 e^{-i\delta}) l_R + \overline{(N_R)^c} Y_s S^\dagger N_R + \text{h.c.}, \end{aligned} \quad (3.56)$$

where $Y_{1,2,3}$ are 3×3 real matrices, and Y_s can be chosen to be real in general. For the lepton sector the Higgs singlet S is also coupled to the right-handed neutrinos. After spontaneous symmetry breaking, the relevant lepton mass terms are shown as

$$\mathcal{L} = -\bar{l}_L M_l l_R - \bar{\nu}_L M_D N_R - \frac{1}{2} \overline{(N_R)^c} M_R N_R + \text{h.c.}; \quad (3.57)$$

with M_l , M_D , and M_R defined by

$$\begin{aligned} \text{Model (a): } \quad & M_l = -\frac{1}{\sqrt{2}} Y_3 v_3, \quad M_D = -\frac{1}{\sqrt{2}} (Y_1 v_1 + Y_2 v_2 e^{i\delta}), \quad M_R = -\sqrt{2} Y_s v_s; \\ \text{Model (b): } \quad & M_l = -\frac{1}{\sqrt{2}} (Y_1 v_1 + Y_2 v_2 e^{-i\delta}), \quad M_D = -\frac{1}{\sqrt{2}} Y_3 v_3, \quad M_R = -\sqrt{2} Y_s v_s. \end{aligned} \quad (3.58)$$

To get neutrino masses, we express the neutrino mass terms in the usual mass matrix for seesaw mechanism, and it is convenient to define the 6×6 mass matrix

$$M_{\text{seesaw}} = \begin{pmatrix} 0 & M_D^* \\ M_D^\dagger & M_R \end{pmatrix}. \quad (3.59)$$

Note that since $v_s \gg v_1, v_2$, the M_R should also be larger than M_D . We can apply the seesaw mechanism (discussed in Sec. 4.1 and Appendix B) to our model. Then we obtain the familiar relation

$$M_D \hat{M}_N^{-1} M_D^T = -V_L^{\nu\dagger} \hat{M}_\nu V_L^{\nu*} = (iV_L^{\nu\dagger}) \hat{M}_\nu (iV_L^{\nu*}), \quad (3.60)$$

where \hat{M}_N is the 3×3 diagonal matrix with three heavy eigenvalues of M_{seesaw} as its diagonal elements, and \hat{M}_ν is the three light neutrino diagonal mass matrix. V_L^ν is the transformation matrix to transform the weak eigenstate ν_L into mass eigenstate. The general solution for M_D of Eq. (3.60) is given by [70]

$$M_D = (iV_L^{\nu\dagger})\hat{M}_\nu^{1/2}O\hat{M}_N^{1/2}, \quad (3.61)$$

where O is a arbitrary complex matrix satisfying $OO^T = 1$. It is difficult to determine the explicit form of O , so we will take it identity in the following.

In Model(a), in the mass basis of charged leptons, the Dirac mass matrix for neutrinos are given by

$$M_D = M_{D1} + M_{D2}e^{i\delta} = V_{\text{PMNS}}\hat{M}_\nu^{1/2}O\hat{M}_N^{1/2}. \quad (3.62)$$

The right-handed side of the above equation is more complicated than its analogue, Eq. (3.21) for quark sector, since there are more than one complex phases which are required to be considered there. In general V_{PMNS} has a Dirac phase and two Majorana phases. It is also not easy to decompose and parametrize the complex orthogonal matrix O into the addition of two matrix with a uniform related phase. Here we will just consider the PMNS matrix with the Dirac phase existing in the model. As a first example we express the PMNS matrix in the modified standard parametrization

$$V_{\text{PMNS}}^{\text{M}} = \begin{pmatrix} c_{12}^\ell c_{13}^\ell e^{i\delta_{13}^\ell} & s_{12}^\ell c_{13}^\ell e^{i\delta_{13}^\ell} & s_{13}^\ell \\ -s_{12}^\ell c_{23}^\ell - c_{12}^\ell s_{23}^\ell s_{13}^\ell e^{i\delta_{13}^\ell} & c_{12}^\ell c_{23}^\ell - s_{12}^\ell s_{23}^\ell s_{13}^\ell e^{i\delta_{13}^\ell} & s_{23}^\ell c_{13}^\ell \\ s_{12}^\ell s_{23}^\ell - c_{12}^\ell c_{23}^\ell s_{13}^\ell e^{i\delta_{13}^\ell} & -c_{12}^\ell s_{23}^\ell - s_{12}^\ell c_{23}^\ell s_{13}^\ell e^{i\delta_{13}^\ell} & c_{23}^\ell c_{13}^\ell \end{pmatrix}, \quad (3.63)$$

where the angles and phases belong to the lepton mixing matrix. Make the crucial assumption $\delta_{13}^\ell = \delta$, and then we have $\delta_{13}^\ell = -\delta_{13} = -(69 \pm 4)^\circ$, where the last step comes from the assumption in quark sector. The magnitudes of the phase in CKM and PMNS matrices are then identical. The mass matrices M_{D1} and M_{D2} can be

obtained as follows

$$M_{D1}^M = \begin{pmatrix} 0 & 0 & s_{13}^\ell \\ -s_{12}^\ell c_{23}^\ell & c_{12}^\ell c_{23}^\ell & s_{23}^\ell c_{13}^\ell \\ s_{12}^\ell s_{23}^\ell & -c_{12}^\ell s_{23}^\ell & c_{23}^\ell c_{13}^\ell \end{pmatrix} \hat{M}_\nu^{1/2} O \hat{M}_N^{1/2}, \quad (3.64)$$

$$M_{D2}^M = \begin{pmatrix} c_{12}^\ell c_{13}^\ell & s_{12}^\ell c_{13}^\ell & 0 \\ -c_{12}^\ell s_{23}^\ell s_{13}^\ell & -s_{12}^\ell s_{23}^\ell s_{13}^\ell & 0 \\ -c_{12}^\ell c_{23}^\ell s_{13}^\ell & -s_{12}^\ell c_{23}^\ell s_{13}^\ell & 0 \end{pmatrix} \hat{M}_\nu^{1/2} O \hat{M}_N^{1/2}. \quad (3.65)$$

Since in this model we can determine the PMNS matrix phase, which is identical to CKM matrix phase up to a minus sign, the Jarlskog, the rephasing invariant of PMNS matrix can also be predicted. By using the fitting angles and mass square differences with 1σ in Ref. [6]

$$\sin^2 \theta_{12}^\ell = 0.312_{-0.015}^{+0.018}, \quad \sin^2 \theta_{23}^\ell = 0.42_{-0.03}^{+0.08}, \quad \sin^2 \theta_{13}^\ell = 0.0251 \pm 0.0034, \\ \Delta m_{21}^2 = (7.58_{-0.26}^{+0.22}) \times 10^{-5} \text{eV}^2, \quad |\Delta m_{32}^2| = (2.35_{-0.09}^{+0.12}) \times 10^{-3} \text{eV}^2, \quad (3.66)$$

we obtain directly $J^\ell(M) = -(0.033 \pm 0.002)$.

The KM-parametrization for PMNS matrix can also be taken as another example

$$V_{\text{PMNS}}^{\text{KM}} = \begin{pmatrix} c_1^\ell & -s_1^\ell c_3^\ell & -s_1^\ell s_3^\ell \\ s_1^\ell c_2^\ell & c_1^\ell c_2^\ell c_3^\ell - s_2^\ell s_3^\ell e^{i\delta^\ell} & c_1^\ell c_2^\ell s_3^\ell + s_2^\ell c_3^\ell e^{i\delta^\ell} \\ s_1^\ell s_2^\ell & c_1^\ell s_2^\ell c_3^\ell + c_2^\ell s_3^\ell e^{i\delta^\ell} & c_1^\ell s_2^\ell s_3^\ell - c_2^\ell c_3^\ell e^{i\delta^\ell} \end{pmatrix}. \quad (3.67)$$

With the assumption parallel to the modified standard parametrization case, $\delta^\ell = \delta = -(91 \pm 4)^\circ$, the mass matrices $M_{D1,2}$ are obtained directly and given by

$$M_{D1}^{\text{KM}} = \begin{pmatrix} c_1^\ell & -s_1^\ell c_3^\ell & -s_1^\ell s_3^\ell \\ s_1^\ell c_2^\ell & c_1^\ell c_2^\ell c_3^\ell & c_1^\ell c_2^\ell s_3^\ell \\ s_1^\ell s_2^\ell & c_1^\ell s_2^\ell c_3^\ell & c_1^\ell s_2^\ell s_3^\ell \end{pmatrix} \hat{M}_\nu^{1/2} O \hat{M}_N^{1/2}, \quad (3.68)$$

$$M_{D2}^{\text{KM}} = \begin{pmatrix} 0 & 0 & 0 \\ 0 & -s_2^\ell s_3^\ell & s_2^\ell c_3^\ell \\ 0 & c_2^\ell s_3^\ell & -c_2^\ell c_3^\ell \end{pmatrix} \hat{M}_\nu^{1/2} O \hat{M}_N^{1/2}. \quad (3.69)$$

In order to obtain the Jaroskog J_{KM}^ℓ it is necessary to know the three mixing angles in KM parametrization. The corresponding angles can be obtained from the magnitudes $|V_{e1}|$, $|V_{e2}|$, and $|V_{e3}|$ with the input parameters from Eq. (3.66). We get

$$\sin \theta_1^\ell = 0.57 \pm 0.02, \quad \sin \theta_3^\ell = 0.28 \pm 0.02. \quad (3.70)$$

The derived phase δ^ℓ given from the assumption with the above two angles can help to determine the last angle from the magnitudes $|V_{\mu 3}|$ and $|V_{\tau 3}|$. The result is given by

$$\sin \theta_2^\ell = 0.64 \pm 0.07, \quad (3.71)$$

The rephasing invariant of PMNS matrix then is obtained as $J^\ell(\text{KM}) = -(0.035 \pm 0.003)$ by using the above derived values for mixing angles and phase. We emphasize that the above two ways of parametrizing the mixing matrices are two different ways. In principle measurement of J can be used to distinguish different models, but the difference is small making it practically difficult.

The probe of neutrinoless double beta decay is one of the useful processes to observe the exist of Majorana neutrinos. With the central values of PMNS parameters for M- and KM-parametrization and the central value of mass square differences in Eq. (3.66), We plot the effective Majorana mass $\langle m_{\beta\beta} \rangle = |\sum_i m_{\nu_i} V_{ei}^2|$ as a function of the light neutrino mass m_{ν_1} for the normal hierarchy in Fig. 3.1. The range of m_{ν_1} is taken from 0 to 0.088, which satisfies one of the stringent cosmological constraints $\sum_i m_{\nu_i} < 0.28\text{eV}$ for the model $\Lambda\text{CDM} + m_\nu$ [72]. Here we emphasize that the two different PMNS matrix parametrization lead to different models. It explains why there is some deviation between two parametrization for $\langle m_{\beta\beta} \rangle$. However, the tiny deviation results in the difficulty to distinguish them by the future experiments.

Another quantity related to neutrino mass is $\langle m_{\nu_e} \rangle = (\sum_i m_{\nu_i}^2 |V_{ei}|^2)^{1/2}$, which can be measured in tritium decay. This quantity is the same for the two models we considered above. With the central values for mixing angles, it is given by 0.089 eV for a normal hierarchy, with $m_{\nu_1} = 0.089\text{ eV}$ taken to approach the upper bound on the sum of light neutrino masses, for example. For an inverted hierarchy with the

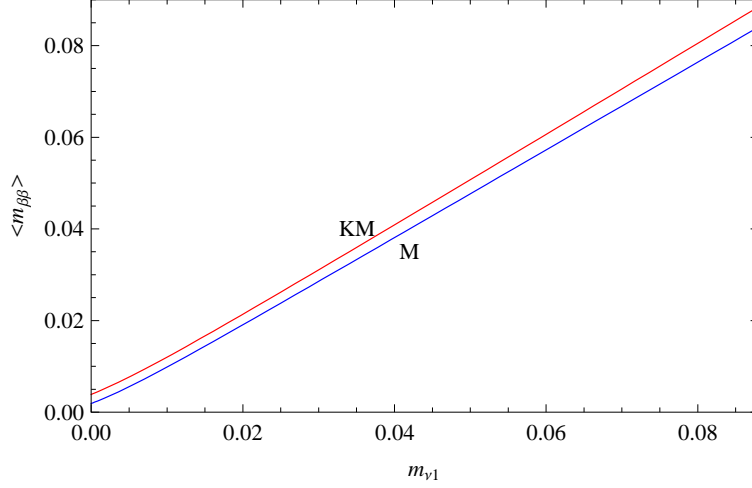


Figure 3.1: Comparison of Model (a-M) and Model (a-KM) by $\langle m_{\beta\beta} \rangle$ as a function of light neutrino mass m_{ν_1} .

same m_{ν_1} , we get almost the same results as we have in a normal hierarchy. This quantity is again not useful in distinguishing different models considered above.

For Model (b), the charged leptons are coupled by two Higgs doublets. The form of Dirac mass matrix for neutrinos in this model is simpler than that in Model (a). The lepton sector of Model (b) can completely parallel the quark sector of this model. For simplicity we will work in a basis with $V_L^\nu = i$. The Dirac mass term is given by

$$M_D = \hat{M}_\nu^{1/2} O \hat{M}_N^{1/2}. \quad (3.72)$$

Again, O is arbitrary matrix satisfying $OO^\dagger = 1$. The charged lepton mass matrix is given by

$$M_l = M_{l1} + M_{l2} e^{-i\delta} = V_{\text{PMNS}}^\dagger \hat{M}_l. \quad (3.73)$$

Taking the M-parametrization in the basis $V_{\text{PMNS}} = -iV_L^l$, we apply the same idea in Model (a) that the Dirac phase δ_{13}^ℓ is identified with δ , and the mass matrices are obtained directly as

$$M_{l1}^{\text{M}} = \begin{pmatrix} 0 & -s_{12}^\ell c_{23}^\ell & s_{12}^\ell s_{23}^\ell \\ 0 & c_{12}^\ell c_{23}^\ell & -c_{12}^\ell s_{23}^\ell \\ s_{13}^\ell & s_{23}^\ell c_{13}^\ell & c_{23}^\ell c_{13}^\ell \end{pmatrix} \hat{M}_l; \quad (3.74)$$

$$M_{l2}^M = \begin{pmatrix} c_{12}^\ell c_{13}^\ell & -c_{12}^\ell s_{23}^\ell s_{13}^\ell & -c_{12}^\ell c_{23}^\ell s_{13}^\ell \\ s_{12}^\ell c_{13}^\ell & -s_{12}^\ell s_{23}^\ell s_{13}^\ell & -s_{12}^\ell c_{23}^\ell s_{13}^\ell \\ 0 & 0 & 0 \end{pmatrix} \hat{M}_l. \quad (3.75)$$

Similarly, the KM-parametrization with $\delta^\ell = \delta$ will lead to

$$M_{l1}^{KM} = \begin{pmatrix} c_1^\ell & s_1^\ell c_2^\ell & s_1^\ell s_2^\ell \\ -s_1^\ell c_3^\ell & c_1^\ell c_2^\ell c_3^\ell & c_1^\ell s_2^\ell c_3^\ell \\ -s_1^\ell s_3^\ell & c_1^\ell c_2^\ell s_3^\ell & c_1^\ell s_2^\ell s_3^\ell \end{pmatrix} \hat{M}_l, \quad (3.76)$$

$$M_{l2}^{KM} = \begin{pmatrix} 0 & 0 & 0 \\ 0 & -s_2^\ell s_3^\ell & c_2^\ell s_3^\ell \\ 0 & s_2^\ell c_3^\ell & -c_2^\ell c_3^\ell \end{pmatrix} \hat{M}_l. \quad (3.77)$$

The mass matrices only depend on charged lepton masses and mixing angles. The Jarlskog invariant in Model (b) is identical to that in Model (a).

The choices of $O = I$ and $V_R = i$ in Model (b) are by assumptions. it would be interesting to see if models with some symmetries can naturally give such options. We have not been able to find a model to achieve this. Our choices should only be taken as some particular working ansatz.

3.3.2 Effect on Charged Lepton Flavor Violating Processes

The different ways to identify the CP violating phase from the lepton mixing matrix with that from the the spontaneous symmetry breaking sector also restrict the forms of the Yukawa couplings in the model differently. New interactions due to Higgs exchange can generate some interesting phenomena. The Yukawa couplings for Model (a) and Model (b) are given by

$$\begin{aligned} \text{Model (a): } \mathcal{L}_{lh^0} &= -\bar{l}_L \hat{M}_l l_R \left[\frac{v_{12}^2 v_s}{N_A v_3} (H_2^0 - ia_2) + \frac{1}{v} H_3^0 + v_{12}^2 / N_a (H_4 - ia) \right] + \text{h.c.} , \\ \text{Model (b): } \mathcal{L}_{lh^0} &= -\bar{l}_L \left(-\frac{v_1}{v_2 v_{12}} \hat{M}_l + \frac{v_{12}}{v_1 v_2} V_{\text{PMNS}} M_{l1} \right) l_R (H_1^0 - ia_1) \\ &\quad + \bar{l}_L \hat{M}_l l_R \left[\frac{v_3 v_s}{N_A} (H_2^0 - ia_2) - \frac{1}{v} H_3^0 + \frac{v_3^2}{N_a} (H_4 - ia) \right] + \text{h.c.} . \end{aligned} \quad (3.78)$$

There is no FCNC process for charged leptons in Model (a). In contrast, there exists tree level FCNC interaction for charged leptons when coupling with H_1^0 and a_1 in the Model (b), which can be expressed by only mixing angles and charged lepton masses

$$\begin{aligned}
V_{\text{PMNS}}^{\text{M}} M_{l1}^{\text{M}} &= \begin{pmatrix} (s_{13}^\ell)^2 & s_{23}^\ell s_{13}^\ell c_{13}^\ell & c_{23}^\ell s_{13}^\ell c_{13}^\ell \\ s_{23}^\ell s_{13}^\ell c_{13}^\ell & (c_{23}^\ell)^2 + (s_{23}^\ell)^2 (c_{13}^\ell)^2 & -s_{23}^\ell c_{23}^\ell s_{13}^2 \\ c_{23}^\ell c_{13}^\ell s_{13}^\ell & -s_{23}^\ell c_{23}^\ell (s_{13}^\ell)^2 & (s_{23}^\ell)^2 + (c_{23}^\ell)^2 (c_{13}^\ell)^2 \end{pmatrix} \hat{M}_l, \\
V_{\text{PMNS}}^{\text{KM}} M_{l1}^{\text{KM}} &= \begin{pmatrix} 1 & 0 & 0 \\ 0 & (c_2^\ell)^2 & c_2^\ell s_2^\ell \\ 0 & c_2^\ell s_2^\ell & (s_2^\ell)^2 \end{pmatrix} \hat{M}_l.
\end{aligned} \tag{3.79}$$

For Model (b-M), Yukawa coupling constants for $\tau - e$ interaction and $\tau - \mu$ interaction are larger than $e - \mu$ interaction, while in Model (b-KM), only $\tau - e$ interaction exists, with other two coupling constants vanish at tree level. Present experiments provide tight constraints on $l_i \rightarrow l_1 \bar{l}_2 l_3$, which are listed as follows

$$\begin{aligned}
\text{Br}(\tau \rightarrow e \bar{e} e)_{\text{exp}} &< 3.6 \times 10^{-8} [73], \text{Br}(\tau \rightarrow \mu \bar{\mu} \mu)_{\text{exp}} < 3.2 \times 10^{-8} [73], \\
\text{Br}(\tau \rightarrow \mu \bar{e} e)_{\text{exp}} &< 2.7 \times 10^{-8} [73], \text{Br}(\tau \rightarrow e \bar{\mu} \mu)_{\text{exp}} < 3.7 \times 10^{-8} [74], \\
\text{Br}(\tau \rightarrow \mu \bar{e} \mu)_{\text{exp}} &< 2.3 \times 10^{-8} [73], \text{Br}(\tau \rightarrow e \bar{\mu} e)_{\text{exp}} < 2.0 \times 10^{-8} [73], \\
\text{Br}(\mu \rightarrow e \bar{e} e)_{\text{exp}} &< 1.0 \times 10^{-12} [75].
\end{aligned} \tag{3.80}$$

In the following we study these decay modes in more detail to see if it is also possible to distinguish Model (b-M) and Model (b-KM). If H_1 is the lightest higgs boson, then the tree level contribution with H_1^0 exchanged should dominate the above processes. As an illustration, take $v_{1,2} \ll v_3$, with $v_{1,2}$ are of order a few GeV, and $H_1^0 = 100\text{GeV}$, with flavor mixing angles chosen to the central values given previously for each kind of parametrization, we plot in Fig 3.2 to show the allowed regions in v_1 - v_2 plane constrained by the above lepton flavor violating processes. For Model (b-M), all $l_i \rightarrow l_1 \bar{l}_2 l_3$ processes can constrain v_1 and v_2 . The most stringent constraints come from the $\tau \rightarrow e \bar{\mu} \mu$ and $\mu \rightarrow e \bar{e} e$ current experimental upper bounds, for which $v_1 > 10\text{ GeV}$ and $v_2 > 3\text{ GeV}$. For Model (b-KM), only $\tau \rightarrow \mu \bar{\mu} \mu$

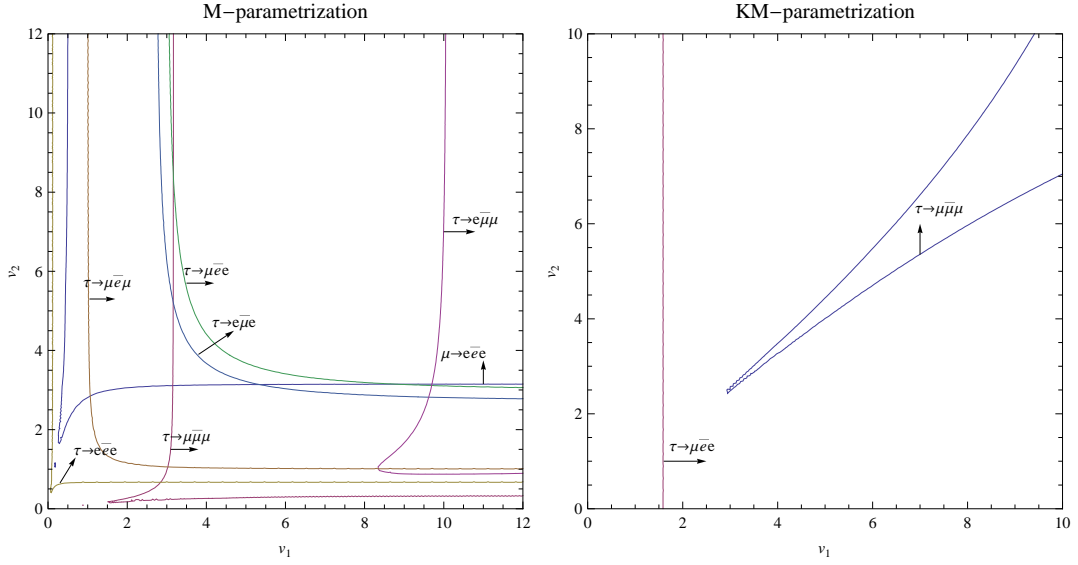


Figure 3.2: The allowed range in $v_{1,2}$ plane constrained by $\mu \rightarrow e\bar{e}e$ and $\tau \rightarrow l_1\bar{l}_2l_3$, where M- and KM- indicate the modified standard parametrization and KM parametrization, respectively.

and $\tau \rightarrow \mu\bar{e}e$ can constrain $v_{1,2}$, and the present $\tau \rightarrow \mu\bar{\mu}\mu$ upper bound leads to the most severe limit. The future experimental signals for any of the processes, for example, $\mu \rightarrow e\bar{e}e$ at MUSIC [115], may help to fix the $v_{1,2}$ or rule out these models if no intersection allowed among these curves.



Chapter 4

Higgs Decay in Large Heavy-Light Mixing Seesaw Model

The observation of neutrino oscillation forces the SM to be extended in order to have the massive active neutrinos. The simplest way to extend the SM is to add the right-handed gauge singlet fermions. The seesaw mechanism can be applied if the Majorana mass term of the gauge singlet fermions is allowed. The seesaw mechanism explains the light neutrino mass successfully by taking the very huge Majorana mass for the right-handed neutrinos, but these heavy neutrinos are too heavy to be detected at LHC, and the related heavy-light mixing is also too small. A specific type of seesaw mechanism with large heavy-light mixing might be possibly verified in the future experiments. The search of Higgs decay is a good way to prove such kind of seesaw models. In this chapter we will introduce briefly the Higgs decay channels in the SM, and then discuss the type-I and type-III seesaw with the large heavy-light mixing and the corresponding effect on Higgs decay.

4.1 Higgs Decay

The probing of Higgs decay is a direct way to search the existence of Higgs. The study of the Higgs decay in the SM and in many other models have been performed in detailed in many years. We will follow the discussion of Higgs decay from Ref. [76]

in this section. In the SM the related Lagrangian is shown as

$$\begin{aligned}\mathcal{L}_h = & \frac{1}{2}(\partial_\mu h)(\partial^\mu h) - \frac{1}{2}m_h^2 h^2 - \frac{3m_h^2 h^3}{v \cdot 3!} - \frac{3m_h^2 h^4}{v^2 \cdot 4!} + \frac{1}{2}\left(\frac{2m_Z^2}{v}h + \frac{m_Z^2}{v^2}h^2\right)Z_\mu^0 Z^{0\mu} \\ & + \left(\frac{2m_W^2}{v}h + \frac{m_W^2}{v^2}h^2\right)W_\mu^+ W^{\mu-} - \frac{h}{v} \sum_f m_f \bar{f} f, \quad (4.1)\end{aligned}$$

where the couplings $h-f-\bar{f}$ are proportional to fermion mass; $h-V-V$ and $h-h-V-V$ are proportional to m_V^2 . The two body decay channels and the corresponding subsequent channels are dominant Higgs decay processes. In theoretical point of view, all possible Higgs decay channels can be predicted for different choice of m_h . The main channel of Higgs decay are the two body decays $h \rightarrow f\bar{f}$ and $h \rightarrow VV$, with V can be on-shell or off-shell massive gauge boson.

One of Higgs decay channels is of the type $h \rightarrow f\bar{f}$, the Higgs decay into two fermions. Tree level diagrams dominate these type of processes. Since the relevant Yukawa coupling is proportional to the fermion mass m_f , $h \rightarrow b\bar{b}$ should be dominant mode among these type of decay rates if $m_h \lesssim 130\text{GeV}$. The tree level formula related to this type of processes is given by [76]

$$\Gamma(h \rightarrow f\bar{f}) = \frac{3G_F}{4\sqrt{2}\pi} m_h m_f^2 (1 - 4m_f^2/m_h^2)^{3/2}. \quad (4.2)$$

The $h \rightarrow VV$ channels, with V to be the gauge boson W or Z are important and dominated for $m_h \gtrsim 150\text{GeV}$. In the SM the decay channels $h \rightarrow WW$ and $h \rightarrow ZZ$ occur at tree level. If the Higgs mass is less than $2m_W$ or $2m_Z$, then the corresponding channel $h \rightarrow VV$ will become off-shell and it will lead to a three or four body decay. The two body decay is given by [76]

$$\Gamma(h \rightarrow VV) = \frac{G_F m_h^3}{16\sqrt{2}\pi} \delta_V \sqrt{1 - 4x} (1 - 4x + 12x^2), \quad x = \frac{m_V^2}{m_h^2}, \quad (4.3)$$

where for W boson $\delta_W = 2$ and for Z boson $\delta_Z = 1$.

The $h \rightarrow \gamma\gamma$ can provide cleaner signal to probe physics beyond the SM, although its leading order contribution from one loop processes is small. $h \rightarrow gg$ is the process which could be found from analysis of jets including hadronic final states at LHC. We can summarize this section by Fig. 4.1, in which the plots of the Higgs branching

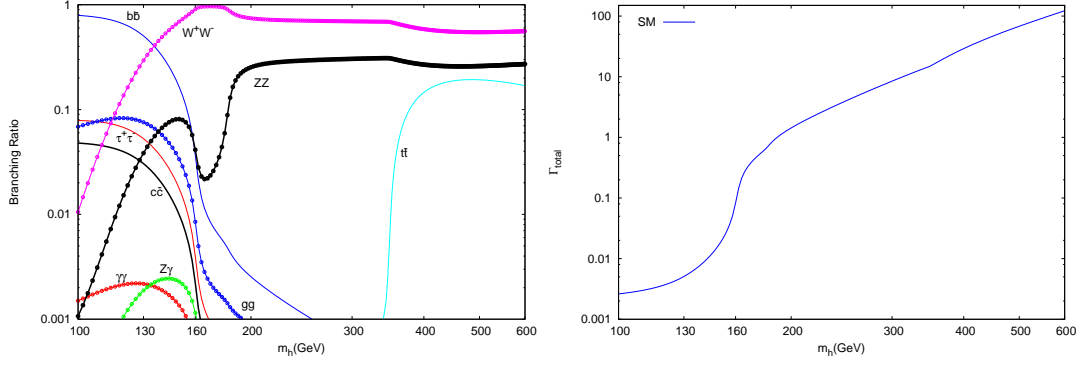


Figure 4.1: The left panel is the mainly branching ratios of the Higgs decay channels as a function of m_h , and the right panel is the total decay rate of Higgs as a function of m_h . The numerical results is calculated by the package HDECAY [81].

ratios and total decay rate versus m_h are given, with numerical results calculated by HDECAY [81]. Note that $h \rightarrow W^+W^-$ and $h \rightarrow ZZ$ have already included the subsequent three body decays and four body decays. From the right panel of the figure, for $100\text{GeV} < m_h < 130\text{GeV}$ the total decay rate is about $0.02 \sim 0.04\text{GeV}$, with the channel $h \rightarrow b\bar{b}$ dominated; for $130\text{GeV} < m_h < 160\text{GeV}$, the two body decay $h \rightarrow W^+W^-$ channel are almost open and dominates over other channels. For $160 < m_h < 180\text{GeV}$, Γ_h is around $0.08\text{GeV} \sim 0.6\text{GeV}$ with the open of the decay channel $h \rightarrow Z^0Z^0$. Finally, $h \rightarrow t\bar{t}$ channel will be open at $m_h \gtrsim 300\text{GeV}$.

4.2 Type-I Seesaw

4.2.1 Introduction

Type-I seesaw is the original and simplest seesaw model, in which one or more gauge singlet fermions are introduced into the SM [77]. It will induce not only the Dirac neutrino mass term but also a Majorana mass term which will violate the lepton number conservation. In the following and later we will focus on models with three such fermions included. In type-I seesaw the new interaction beyond the SM

is shown as

$$\mathcal{L}_{\text{new}} = \overline{N_R} i \not{D} N_R - [\overline{L_L} Y_R \tilde{H} N_R - \frac{1}{2} \overline{N_R^c} \hat{M}_R N_R + \text{h.c.}] , \quad (4.4)$$

where \hat{M}_R is the Majorana mass matrix, which can be transformed by a unitary matrix into real diagonal form in general. After spontaneous symmetry breaking, the relevant neutrino mass terms is given by

$$\mathcal{L}_{\text{mass}} = -\overline{L_L} M_D N_R - \frac{1}{2} \overline{N_R^c} \hat{M}_R N_R + \text{h.c.} , \quad (4.5)$$

where $M_D = (v/\sqrt{2})Y_R$ are 3×3 Dirac mass matrices. By re-arranging the above formula, we obtain

$$\mathcal{L}_{\text{mass}} = -\frac{1}{2} (\overline{\nu_L}, \overline{N_R^c}) M_{\text{seesaw}}^\dagger \begin{pmatrix} \nu_L^c \\ N_R \end{pmatrix} + \text{h.c.} , \quad (4.6)$$

where M_{seesaw} is defined as a 6×6 matrices

$$M_{\text{seesaw}} = \begin{pmatrix} 0 & M_D^* \\ M_D^\dagger & \hat{M}_R \end{pmatrix} = \begin{pmatrix} 0 & m_D^T \\ m_D & \hat{M}_R \end{pmatrix} , \text{ with } m_D = M_D^\dagger. \quad (4.7)$$

In order to diagonalize M_{seesaw} , we define the transformation matrix U by the left-handed fermions redefinition

$$\begin{pmatrix} \hat{M}_\nu & 0 \\ 0 & \hat{M}_N \end{pmatrix} = U^T M_{\text{seesaw}} U , \text{ with } U \text{ is defined as}$$

$$\begin{pmatrix} \nu_L \\ (N_R)^c \end{pmatrix} = U \begin{pmatrix} \nu_{mL} \\ N_{mL} \end{pmatrix} = \begin{pmatrix} U_{\nu\nu} & U_{\nu N} \\ U_{N\nu} & U_{NN} \end{pmatrix} \begin{pmatrix} \nu_{mL} \\ N_{mL} \end{pmatrix} , \quad (4.8)$$

where $U_{\nu\nu} \equiv V_L^{\nu\dagger}$ is approximately unitary, and $\hat{M}_{\nu,N}$ are diagonalized mass matrices for light and heavy neutrino mass eigenstates, respectively. From the above equation we directly obtain the following relation

$$U_{\nu\nu} \hat{M}_\nu U_{\nu\nu}^T = -U_{\nu N} \hat{M}_N U_{\nu N}^T . \quad (4.9)$$

The above formula provides us an important information, that is, if $U_{\nu\nu}$ is of order $\mathcal{O}(1)$, then $U_{\nu N}$ should be of the order $(m_\mu/m_N)^{1/2}$. According to the procedure in Appendix B we get the following relation

$$-M_D \hat{M}_N^{-1} M_D^T \simeq U_{\nu\nu} \hat{M}_\nu U_{\nu\nu}^T . \quad (4.10)$$

This is the famous seesaw relation. The heavy neutrino mass can generate a very light neutrino mass, like a “seesaw”. In the other hand, the scale of the light neutrino also sets the lower bound for the heavy neutrino mass to be around hundreds GeV to TeV scale, even if M_D is set to be 1MeV. The next section will provide an interesting and special way to circumvent the constraints from Eq. (4.10), or in equivalence from Eq. (4.9).

4.2.2 Heavy-Light Large Mixing

Type-I seesaw has solved the problem about the origin of the very light active neutrino mass. The observation of light neutrino masses also provides the lower bounds of heavy neutrino masses. By looking at Eq. (4.9), we find that the order of magnitude of elements in $U_{\nu N}$ should be about $(m_\nu/m_N)^{1/2}$, which is too small to be proved in the experiment such like LHC. In the presence of more than one generation of light and heavy neutrinos, there are circumstances in which the mixing can be much larger [82, 83, 84], offering greater hope of observing its effects on various processes. The combination of such large mixing, with $m_N \sim 100$ GeV, and the tiny light-neutrino masses can occur naturally if the underlying theory has some symmetry that is slightly broken [84]. Ref. [85] provides a special type of $U_{\nu N}$, which can be large and evade the limitation from Eq. (4.9). We will show how to achieve it in the following. Consider the heavy-light mixing $U_{\nu N}$ which is expressed in the sum of a dominant part U_0 and a small perturbation U_δ , which is given by [85]

$$U_{\nu N} = U_0 + U_\delta . \quad (4.11)$$

It is also assumed that U_0 satisfying the equation [85]

$$U_0 \hat{M}_N U_0^T = (U_0 \hat{M}_N^{1/2})(U_0 \hat{M}_N^{1/2})^T = 0 , \quad (4.12)$$

in which U_0 can be of arbitrary unlimited size. The next step is to find the general solution for such a U_0 . It is convenient to consider the rank of the matrix $K = U_0 \hat{M}_N^{1/2}$. From mathematical analysis we know that K can not be of rank three because there is no such a nonzero vector whose hermitian products with all elements

of a basis are all vanished. If K is of rank two, then the corresponding orthogonal space should be of only dimension 1, but this conflicts with the fact that the rank of K should be equal to that of K^T . So the only possible choice is a rank-1 one matrix for K . This means that U_0 should be also of rank one if \hat{M}_N is of rank-3.

Since K satisfying $KK^T = 0$, with the understanding that K is a rank-1 matrix, in general K can be expressed in the form

$$K \propto \begin{pmatrix} a \mathbf{v}^T \\ b \mathbf{v}^T \\ c \mathbf{v}^T \end{pmatrix}, \text{ where } a, b, c \in \mathbb{C}, \quad (4.13)$$

with \mathbf{v} a 3×1 complex column vector satisfying $\mathbf{v}^T \mathbf{v} = 0$. This form of K helps us to get the form of U_0 as follows [85]

$$U_0 = \begin{pmatrix} a \mathbf{v}^T \\ b \mathbf{v}^T \\ c \mathbf{v}^T \end{pmatrix} \cdot \mathcal{R} \text{ with } \mathcal{R} = \text{diag}(\sqrt{\frac{m_N}{M_1}}, \sqrt{\frac{m_N}{M_2}}, \sqrt{\frac{m_N}{M_3}}), \quad (4.14)$$

where $M_{1,2,3}$ are the masses of heavy neutrinos, and we can take m_N to be the smallest of $M_{1,2,3}$. The parameters a, b , and c and the perturbation term U_δ are constrained by the experimental results of neutrino mass square differences Δm_{ij}^2 . the detail is given in Appendix C. We will use the scenario of large $U_{\nu N}$ to investigate the Higgs decay in the following.

4.2.3 $h \rightarrow \nu N$

From the idea of Section 4.2.2, there is a special structure of $U_{\nu N}$ which can make the magnitudes of its elements become larger than before. Some of the effect and implication has been discussed in Ref. [85]. In this chapter, we will focus on the effect of such a large $U_{\nu N}$ on Higgs decay, and also the related implications.

In Type-I seesaw, The SM Higgs decay width increases by the channels in which the final states includes a light neutrino and a heavy neutrino. The amplitude of such a process is given by

$$\mathcal{M}(h \rightarrow \nu_i N_j) = \frac{g_2 M_j}{2m_W} \bar{u}_\nu [(U_{\nu\nu}^T U_{\nu N}^*)_{ij} P_L + (U_{\nu\nu}^\dagger U_{\nu N})_{ij} P_R] v_N, \quad (4.15)$$

where M_j is the mass of heavy neutrino N_j ; v_N and u_ν are the 4-spinors of heavy and light neutrino, respectively. The projection operators in Dirac space are defined by $P_L \equiv (1 - \gamma_5)/2$ and $P_R \equiv (1 + \gamma_5)/2$. By ignoring all the light neutrino masses and applying the approximation $U_{\nu\nu}U_{\nu\nu}^\dagger \simeq 1$ to the calculation, the total decay rate of $h \rightarrow \nu N$ is given by

$$\Gamma(h \rightarrow \nu N) = \sum_{i=1}^3 \frac{g_2^2 m_h M_i^2 (U_{\nu N}^\dagger U_{\nu N})_{ii}}{32\pi m_W^2} \left(1 - \frac{M_i^2}{m_h^2}\right)^2. \quad (4.16)$$

Before obtaining the decay rate of this channel, it requires to choose a appropriate $U_{\nu N}$ as our input. $U_{\nu N}$ can be as large as we hope theoretically, but it is still constrained by several experiments. From the gauge-boson mass fitting we can constrain the diagonal elements of the matrix $\epsilon = U_{\nu N}U_{\nu N}^\dagger$ as follows [87, 88]

$$\epsilon_{11} \leq 3.0 \times 10^{-3}, \quad \epsilon_{22} \leq 3.2 \times 10^{-3}, \quad \epsilon_{33} \leq 6.2 \times 10^{-3}. \quad (4.17)$$

On the other hand, the off-diagonal elements can be constrained by lepton flavor violating process such as $\ell_i \rightarrow \ell_j \gamma$ [87, 89]

$$|\epsilon_{12}| \leq 1.0 \times 10^{-4}, \quad |\epsilon_{13}| \leq 0.01, \quad |\epsilon_{23}| \leq 0.01. \quad (4.18)$$

The most stringent constraint comes from neutrinoless double beta decay [79]

$$\left| \sum_{i=1}^3 (U_{\nu N})_{1i}^2 / M_i \right| \leq 5 \times 10^{-8} \text{GeV}. \quad (4.19)$$

The L3 and DELPHI in LEP [80] for neutrino singlet search from $Z \rightarrow \nu N$ also constrain $(U_{\nu N})_{2i}$ and $(U_{\nu N})_{3i}$, which might be more stringent than Eqs. (4.17, 4.18).

Now we turn to take some $U_{\nu N}$ in Appendix C as our examples, for which we will ignore the small perturbation terms U_δ . As the first example we take $U_{\nu N} = U_0^a$ with the only free parameter $\bar{b} = 0.006$ which is the largest allowed values by experimental constraints. Also note that this choice of $U_{\nu N}$ satisfying Eq. (4.19) since we take M_i 's to be almost degenerate, and from this inequality the deviation between these M_i 's should be less than 1GeV. This property is similar for other choices in Appendix C. As the illustration, we plot the ratio of new Higgs decay channel to the SM total Higgs decay width as a function of m_h from 100GeV to 180GeV, with m_N

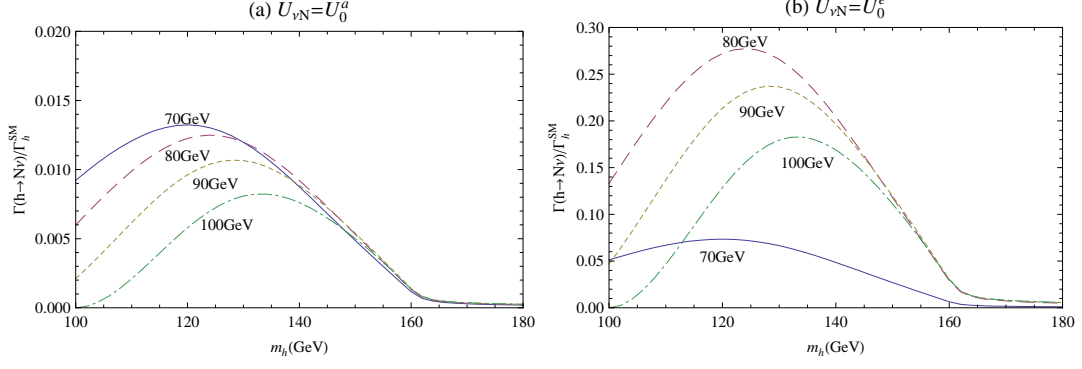


Figure 4.2: The ratio of decay width of $h \rightarrow \nu N$ to total Higgs decay width in SM as a function of m_h , for $m_N = 70, 80, 90, 100\text{GeV}$ as marked in the figures, with (a) $U_{\nu N} = U_0^a$, and (b) $U_{\nu N} = U_0^e$. The numerical result of the SM Higgs decay width is calculated by the package HDECAY [81].

chosen to 70, 80, 90, and 100GeV, as shown in Fig. 4.2(a). In the plot we find that the largest enhancement of Higgs decay width is around 1% for $m_N = 70\text{GeV}$ with $m_h \simeq 120\text{GeV}$. If we take $U_{\nu N} = U_0^d$ with free parameter $\bar{a} = 0.0089$ allowed in maximum, the corresponding graph will be similar to that for U_0^a . We emphasize that the recently experiments for the detection of $\mu \rightarrow e\gamma$ by MEG collaboration with the results $B(\mu \rightarrow e\gamma) < 2.4 \times 10^{-12}$ [112] should lead to a more stringent constraint on the allowed magnitudes of U_0^a and U_0^d .

It is possible to make a larger enhancement for Higgs decay width if we take the other kind of $U_{\nu N}$. Choosing $U_{\nu N} = U_0^e$ with $a = 0.02(0.04)$ for $m_N = 70\text{GeV}(\geq 80\text{GeV})$, or $U_{\nu N} = U_0^f$ with $a = 0.02(0.039)$ for $m_N = 70\text{GeV}(\geq 80\text{GeV})$ can achieve the goal, with the special case for $m_N = 70\text{GeV}$ constrained by LEP [80]. The data of total decay rate and branching ratio of SM we use here and later comes from the program HDECAY [81]. These choices evade the stringent constraint for $|\epsilon_{12}|$ in Eq. (4.18) because the first or second row of $U_{\nu N}$ vanishes. The result relevant for U_0^e is given in Fig 4.2(b), in which the enhancement can achieve to more than 25% for $m_N = 80\text{GeV}$ with $m_h \simeq 125\text{GeV}$. The graph for U_0^f is similar to that for U_0^e .

The enlarged $U_{\nu N}$ increases the total Higgs decay rate significantly. However, it should also increase the decay rate of Z boson, for which the SM prediction $\Gamma_Z^{\text{SM}} =$

$2.4954 \pm 0.0010 \text{ GeV}$ [90] is in agreed with experimental results $\Gamma_Z^{\text{exp}} = 2.4952 \pm 0.0023 \text{ GeV}$ [8]. So it is necessary to check if the decay rate $Z \rightarrow \nu N$ becomes so large that makes such a model be ruled out. The leading order transition amplitude of $Z \rightarrow \nu N$ which comes from tree level interaction, is given by

$$\mathcal{M}(Z \rightarrow \nu_i N_j) = \frac{g_2 \epsilon_Z^\mu}{2c_W} \bar{u}_\nu \gamma_\mu [(U_{\nu\nu}^T U_{\nu N}^*)_{ij} P_R - (U_{\nu\nu}^\dagger U_{\nu N})_{ij} P_L] v_N. \quad (4.20)$$

Square and sum over all mass eigenstates to get the total decay rate

$$\Gamma(Z \rightarrow \nu N) = \sum_{i=1}^3 \frac{g_2^2 m_Z^3 (U_{\nu N}^\dagger U_{\nu N})_{ii}}{48\pi m_W^2} \left(1 - \frac{3m_N^2}{2m_Z^2} + \frac{m_N^6}{2m_Z^6} \right), \quad (4.21)$$

where we have used $U_{\nu\nu} U_{\nu\nu}^\dagger \simeq 1$. By the formula, the most influential choices, $U_{\nu N} = U_0^{e,f}$ will lead to $\Gamma(Z \rightarrow \nu N) \simeq 0.12, 0.16, 0.002 \text{ MeV}$ for m_N to be 70, 80, and 90 GeV, respectively. It is clear that these channels are too small compared with both the deviation of experimental result and SM prediction.

In type-I seesaw the dominant decay mode of heavy neutrino is the decays into three light fermions, which will be described in more details later on. The heavy neutrino three body decay following the electron-positron annihilation $e^+ e^- \rightarrow Z^* \rightarrow \nu N$ will lead to the scattering into four fermions, whereas in the SM such processes are dominated by that with two W boson mediating. The spin-averaged amplitude square for $e^+ e^- \rightarrow \nu N$ in type-I seesaw is given by

$$\begin{aligned} \overline{|\mathcal{M}(e^+ e^- \rightarrow \nu_i N_j)|^2} &= \frac{g_2^4 (l_e^2 + r_e^2)}{4c_W^4} |(U_{\nu\nu}^\dagger U_{\nu N})_{ij}|^2 \frac{(t - m_N^2)t + (u - m_N^2)u}{(s - m_Z^2)^2} \\ &\quad + \frac{g_2^4}{4} |(U_{\nu\nu}^\dagger)_{i1} (U_{\nu N})_{1j}|^2 \left[\frac{(u - m_N^2)u}{(t - m_W^2)^2} + \frac{(t - m_N^2)t}{(u - m_W^2)^2} \right] \\ &\quad + \frac{g_2^4 l_e \text{Re}[(U_{\nu\nu}^\dagger U_{\nu N})_{ij} (U_{\nu\nu}^\dagger)_{1i} (U_{\nu N})_{j1}]}{2c_W^2 (s - m_Z^2)} \left[\frac{(u - m_N^2)u}{t - m_W^2} + \frac{(t - m_N^2)t}{u - m_W^2} \right], \end{aligned} \quad (4.22)$$

where the Mandelstam variables $s = (p_{e^+} + p_{e^-})^2$, $t = (p_{e^+} - p_N)^2$ and $u = m_N^2 - s - t$; $l_e = s_W^2 - 1/2$ and $r_e = s_W^2$, with $s_W = \sin \theta_W$. All external fermion masses are ignored except for m_N . The approximate cross section $\sigma(e^+ e^- \rightarrow \nu N \rightarrow \nu l_1^+ \nu l_2^-)$ is approximately equal to $\sigma(e^+ e^- \rightarrow \nu N)$ multiplying by branching ratio $\text{Br}(N \rightarrow \nu l_1^+ \nu l_2^-) \simeq 0.3$, which will be given in details later. LEP2 collaborations [91, 92] have already obtained the cross section for different lepton flavor final states with

$U_0^e : \sqrt{s} / m_N$	70GeV	80GeV	90GeV	100GeV	Data [92]
161GeV	0.001	0.005	0.005	0.004	0.28 ± 0.22
183GeV	0.001	0.003	0.003	0.003	1.63 ± 0.21
207GeV	0.001	0.002	0.003	0.002	1.87 ± 0.13
$U_0^f : \sqrt{s} / m_N$	70GeV	80GeV	90GeV	100GeV	Data [92]
161GeV	0.013	0.047	0.050	0.040	0.28 ± 0.22
183GeV	0.014	0.052	0.057	0.048	1.63 ± 0.21
207GeV	0.014	0.056	0.063	0.055	1.87 ± 0.13

Table 4.1: Cross section for different center-mass energy \sqrt{s} with different m_N , which is compared with experiment result. The values in last column are taken from Ref. [92]. All cross-section numbers are in pb.

the center-mass-energy 161, 183, and 207GeV. The related new contribution to the cross section for the choices U_0^e and U_0^f is given in Table 4.1, where the last column shows the corresponding experimental results [92]. It is found that the effect on such process for U_0^f is larger than that for U_0^e due to the vanishing of first row in U_0^e , but both are smaller than experiment deviations given in Ref. [92].

4.2.4 Three-Body Decays of N and Four-Body Decays of Higgs

The heavy neutrino N is produced by $h \rightarrow \nu N$. To explore such a process we need to understand the property of N first. The dominant decay mode of N is the three body decay, and we write down the related transition amplitudes as follows. For $N \rightarrow \nu \nu \bar{\nu}$, the main contribution is from the processes with Z boson intermediated, which is given by

$$\mathcal{M}(N_i \rightarrow \nu_j \nu_k \bar{\nu}_k) = \frac{g_2^2}{4c_W^2} \frac{\bar{u}'_\nu \gamma^\alpha [(U_{\nu\nu}^\dagger U_{\nu N})_{ji} P_L - (U_{\nu\nu}^T U_{\nu N}^*)_{ji} P_R] u_N \bar{u}_\nu \gamma_\alpha P_L v_\nu}{m_Z^2 - (p_\nu + p_{\bar{\nu}})^2 - i\Gamma_Z m_Z}, \quad (4.23)$$

where the same index k for ν and $\bar{\nu}$ means that we only consider the approximation $U_{\nu\nu} U_{\nu\nu}^\dagger \simeq 1$ in Z boson gauge interaction between ν 's. There are two kinds of

processes for $N \rightarrow \nu l^- l^+$. One is related to the different lepton flavor final states. The amplitude is given by

$$\mathcal{M}(N_i \rightarrow \nu_j l_m^- l_n^+) = \frac{g_2^2}{2} \frac{(U_{\nu N})_{mi} (U_{\nu\nu}^\dagger)_{jn} \bar{u}_l \gamma^\alpha P_L u_N \bar{u}_\nu \gamma_\alpha P_L v_l}{m_W^2 - (p_\nu + p_+)^2 - i\Gamma_W m_W} + \frac{g_2^2}{2} \frac{(U_{\nu N}^*)_{ni} (U_{\nu\nu}^T)_{jm} \bar{u}_\nu \gamma^\alpha P_R u_N \bar{u}_l \gamma_\alpha P_L v_l}{m_W^2 - (p_\nu + p_-)^2 - i\Gamma_W m_W}, \quad (4.24)$$

where $m \neq n$, and the Z mediated processes are ignored. The other one is for the processes in which charged lepton pair in the final state is of the same flavor. Such processes are constituted by three sub-amplitudes

$$\begin{aligned} \mathcal{M}(N_i \rightarrow \nu_j l_k^- l_k^+) &= \frac{g_2^2}{2} \frac{(U_{\nu N})_{ki} (U_{\nu\nu}^\dagger)_{jk} \bar{u}_l \gamma^\alpha P_L u_N \bar{u}_\nu \gamma_\alpha P_L v_l}{m_W^2 - (p_\nu + p_+)^2 - i\Gamma_W m_W} \\ &+ \frac{g_2^2}{2} \frac{(U_{\nu N}^*)_{ki} (U_{\nu\nu}^T)_{jk} \bar{u}_\nu \gamma^\alpha P_R u_N \bar{u}_l \gamma_\alpha P_L v_l}{m_W^2 - (p_\nu + p_-)^2 - i\Gamma_W m_W} \\ &- \frac{g_2^2}{2c_W^2} \frac{\bar{u}_\nu \gamma^\alpha [(U_{\nu\nu}^\dagger U_{\nu\nu})_{ji} P_L - (U_{\nu\nu}^T U_{\nu N}^*)_{ji} P_R] u_N \bar{u}_l \gamma_\alpha (l_l P_L + r_l P_R) v_l}{m_Z^2 - (p_+ + p_-)^2 - i\Gamma_Z m_Z}. \end{aligned} \quad (4.25)$$

The amplitudes of the processes $N \rightarrow \nu q \bar{q}$ are given by

$$\mathcal{M}(N_i \rightarrow \nu_j q \bar{q}) = \frac{g_2^2}{2c_W^2} \frac{\bar{u}_\nu \gamma^\alpha [(U_{\nu\nu}^\dagger U_{\nu N})_{ji} P_L - (U_{\nu\nu}^T U_{\nu N}^*)_{ji} P_R] u_N \bar{u}_q \gamma_\alpha (l_q P_L + r_q P_R) v_q}{m_Z^2 - (p_q + p_{\bar{q}})^2 - i\Gamma_Z m_Z}, \quad (4.26)$$

in which only five quarks are involved. The processes $N \rightarrow l u \bar{d}$ with u and d denoted to up or down type quarks respectively are dominated by tree level process with W boson exchange

$$\mathcal{M}(N_i \rightarrow l_j^- u \bar{d}) = \frac{g_2^2}{2} \frac{(U_{\nu N})_{ji} V_{ud} \bar{u}_l \gamma^\alpha P_L u_N \bar{u}_u \gamma_\alpha P_L v_d}{m_W^2 - (p_u + p_d)^2 - i\Gamma_W m_W}, \quad (4.27)$$

where V_{ud} is the related CKM matrix element.

The decay rates of N of the above three body decay processes are shown in Table 4.2. The decay rates for $m_N = 90\text{GeV}$ and $m_N = 100\text{GeV}$ increase sharply due to the open of W and Z channels separately. The travelling distance for N born from Higgs decay is estimated to be less than 10^{-10}m , which is so small that it is very hard to detect it directly.

Decay mode	70GeV	80GeV	90GeV	100GeV
$N \rightarrow \nu\nu\bar{\nu}$	0.06	0.6	2	16
$N \rightarrow \nu l^+ l'^-$	0.24	3.4	38	128
$N \rightarrow \nu l^+ l^-$	0.11	1.5	19	71
$N \rightarrow \nu q\bar{q}$	0.25	2.4	7	63
$N \rightarrow l^- u\bar{d}$	0.37	5.1	57	192
$N \rightarrow l^+ d\bar{u}$	0.37	5.1	57	192
$N \rightarrow 3 \text{ fermions}$	1.40	18.1	180	662

Table 4.2: Decay rates of three body decay modes for different m_N .

The effective four-body decays of Higgs following $h \rightarrow \nu N$ include $H \rightarrow \nu\nu\nu\nu$, $H \rightarrow \nu\nu l\bar{l}$, $H \rightarrow \nu\nu q\bar{q}$, and $H \rightarrow \nu\nu ud$. In the SM these channels are dominated by Higgs decaying into two gauge bosons and then subsequently decaying into two fermions for each vector bosons. The branching ratios of these processes are evaluated approximately by multiplying the branching ratio of gauge boson decaying into two leptons to that of the Higgs three body decays with one gauge boson. This means that $\text{Br}(h \rightarrow \nu f f' f'') \cong \text{Br}(h \rightarrow V \nu f) \text{Br}(V \rightarrow f' f'')$. The new contribution to the above four-body decays in this model is $h \rightarrow \nu N$ followed by the three body decay $N \rightarrow f f' f''$. The results is shown in Fig 4.3.

Evidently, for m_h less than 140GeV or so, the N-mediated contributions to each of the four-body modes are comparable to, and can be a few times bigger than, the corresponding SM contributions. This is clearly the case when it comes to the $\nu l u d$ and $\nu\nu l\bar{l}$ curves for the three values of m_N considered. We remark that it doesn't include possible interference between the N-mediated and SM contributions for our analysis here, but it should be taken into account in a more refined analysis. Nevertheless, this exercise serves to demonstrate the potential importance of the effect of large light-heavy mixing on Higgs decays. Accordingly, if the Higgs boson is detected, with $m_h \lesssim 140\text{GeV}$, and its decay modes can be studied with sufficient precision, these four-body Higgs decays may offer useful information on the seesaw

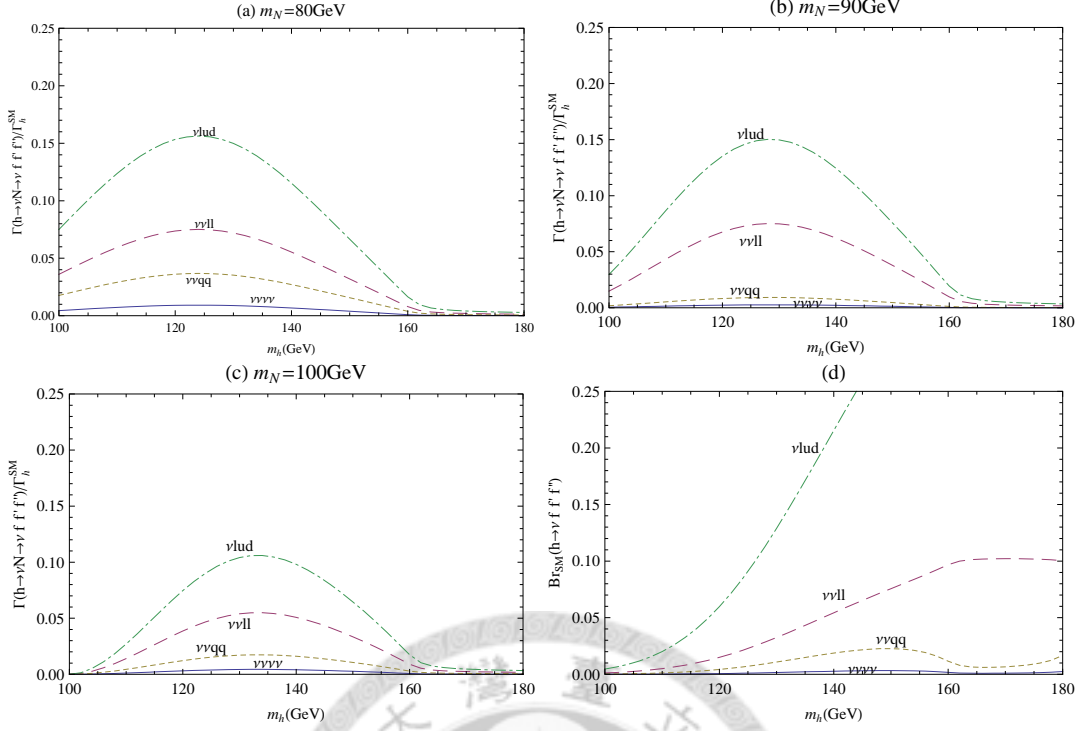


Figure 4.3: (a,b,c) Decay widths of the channels $h \rightarrow \nu N \rightarrow \nu f f' f''$ versus m_h with $m_N = 80, 90, 100 \text{ GeV}$, respectively, with heavy-light mixing $U_{\nu N} = U_0^e$. (d) The branching ratios of four body decay channels in SM. The numerical result of SM total and partial decay rates in these figures is calculated by package HDECAY [81]. mechanism.

4.3 Type-III Seesaw

4.3.1 Introduction

For this type of seesaw the fermion $\text{SU}(2)_L$ triplets are introduced into the SM [86]. The gauge transformation of this type of fermions is $N_R : (1, 3, 0)$, which can be expressed in symmetric tensor form $(N_R)_{ij}$

$$(N_R)_{11} = N_R^+, (N_R)_{12} = \frac{1}{\sqrt{2}} N_R^0, (N_R)_{22} = N_R^- . \quad (4.28)$$

Under $\text{SU}(2)$ transformation $(N_R)_{ij}$ becomes

$$(N_R)_{ij} \longrightarrow u_{ii'} u_{jj'} (N_R)_{i'j'} , \quad (4.29)$$

where u is the transformation matrix in $SU(2)$ fundamental representation. We can define another matrix form to represent N_R , which is usually given by $\Sigma_{ij} = -(N_R)_{ik}\epsilon_{kj}$, where

$$\Sigma = \begin{pmatrix} (N_R^0/\sqrt{2}) & E_R^+ \\ E_R^- & -(N_R^0/\sqrt{2}) \end{pmatrix}, \text{ with } E_R^+ = -N_R^+, E_R^- = N_R^-, \quad (4.30)$$

and it transforms under $SU(2)_L$ as

$$\Sigma_R \longrightarrow -(u N_R u^T \epsilon) = -u(N_R \epsilon)u^\dagger = u \Sigma_R u^\dagger. \quad (4.31)$$

where ϵ is the antisymmetric rank-2 tensor with $\epsilon_{12} = 1$. Also note that the transformation of $\bar{\Sigma}$ and $(\Sigma_R)^c \equiv C \bar{\Sigma}_R^T$ with the 4×4 matrix C and the transpose T acting on only spinors, is shown as

$$\bar{\Sigma}_R \longrightarrow u \bar{\Sigma}_R u^\dagger, (\Sigma_R)^c \longrightarrow u (\Sigma_R)^c u^\dagger. \quad (4.32)$$

Apply the materials given in the above to write down all the possible gauge invariant renormalizable new interaction terms

$$\mathcal{L}_{\text{new}} = \text{Tr}(\bar{\Sigma}_R i \not{D} \Sigma_R) + [-\sqrt{2} L_L Y_\Sigma^\dagger \Sigma_R \tilde{H} - \frac{1}{2} \text{Tr}(\bar{(\Sigma_R)^c} \hat{M}_\Sigma \Sigma_R) + \text{h.c.}] , \quad (4.33)$$

where \hat{M}_Σ is a 3×3 matrix, which should be real and diagonal in general. The form of mass matrix for neutral fermions is exactly the same as that in type-I seesaw. Note that for the heavy charged fermions one can define $E^\mp = E_R^\mp + (E_R^\pm)^c$ and then $E^+ = (E^-)^c$. The corresponding mass eigenstates are also the mixing of heavy and light charged leptons. The Yukawa coupling about heavy-light interaction is given in the form

$$\mathcal{L}_E = \frac{-g_2}{\sqrt{2}m_W} (\bar{l}_{mL} U_{\nu N} M_\Sigma E_{mR} + \bar{E}_{mR} M_\Sigma U_{\nu N}^\dagger l_{mL}) h + \dots, \quad (4.34)$$

where $l_{mR,L}$ and $E_{mR,L}$ are the heavy and light mass eigenstates, respectively.

4.3.2 $h \rightarrow \nu N$ and $h \rightarrow \ell E$

The effect on Higgs decay in type-III seesaw is more complicated than that in type-I seesaw, because there are additional Higgs decay channels with heavy and

light charged leptons included in the final states. The amplitude for $h \rightarrow \nu N$ is the same as that for type-I seesaw. For $h \rightarrow \ell E$, the corresponding amplitude is written as

$$\mathcal{M}(h \rightarrow l_i^- E_j^+) = \frac{g_2 M_i}{\sqrt{2} m_W} (U_{\nu N})_{ij} \bar{u}_l P_R v_E, \quad (4.35)$$

where v_E and u_l are the spinors for E^+ and l^- , respectively. The decay rate by the summation over all charged leptons is

$$\Gamma(h \rightarrow l^- E^+) = \sum_i \frac{g_2^2 m_h M_i^2 (U_{\nu N}^\dagger U_{\nu N})_{ii}}{32 \pi m_W^2} \left(1 - \frac{M_i^2}{m_h^2}\right)^2. \quad (4.36)$$

In type-III the experimental constraints for the FCNC factor ϵ are more stringent than in type-I seesaw, since FCNC can be generated by tree level interaction at this moment. The FCNC constraints for type-III seesaw are given by [87, 88]

$$\epsilon_{11} \leq 3.6 \times 10^{-4}; \quad \epsilon_{22} \leq 2.9 \times 10^{-4}; \quad \epsilon_{33} \leq 7.3 \times 10^{-4}. \quad (4.37)$$

The off diagonal elements of ϵ are constrained as [93]

$$|\epsilon_{12}| \leq 1.7 \times 10^{-7}; \quad |\epsilon_{13}| \leq 4.2 \times 10^{-4}; \quad |\epsilon_{23}| \leq 4.9 \times 10^{-4}. \quad (4.38)$$

The $U_{\nu N}$ can be chosen to be U_e^0 or U_f^0 given from Ref. [85], in order to evade the most stringent constraints on ϵ_{12} . For the choice $U_{\nu N} = U_e^0$ with $a = b$, the largest allowed value is $a = 0.012$; it is similar for the choice $U_{\nu N} = U_f^0$ in which $b = (0.0013 + 1.03i)a$ with $a = 0.013$ is allowed. These allowed values are smaller than what we took in type-I case. The new Higgs decay width including $h \rightarrow \nu N$ and $h \rightarrow l^- E^+$ are plotted as a function of m_h , shown in Fig. 4.4. In both figures the enhancement can only reach to 5% in type-III seesaw. This is due to the stronger experimental constraints on the elements of the mixing matrix $U_{\nu N}$ and also to the lower-limit on the heavy-lepton masses. As a consequence, the Higgs decays into four light fermions in this case would be less sensitive for probing the underlying seesaw mechanism than their type-I counterparts.

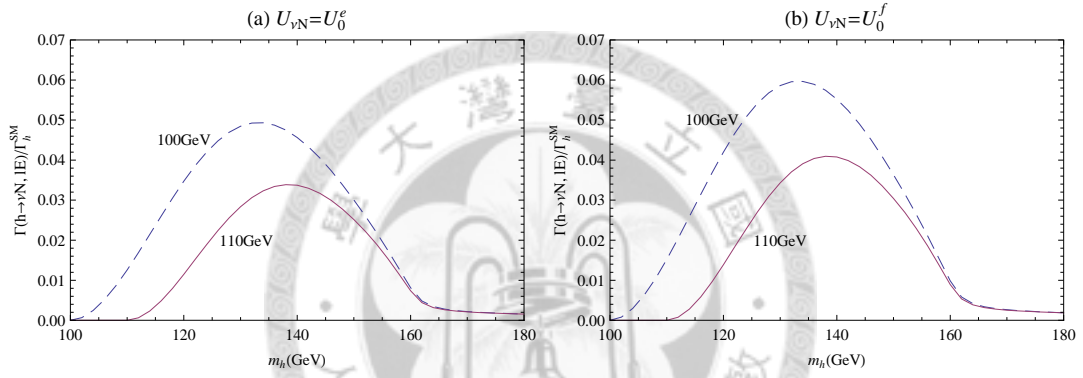


Figure 4.4: The ratios of decay width including the channels $h \rightarrow \nu N$ and $h \rightarrow l^- E^+$ to total SM Higgs decay width, as the functions of m_h , with $m_N = 100, 110$ GeV for (a) $U_{\nu N} = U_0^e$; for (b) $U_{\nu N} = U_0^f$. The numerical result for the SM Higgs total decay width is calculated by package HDECAY [81].

Chapter 5

Lepton Flavor Violation in Standard Model with Four Generations

The standard model is built with three fermion generations included, which is the minimal numbers of generation to generate CP violation. Although most of the present experimental results are in agreement with three-generation standard model (SM3), the existence of fourth generation fermions (SM4) is still not be decisively ruled out by experiments. Considering the SM3 with right-handed neutrinos, the massive neutrinos lead to the non-identity PMNS matrix appearing in the charged current interaction, which results in the lepton flavor violation (LFV). The light neutrinos in the SM can only violate the lepton flavor with very small amount, which is also consistent with current experimental results. If the fourth generation fermion exist, their masses should be very heavy, and their loop contribution to flavor violating processes could be large enough to be verified.

In order to keep the cancellation of the gauge anomaly, each type of fermions for the fourth generation should be introduced, which are denoted by t' , b' , l' , and ν_4 for up-type quark, down-type quark, charged lepton, and neutrino of the fourth generation, respectively. Their quantum numbers of the SM gauge group are the

same as their counterparts of other three generations. Such model is named as the sequential four generation SM. The SM4 is constrained by the “oblique” parameters S, T and U in studying the electroweak precision. One of the parameter, S , which is related to the deviation of the self-energy from the scales 0 to m_Z^2 , changes from the SM3 when appending a additional generation of fermions to SM. The result is given by [94, 95]

$$\delta S = \frac{2}{3\pi} - \frac{1}{3\pi} \left[\log \frac{m_{l'}}{m_{b'}} - \log \frac{m_{\nu_4}}{m_{l'}} \right]. \quad (5.1)$$

In order to reduce the deviation δS due to the fourth generation, the condition $m_{l'} > m_{b'}$ and $m_{l'} > m_{\nu_4}$ is required [94, 95]. Precisely speaking, it implies that $m_{l'} - m_{b'} \simeq 55 \text{ GeV}$ and $m_{l'} - m_{\nu_4} \simeq 60 \text{ GeV}$ [95] as the necessary condition for the existence of fourth generation. From the study of the perturbative unitarity bound, critical masses determined by perturbativity for charged leptons and neutrinos are about 1.2 TeV [96].

There are also some direct bounds on masses of fourth generation fermions from experiments. The probe of the process $pp \rightarrow t'\bar{t}' \rightarrow W^+ b W^- \bar{b}$ by CMS at the LHC with $\sqrt{s} = 7 \text{ TeV}$ gives a lower bound $m_{l'} > 557 \text{ GeV}$ [97]. Also from the study of $b'\bar{b}' \rightarrow tW^- \bar{t}W^+$ the range $m_{b'} < 611 \text{ GeV}$ has been ruled out at 95% C.L. [98]. The bounds on l' and ν_4 from LEP II experiment has been discussed in Ref. [99]. For unstable charged lepton heavier than heavy neutrino, the bound is given by $m_{l'} > 101.9 \text{ GeV}$ at 95% C.L. [99], while a heavy Dirac neutrino with $\nu_4 \rightarrow eW$ as its dominant decay mode the bound is $m_{\nu_4} > 101.3 \text{ GeV}$ at 95% C.L. [99]. It means that the fourth generations, if exists, with a large mass in the range of about 100 GeV to the unitarity bound are not ruled out. The current experimental bounds can be used to constrain model parameters, FCNC interaction with SM4 has been studied for a long time [100] and can also help for solving some of open questions in FCNC quark interaction [101, 94]. Leptonic FCNC effects, including $\mu - e$ conversion, in SM4 have also been studied extensively [102, 103, 104, 105]. In this chapter we carry out a more detailed systematic study by taking account of all available $\mu - e$ conversion experimental results, which has been measured in several kinds of nuclei

as the targets by experiments, and also been studied theoretically [110, 111]. The experimental upper bounds for different nuclei are given by $B_{\mu \rightarrow e}^{\text{Au}} < 7 \times 10^{-13}$ [106], $B_{\mu \rightarrow e}^{\text{S}} < 7 \times 10^{-11}$ [107], $B_{\mu \rightarrow e}^{\text{Ti}} < 4.3 \times 10^{-12}$ [108], and $B_{\mu \rightarrow e}^{\text{Pb}} < 4.6 \times 10^{-11}$ [109]. We will also compare constraints obtained from $\mu - e$ conversion using experimental bounds on various nuclei with those from $\mu \rightarrow e\gamma$ and $\mu \rightarrow e\bar{e}e$.

5.1 Charged Lepton Flavor Changing Processes

We focus on the model with massive neutrinos in order to satisfying the results from the neutrino oscillation experiments. Depending on the nature of the neutrinos, there may be right-handed neutrinos, $\nu_R : (1, 1, 0)$ which may pair up with the left-handed neutrinos to have Dirac or by themselves to have Majorana masses. For a model without Majorana neutrino mass, the charged lepton and neutrino masses are generated by the Yukawa interaction

$$\mathcal{L}_Y^\ell = -\overline{L}_{Li} Y_l^{ij} H l_{Rj} - \overline{L}_{Li} Y_\nu^{ij} \tilde{H} \nu_{Rj} + \text{h.c.} \quad (5.2)$$

In four-generation case $i, j = 1, \dots, 4$. After spontaneous symmetry breaking, the lepton mass terms appear, which are given by

$$\begin{aligned} \mathcal{L}_{\text{CC+mass}}^\ell &= -\frac{g_2}{\sqrt{2}} (\overline{l}_L \gamma_\mu \nu_L W^{\mu-} + \overline{\nu}_L \gamma_\mu l_L W^{\mu+}) \\ &\quad - \overline{L}_L M_l l_R - \overline{L}_L M_\nu \nu_R + \text{h.c.} \end{aligned} \quad (5.3)$$

The diagonalization of lepton mass matrices M_l and M_ν leads to the mixing in charged current interaction

$$\begin{aligned} \mathcal{L}_{\text{CC+mass}}^\ell &= -\frac{g_2}{\sqrt{2}} (\overline{l}_L \gamma_\mu V_{\text{PMNS}} \nu_L W^{\mu-} + \overline{\nu}_L \gamma_\mu V_{\text{PMNS}}^\dagger l_L W^{\mu+}) \\ &\quad - \overline{L}_L \hat{M}_l l_R - \overline{L}_L \hat{M}_\nu \nu_R + \text{h.c.}, \end{aligned} \quad (5.4)$$

where lepton mixing matrix V_{PMNS} of dimension 3×3 has been discussed in Sec. 2.3.1. In the SM4 the V_{PMNS} becomes a 4×4 matrix. There are a lot of FCNC processes for charged leptons, and most of which is induced at one loop level. Due to the GIM mechanism the terms independent of fermion mass are cancelled with each

other. The leading order contribution of these processes should be proportional to $(m_{\nu_i}^2/m_W^2)$, which is very tiny for SM3 neutrinos in the loop. The SM4 can enhance the contribution to these LFV processes with the fourth generation neutrino ν_4 in the loop. What we will focus on in the following are the following processes: $\mu \rightarrow e\gamma$, $\mu - e$ conversion, and $\mu \rightarrow ee\bar{e}$. The strength of these processes are governed by the factor $\lambda_{\mu e} = V_{\mu 4}^* V_{e 4}$, the multiplication of the PMNS matrix elements.

The $\mu \rightarrow e\gamma$ can be described by a dimension 5 dipole operator. In SM4, the main contribution comes from the fourth generation neutrino ν_4 in the loop, and it is written down explicitly in the leading order as

$$\mathcal{L}(\mu \rightarrow e\gamma) = -\frac{4G_F}{\sqrt{2}} \frac{e}{32\pi^2} \lambda_{\mu e} G_2(x_4) \bar{e} \sigma^{\mu\nu} (m_\mu P_R + m_e P_L) \mu F_{\mu\nu}, \quad (5.5)$$

$$\text{where } G_2(x) = \frac{x(1-5x-2x^2)}{4(x-1)^3} + \frac{3x^3}{2(x-1)^4} \ln x, \quad (5.6)$$

with $x_4 = (m_{\nu_4}^2/m_W^2)$. Note that the mass inversion for initial and final state fermions makes the right-handed coupling larger than left-handed one by a factor (m_μ/m_e) .

Another useful process is the $\mu - e$ conversion which occurs by the scattering with the target nuclei. It is convenient to normalize it in the ratio of the $\mu - e$ conversion rate to the rate of capture of muon by the same atom, which is given by

$$B_{\mu \rightarrow e}^A = \frac{\Gamma(\mu^- + A(N, Z) \rightarrow e^- + A(N, Z))}{\Gamma(\mu^- + A(N, Z) \rightarrow \nu_\mu + A(N+1, Z-1))}, \quad (5.7)$$

where A indicates the type of atom in which the nucleus is taken as the target. Different types of targets would lead to different conversion-to-capture ratios. In SM4, the interaction related to $\mu - e$ conversion is dominated by penguin and box diagrams with ν_4 exchanging in the loop, which is given by

$$\begin{aligned} \mathcal{L}(\mu \rightarrow eq\bar{q}) = & -\frac{G_F}{\sqrt{2}} \frac{e^2}{4\pi^2} \lambda_{\mu e} [V_u(x_4) \bar{u} \gamma_\mu u + V_d(x_4) \bar{d} \gamma_\mu d \\ & + A_u(x_4) \bar{u} \gamma_\mu \gamma_5 u + A_d(x_4) \bar{d} \gamma_\mu \gamma_5 d] \bar{e} \gamma^\mu P_L \mu, \end{aligned} \quad (5.8)$$

where $\sigma_{\mu\nu} = i[\gamma^\mu, \gamma^\nu]/2$, and

$$V_q(x) = -Q^q G_1(x) + \frac{1}{2s_W^2}(I_3^q - Q^q s_W^2)G_Z(x) - \frac{1}{4s_W^2}G_B^q(x), \quad (5.9)$$

$$A_q(x) = -\frac{1}{s_W^2}I_3^q G_Z(x) + \frac{1}{4s_W^2}G_B^q(x), \quad (5.10)$$

$$G_1(x) = \frac{x(12+x-7x^2)}{12(x-1)^3} - \frac{x^2(12-10x+x^2)}{6(x-1)^4} \ln x, \quad (5.11)$$

$$G_Z(x) = \frac{x(x^2-7x+6)}{4(x-1)^2} + \frac{x(2+3x)}{4(x-1)^2} \ln x, \quad (5.12)$$

$$G_B(x) = \frac{x}{x-1} - \frac{x}{(x-1)^2} \ln x, \quad G_B^u(x) = 4G_B(x), \quad G_B^d(x) = G_B(x). \quad (5.13)$$

I_3^q and Q^q are the isospin and electric charge of q , respectively.

The effective interaction for $\mu \rightarrow e\bar{e}e$ in SM4 is given by

$$\begin{aligned} \mathcal{L}(\mu \rightarrow e\bar{e}e) = & -\frac{G_F}{\sqrt{2}} \frac{e^2}{4\pi^2} \lambda_{\mu e} [G_2(x_4) \bar{e} \gamma_\mu e \frac{q_\nu}{q^2} \bar{e} i \sigma^{\mu\nu} (m_\mu P_R + m_e P_L) \mu \\ & + \bar{e} \gamma^\mu (a_L(x_4) P_L + a_R(x_4) P_R) e \bar{e} \gamma_\mu P_L \mu], \end{aligned} \quad (5.14)$$

which is constituted by the contribution from the penguin diagrams and the box diagrams, with the corresponding functions given by

$$a_L(x) = G_1(x) + \frac{1}{s_W^2} \left(-\frac{1}{2} + s_W^2 \right) G_Z(x) - \frac{1}{2s_W^2} G_B(x), \quad a_R(x) = G_1(x) + G_Z(x). \quad (5.15)$$

The function $G_2(x)$ is related to the dipole operator, which can also contribute to other LFV processes. $G_1(x)$ corresponds to the charge radius contribution, which contributes to both $\mu \rightarrow e + q\bar{q}$ and $\mu \rightarrow e\bar{e}e$. $G_Z(x)$ is the Z-penguin contribution, which increases linearly with large x , as mentioned in Ref. [104]. Finally, $G_B(x)$ is the box diagram contribution.

5.2 $\mu - e$ Conversion

To calculate the $\mu - e$ conversion in nucleus we need to deal with the related initial and final hadronic states. Ref. [110, 111] have provided several results. In this section we will use these consequences as well as the notation of functions relevant for $\mu - e$ conversion at hadronic level in Ref. [111]. The general interaction related

to $\mu - e$ conversion is given by [111]

$$\begin{aligned}
\mathcal{L}_{\text{eff}} = & -\frac{4G_F}{\sqrt{2}}[m_\mu \bar{e} \sigma^{\mu\nu} (A_R P_R + A_L P_L) \mu F_{\mu\nu} + \text{h.c.}] \\
& -\frac{G_F}{\sqrt{2}}[\bar{e}(g_{LS(q)} P_R + g_{RS(q)} P_L) \mu \bar{q} q + \bar{e}(g_{LP(q)} P_R + g_{RP(q)} P_L) \mu \bar{q} \gamma_5 q + \text{h.c.}] \\
& -\frac{G_F}{\sqrt{2}}[\bar{e}(g_{LV(q)} \gamma^\mu P_L + g_{RV(q)} \gamma^\mu P_R) \mu \bar{q} \gamma_\mu q \\
& + \bar{e}(g_{LA(q)} \gamma^\mu P_L + g_{RA(q)} \gamma^\mu P_R) \mu \bar{q} \gamma_\mu \gamma_5 q + \text{h.c.}] \\
& -\frac{G_F}{\sqrt{2}} \left[\frac{1}{2} \bar{e}(g_{LT(q)} \sigma^{\mu\nu} P_R + g_{RT(q)} \sigma^{\mu\nu} P_L) \mu \bar{q} \sigma_{\mu\nu} q + \text{h.c.} \right].
\end{aligned} \tag{5.16}$$

By comparing with Eq. (5.5) and Eq. (5.8) related to SM4 contribution, it leads to

$$A_R = \frac{e}{32\pi^2} \lambda_{\mu e} G_2(x_4), \quad A_L = \frac{m_e}{m_\mu} A_R, \quad g_{LV(q)} = \frac{e^2}{4\pi^2} \lambda_{\mu e} V_q. \tag{5.17}$$

Note that $g_{L,R}(S, P, T(q))$ vanish in SM4, and the contribution of $g_{L(R)A}$ is suppressed since fraction of the coherent process is larger than incoherent one by approximately the factor of mass number of target nuclei in general [111]. All of the related contributions are proportional to $\lambda_{\mu e}$. The conversion-to-capture ratio is given by

$$B_{\mu \rightarrow e}^A = \frac{2G_F^2 m_\mu^5}{\Gamma_{\text{capt}}^A} |A_R D + \tilde{g}_{LV}^{(p)} V^{(p)} + \tilde{g}_{LV}^{(n)} V^{(n)}|^2, \tag{5.18}$$

where the overlapped functions D , $V^{(p)}$, and $V^{(n)}$ are defined in Appendix D. It is also useful to define the ratio of $\mu - e$ conversion and $\mu \rightarrow e\gamma$ as follows

$$\begin{aligned}
\frac{B_{\mu \rightarrow e}^A}{B(\mu \rightarrow e\gamma)} &= R_{\mu \rightarrow e}^0(A) \left| 1 + \frac{\tilde{g}_{LV}^{(p)} V^{(p)}(A)}{A_R D(A)} + \frac{\tilde{g}_{LV}^{(n)} V^{(n)}(A)}{A_R D(A)} \right|^2, \\
R_{\mu \rightarrow e}^0(A) &= \frac{G_F^2 m_\mu^5}{192\pi^2 \Gamma_{\text{capt}}^A} |D(A)|^2.
\end{aligned} \tag{5.19}$$

We take the numerical values of D , $V^{(p)}$, and $V^{(n)}$ shown in Table 5.1 given from method 1 in Ref. [111], with saturating the conversion-to-capture ratio to the experiment bounds [106, 107, 108, 109]. The bound on coupling $|\lambda_{\mu e}|$ as a function of x_4 is acquired, given in Fig 5.1. It shows that the $\mu - e$ conversion in Au provides the most stringent constraints in the present, mostly due to the tightest upper bound from experiment. With $m_{\nu_4} \gtrsim 100\text{GeV}$, $|\lambda_{\mu e}|$ is constrained to be less than 1.6×10^{-5} , which is still allowed by the current neutrino oscillation observation.

A	$D(A)$	$V^{(p)}(A)$	$V^{(n)}(A)$	$R_{\mu \rightarrow e}^0(A)$
${}_{13}^{27}\text{Al}$	0.0362	0.0161	0.0173	0.0027
${}_{16}^{32}\text{S}$	0.0524	0.0236	0.0236	0.0029
${}_{22}^{48}\text{Ti}$	0.0864	0.0396	0.0468	0.0041
${}_{79}^{197}\text{Au}$	0.189	0.0974	0.146	0.0039
${}_{82}^{208}\text{Pb}$	0.161	0.0834	0.128	0.0028

Table 5.1: The overlapped functions D , $V^{(p)}$, and $V^{(n)}$ related to $\mu - e$ conversion on different atomic nuclei [111]. The numbers in last column is the values of $R_{\mu \rightarrow e}^0$.

5.3 Comparison with $\mu \rightarrow e\gamma$ and $\mu \rightarrow 3e$

Besides the $\mu - e$ conversion with the nuclei of atom, $\mu \rightarrow e\gamma$ and $\mu - e\bar{e}e$ are also useful to give the tight bounds on $|\lambda_{\mu e}|$. The branching ratio of $\mu \rightarrow e\gamma$ is shown as

$$B(\mu \rightarrow e\gamma) = \frac{\Gamma(\mu \rightarrow e\gamma)}{\Gamma(\mu \rightarrow e\nu\bar{\nu})} = 384\pi^2(|A_L|^2 + |A_R|^2). \quad (5.20)$$

In the above formula m_e is neglected. If m_e is kept, one should divide, in the above expression, a phase factor $I(x) = 1 - 8x + 8x^3 - x^4 - 12x^2 \ln x$ with $x = m_e^2/m_\mu^2$. Radiative corrections from QED also modify the above expression by dividing a factor $1 + \delta_{\text{QED}}$ with $\delta_{\text{QED}} = (\alpha_e/2\pi)(25/4 - \pi^2)$. For $\mu \rightarrow e\bar{e}e$, with the functions $G_2(x)$, $a_R(x)$, and $a_L(x)$ given previously, the related branching ratio reads

$$\begin{aligned} B(\mu \rightarrow e\bar{e}e) &= \frac{\alpha_e^2}{16\pi^2} |\lambda_{\mu e}|^2 \left[a_R^2(x_4) + 2a_L^2(x_4) - 4G_2(x_4)(a_R(x_4) + 2a_L(x_4)) \right. \\ &\quad \left. + 4G_2^2(x_4) \left(4 \ln \frac{m_\mu}{m_e} - \frac{11}{2} \right) \right]. \end{aligned} \quad (5.21)$$

Recently MEG obtained a tighter upper bound $\text{Br}(\mu \rightarrow e\gamma) < 2.4 \times 10^{-12}$ [112], which is five times smaller than the older result $\text{Br}(\mu \rightarrow e\gamma) < 1.2 \times 10^{-11}$ [113]. The current experimental bound on $\mu \rightarrow e\bar{e}e$ is $\text{Br}(\mu \rightarrow e\bar{e}e) < 10^{-12}$ [75]. We also plot the bounds on $|\lambda_{\mu e}|$ constrained by experimental bounds on these two processes in the SM4 in Fig. 5.1, too. The constraint on $\mu \rightarrow e\bar{e}e$ becomes tighter with larger x_4 due to the property of Z-penguin contribution. However, it shows that $\mu \rightarrow e\gamma$ and $\mu - e$ conversion can not provide smaller upper bounds on $|\lambda_{\mu e}|$ than

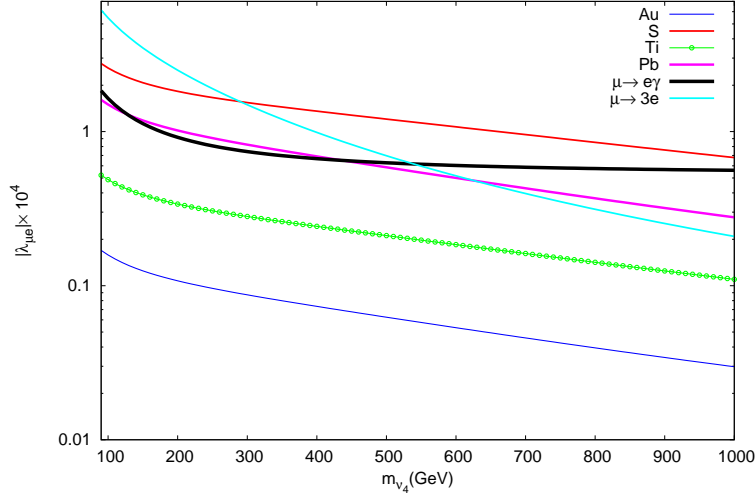


Figure 5.1: The upper bounds of the coupling $|\lambda_{\mu e}|$ from experimental constraints on $\mu - e$ conversion in Au, S, Ti, Pb, $\mu \rightarrow e\gamma$, and $\mu \rightarrow 3e$, as the functions of m_{ν_4} .

that provided by $\mu - e$ conversion in Au or Ti.

Fig. 5.2 shows the ratios $B_{\mu \rightarrow e}^A/B(\mu \rightarrow e\gamma)$ and $B(\mu \rightarrow e\bar{e}e)/B(\mu \rightarrow e\gamma)$ as the functions of m_{ν_4} . These ratios are independent of $|\lambda_{\mu e}|$, and they imply the comparison of constraints on coupling among different LFV processes with the situation that these LFV experimental bounds with the same order. $B_{\mu \rightarrow e}^A/B(\mu \rightarrow e\gamma)$ is larger than 1 for most of the range of m_{ν_4} . $B(\mu \rightarrow e\bar{e}e)/B(\mu \rightarrow e\gamma)$ is smaller than 1 for lower m_{ν_4} , and it becomes larger than 1 when $m_{\nu_4} \gtrsim 800\text{GeV}$. Each curve in the figure increases with x_4 , since the Z-penguin $G_Z(x_4)$ increases faster with x_4 than $G_2(x_2)$ for $\mu \rightarrow e\gamma$.

There are several projected experimental sensitive which may be performed in the future. MEG plans to perform the sensitive for $B(\mu \rightarrow e\gamma)$ with the order 10^{-13} [114]; $B(\mu \rightarrow e\bar{e}e)$ will also be improved to 10^{-14} [115]; $\mu - e$ conversion in Ti and Al may also be done in the future with the sensitive 10^{-18} and 10^{-16} , respectively [116, 117, 118]. We also plot them in Fig. 5.3 to constrain $|\lambda_{\mu e}|$. It shows that the $\mu - e$ conversion in Ti can provide better constraint in the future.

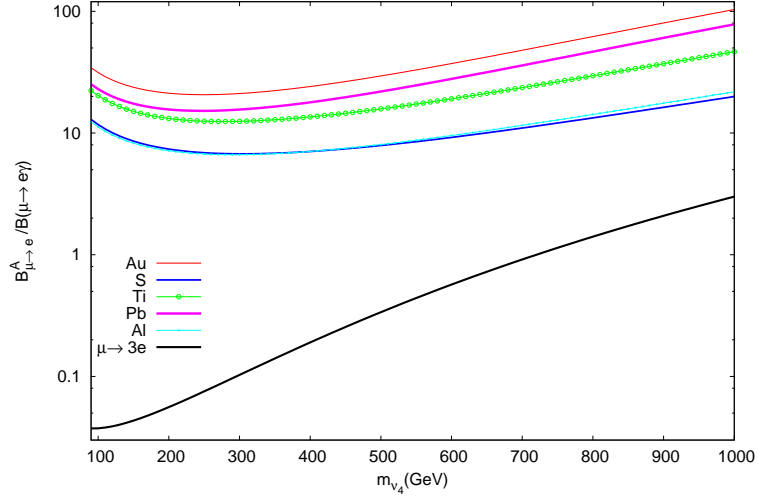


Figure 5.2: The ratios of $\mu - e$ conversion in Au, S, Ti, Pb, Al, and $\mu \rightarrow 3e$ to $\mu \rightarrow e\gamma$, respectively, as the functions of m_{ν_4} .

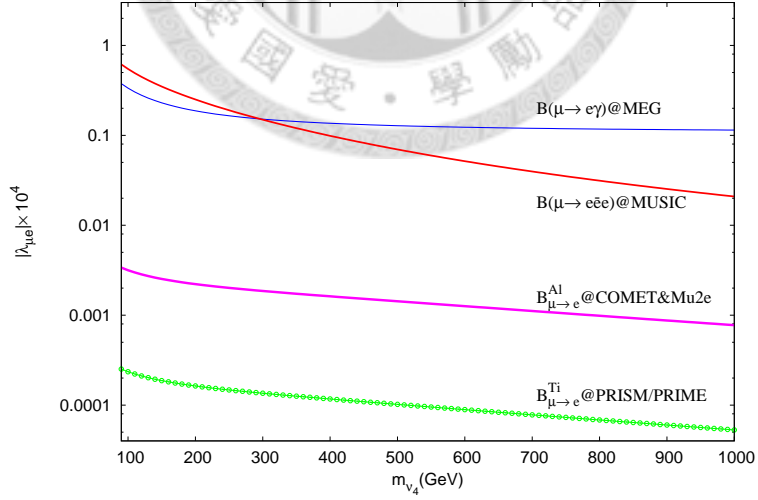


Figure 5.3: The upper bounds of $|\lambda_{\mu e}|$, constrained by projected sensitivities of future experiments for $\mu \rightarrow e\gamma$ [114], $\mu \rightarrow 3e$ [115], and $\mu - e$ conversion on Al [117] and Ti [118], as functions of m_{ν_4} .



Chapter 6

Conclusion

The standard model has been studied for a long period of time. It has been examined and regarded as a very successful model in electroweak precision test, the fitting of CKM matrix parameters. However, there remain some problems in the SM which require further explanation. Three of these have been discussed through this thesis. We conclude these as follows.

We have built a model which constructs the CKM matrix by the spontaneous CP violation, with the assumption that the spontaneous CP violating phase is identical to the CKM matrix phase, up to a minus sign. In order to evade from the strong CP problem for general multi-Higgs model, PQ mechanism should be applied into our model. So we take three Higgs doublets and one Higgs singlet in the model to keep the spontaneous CP violation and PQ symmetry with invisible axion simultaneously. We have classified our model into Model (a), with two Higgs coupled to U_R and Model (b), with two Higgs coupled to D_R . In each of these models different CKM matrix parametrizations lead to different sub-models. Yukawa couplings just depend on CKM mixing angles and quark masses. Then we knew the lightest Higgs mass allowed by neutral meson mixing in experiments. In Model (a-M), $D - \overline{D}^0$ mixing allows the Higgs mass around 100GeV. From $K^0 - \overline{K}^0$ mixing lightest Higgs mass should be at least TeV level in Model (a-KM). In Model (b-KM) 300GeV Higgs mass is allowed by $B_s^0 - \overline{B}_s^0$ mixing. The neutron EDM in our model can also be

close to the current experimental bound.

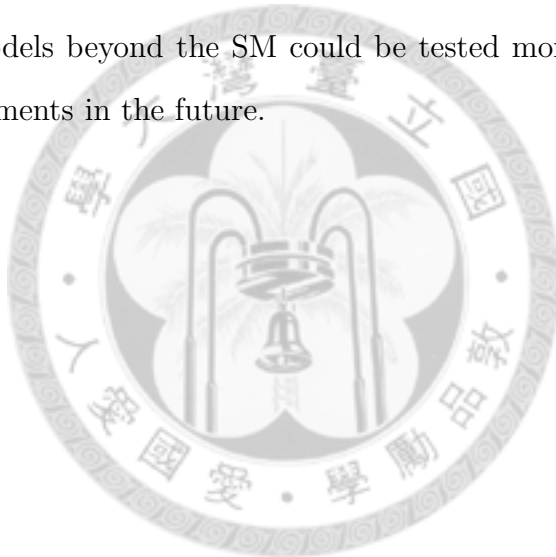
We also applied the same idea to the lepton sector. The three gauge singlet right-handed neutrinos acquire heavy Majorana masses after spontaneous symmetry breaking. In Model (a) we also couple two Higgs to N_R . The situation becomes more complicated since the neutrino Dirac mass matrix depends on not only light and heavy neutrino mass matrix but also a complex orthogonal matrix. In Model (b), the building of Yukawa coupling in the lepton sector is almost the same as that in quark sector. Two Higgs doublets are coupled to l_R . We identified the PMNS matrix phase with the spontaneous CP violating phase, which has already been identified with CKM matrix phase. These models depend on PMNS matrix parametrization. The Jarlskog invariant for modified standard parametrization (M-parametrization) is $-(0.033 \pm 0.002)$; for KM-parametrization it is $-(0.035 \pm 0.003)$, which could be probed to distinguish different model in the future.

In the second topic we discussed the Higgs decay in the seesaw models with large heavy-light mixing $U_{\nu N}$. In type-I seesaw, by the previous choices of $U_{\nu N} = U_{e,f}^0$, the decay channel $h \rightarrow \nu N$ can enhance more than 20% of total Higgs decay width from the SM contribution. The choice of large $U_{\nu N}$ can satisfy experimental constraints from total Z^0 decay width and the cross sections of $e^-e^+ \rightarrow l^-\nu l^+\nu$. The dominant decay channel of heavy neutrino N is the three body decay. Because of the very short propagation distance of N from where h decays, N decays into three light fermions before it can be detected. The detection of four body decay $h \rightarrow \nu f f' f''$ might be a signal to look for such seesaw models. The Higgs decay can also be enhanced in type-III by the decay channels $h \rightarrow \nu N$ and $h \rightarrow lE$. However, the enhancement can be only about a few percent, not as large as that in type-I seesaw.

In the last topic we studied the lepton flavor violating processes $\mu \rightarrow e\gamma$, $\mu - e$ conversion, and $\mu \rightarrow ee\bar{e}$ in the SM with sequential four generations. The one loop contribution involved with the fourth generation neutrino is the dominant contribution to these LFV processes. By comparing with current experimental upper bounds for these processes, we found that $\mu - e$ conversion for Au nucleus provides the most

stringent constraints on the coupling $|\lambda_{\mu e}|$, the couplings relevant for lepton flavor mixing with fourth generation. For m_{ν_4} larger than 100GeV the coupling $\lambda_{\mu e}$ should be less than 1.6×10^{-5} . We also applied the expected experimental upper bounds for these LFV processes in the future to constrain $\lambda_{\mu e}$. The experiment for $\mu - e$ conversion for Ti nucleus could result in the tightest constraint on fourth generation coupling.

In this thesis I have completed the work about the phenomenology of relation between spontaneous CP violation and CKM, PMNS mixing matrices, the Higgs decay in seesaw model, and the comparison among lepton flavor violating processes in SM4. These work may be helpful to improve the SM and solve some of its problems. These models beyond the SM could be tested more precisely and more accurately by experiments in the future.





Appendix A

Higgs Mass Matrices

The neutral mass matrix elements will be given in the basis $(H_1^0, H_2^0, H_3^0, H_4^0, a_1, a_2, a_3, a)$. We will introduce some of the notation for simplicity. A sequent of three characters of s or c appearing in the formula indicates sine or cosine applied to δ , δ_s , and $\delta + \delta_s$, respectively. The prime on the first of the three characters corresponds to 2δ instead of δ . For example, ‘ scs ’ means ‘ $\sin \delta \cos \delta_s \sin(\delta + \delta_s)$ ’ and ‘ $c'ss$ ’ means ‘ $\cos 2\delta \sin \delta_s \sin(\delta + \delta_s)$ ’. The neutral mass matrix elements are shown as

$$\begin{aligned} m_{H_1^0 H_1^0}^2 = & \frac{2v_1^2 v_2^2}{v_{12}^2} (\lambda_1 + \lambda_2 - \lambda_3 - \lambda_4) \\ & - \frac{1}{2v_1 v_2 v_{12}^2 \sin \delta_s \sin(\delta + \delta_s)} \{ \lambda_5 v_1 v_2 [v_1^4 s' cs + 4v_1^2 v_2^2 c' ss - v_2^4 s' sc] \\ & + \lambda_6 v_1^2 [v_1^4 (scs - 3css) + 6v_1^2 v_2^2 css + v_2^4 (-3css - ssc)] \\ & + \lambda_7 v_2^2 [v_1^4 (scs - 3css) + 6v_1^2 v_2^2 css + v_2^4 (css - ssc)] \\ & + ((\lambda_8 + \lambda'_8) v_3^2 + d_{12} v_s^2) [v_1^4 (ccs + scs) + 2v_1^2 v_2^2 css + v_2^4 (css - ssc)] \} ; \end{aligned} \tag{A.1}$$

$$\begin{aligned}
m_{H_2^0 H_2^0}^2 = & \frac{2v_3^2}{v^2 v_{12}^2} (\lambda_1 v_1^4 + \lambda_2 v_2^4 + \lambda_t v_{12}^4 + \lambda_s v_{12}^4 + \lambda_3 v_1^2 v_2^2 - \lambda'_3 v_1^2 v_{12}^2 - \lambda''_3 v_2^2 v_{12}^2 \\
& + \lambda_4 v_1^2 v_2^2 - \lambda'_4 v_1^2 v_{12}^2 - \lambda''_4 v_2^2 v_{12}^2 - f_1 v_1^2 v_{12}^2 - f_2 v_2^2 v_{12}^2 + f_3 v_{12}^4) \\
& - \frac{v_1 v_2}{2v_3^2 v^2 v_{12}^2 \sin \delta_s \sin(\delta + \delta_s)} \{ \lambda_5 v_1 v_2 [v^4 (s'cs - s'sc) - 4v_3^4 c'ss] \\
& + \lambda_6 v_1^2 [v^4 (scs - ssc) - 8v_3^4 css] + \lambda_7 v_2^2 [v^4 (scs - ssc) - 8v_3^4 css] \\
& + (\lambda_8 + \lambda'_8) v_3^2 [v^4 (scs - ssc) + 8v_{12}^2 v_3^2 css] + d_{12} v_s^2 v^4 (scs - ssc) \} ;
\end{aligned} \tag{A.2}$$

$$\begin{aligned}
m_{H_3^0 H_3^0}^2 = & \frac{2}{v^2} \{ \lambda_1 v_1^4 + \lambda_2 v_2^4 + \lambda_t v_3^4 + (\lambda_3 + \lambda_4) v_1^2 v_2^2 + (\lambda'_3 + \lambda'_4) v_1^2 v_3^2 \\
& + (\lambda''_3 + \lambda''_4) v_2^2 v_3^2 \} - \frac{2v_1 v_2}{v^2} \{ -\lambda_5 v_1 v_2 \cos 2\delta \\
& - 2(\lambda_6 v_1^2 + \lambda_7 v_2^2 + (\lambda_8 + \lambda'_8) v_3^2) \cos \delta \} ;
\end{aligned} \tag{A.3}$$

$$\begin{aligned}
m_{H_4^0 H_4^0}^2 = & \frac{2}{v^4 v_s^2} \{ (\lambda_1 v_1^4 + \lambda_2 v_2^4) v_3^4 + \lambda_t v_3^4 v_{12}^4 + \lambda_s v^4 v_s^4 + (\lambda_3 + \lambda_4) v_1^2 v_2^2 v_3^4 \\
& - v_1^2 v_3^4 v_{12}^2 (\lambda'_3 + \lambda'_4) - v_2^2 v_3^4 v_{12}^2 (\lambda''_3 + \lambda''_4) + v_3^2 v_s^2 v^2 (f_1 v_1^2 + f_2 v_2^2 - v_{12}^2 f_3) \} \\
& - \frac{2v_1 v_2}{v^4 v_s^2 \sin \delta \sin(\delta + \delta_s)} \{ \lambda_5 v_1 v_2 [v_{12}^2 v^2 (s'cs - s'sc) - v_3^4 c'ss] \\
& + \lambda_6 v_1^2 [v_{12}^2 v^2 (scs - ssc) - 2v_3^4 css] + \lambda_7 v_2^2 [v_{12}^2 v^2 (scs - ssc) - 2v_3^4 css] \\
& + (\lambda_8 + \lambda'_8) v_3^2 [v_{12}^2 v^2 (scs - ssc) + 2v_{12}^2 v_3^2 css] \\
& + d_{12} v_s^2 [v_{12}^2 v^2 (scs - ssc) + 2(v_{12}^2 - v_3^2) v_3^2 css] \} ;
\end{aligned} \tag{A.4}$$

$$\begin{aligned}
m_{H_1^0 H_2^0}^2 = & \frac{v_1 v_2 v_3}{v_{12}^2 v} (-2v_1^2 \lambda_1 + 2v_2^2 \lambda_2 + \lambda_3(v_1^2 - v_2^2) + \lambda'_3 v_{12}^2 - \lambda''_3 v_{12}^2 \\
& + \lambda_4(v_1^2 - v_2^2) + \lambda'_4 v_{12}^2 - \lambda''_4 v_{12}^2 + f_1 v_{12}^2 - f_2 v_{12}^2) \\
& - \frac{1}{2v_3 v v_{12}^2 \sin \delta_s \sin(\delta + \delta_s)} \{ \lambda_5 v_1 v_2 [v_1^4 s' cs + v_2^4 s' sc + v_1^2 v_2^2 (s' cs + s' sc) \\
& + v_2^2 v_3^2 (2c' ss + s' sc) + v_1^2 v_3^2 (s' cs - 2c' ss)] \\
& + \lambda_6 v_1^2 [v_1^4 scs + v_2^4 ssc + v_1^2 v_2^2 (scs + ssc) \\
& + v_2^2 v_3^2 (6css + ssc) + v_1^2 v_3^2 (scs - 2css)] \\
& + \lambda_7 v_2^2 [v_1^4 scs + v_2^4 ssc + v_1^2 v_2^2 (scs + ssc) \\
& + v_2^2 v_3^2 (2css + ssc) + v_1^2 v_3^2 (scs - 6css)] \\
& + (\lambda_8 + \lambda'_8) v_3^2 [v_1^4 (2css + scs) + v_2^4 (ssc - 2css) + v_1^2 v_2^2 (scs + ssc) \\
& + v_2^2 v_3^2 ssc + v_1^2 v_3^2 scs] + d_{12} v_s^2 [v_1^4 scs + v_2^4 ssc + v_1^2 v_2^2 (scs + ssc) \\
& + v_2^2 v_3^2 ssc + v_1^2 v_3^2 scs] \} ; \tag{A.5}
\end{aligned}$$

$$\begin{aligned}
m_{H_1^0 H_3^0}^2 = & \frac{v_1 v_2}{v_{12} v} (2\lambda_1 v_1^2 - 2\lambda_2 v_2^2 - (\lambda_3 + \lambda_4)(v_1^2 - v_2^2) + (\lambda'_3 - \lambda''_3 + \lambda'_4 - \lambda''_4) v_3^2 \\
& - \frac{1}{v v_{12}} \{ \lambda_5 v_1 v_2 (v_1^2 - v_2^2) \cos 2\delta + \lambda_6 v_1^2 (v_1^2 - 3v_2^2) \cos \delta \\
& + \lambda_7 v_2^2 (3v_1^2 - v_2^2) \cos \delta + (\lambda_8 + \lambda'_8) v_3^2 (v_1^2 - v_2^2) \cos \delta \} ; \tag{A.6}
\end{aligned}$$

$$\begin{aligned}
m_{H_2^0 H_3^0}^2 = & \frac{v_3}{v_{12} v^2} \{ -2\lambda_1 v_1^4 - 2\lambda_2 v_2^4 + 2\lambda_t v_{12}^2 v_3^2 - 2(\lambda_3 + \lambda_4) v_1^2 v_2^2 \\
& + (\lambda'_3 + \lambda'_4) v_1^2 (v_{12}^2 - v_3^2) + (\lambda''_3 + \lambda''_4) v_2^2 (v_{12}^2 - v_3^2) \\
& + (f_1 v_1^2 + f_2 v_2^2 + f_3 v_3^2) v_{12}^2 \} \\
& - \frac{2v_1 v_2}{v^2 v_{12} v_3} \{ (\lambda_5 v_1 v_2 \cos 2\delta + 2\lambda_6 v_1^2 \cos \delta + 2\lambda_7 v_2^2 \cos \delta) v_3^2 \\
& - (\lambda_8 + \lambda'_8) v_3^2 (v_{12}^2 - v_3^2) \cos \delta \} - \frac{d_{12} v_{12} v_1 v_2 v_3 (ssc - scs - 2css)}{v^2 \sin \delta \sin(\delta + \delta_s)} ; \tag{A.7}
\end{aligned}$$

$$\begin{aligned}
m_{H_1^0 H_4^0}^2 = & \frac{v_1 v_2 v_3^2}{v_{12} v^2 v_s} (-2\lambda_1 v_1^2 + 2\lambda_2 v_2^2 + (\lambda_3 + \lambda_4)(v_1^2 - v_2^2) + (\lambda'_3 - \lambda''_3 + \lambda'_4 - \lambda''_4)v_{12}^2 \\
& - \frac{v_1 v_2 v_s}{v_{12}} (f_1 - f_2) \\
& - \frac{1}{v^2 v_{12} v_s} \{ -\lambda_5 v_1 v_2 (v_1^2 - v_2^2) v_3^2 \cos 2\delta - \lambda_6 v_1^2 (v_1^2 - 3v_2^2) v_3^2 \cos \delta \\
& - \lambda_7 v_2^2 (3v_1^2 - v_2^2) v_3^2 \cos \delta + (\lambda_8 + \lambda'_8) v_3^2 (v_1^4 - v_2^4) \cos \delta - d_{12} v_s^2 v_{12}^2 v_3^2 \cos \delta \} ;
\end{aligned} \tag{A.8}$$

$$\begin{aligned}
m_{H_2^0 H_4^0}^2 = & \frac{2v_3}{v_{12} v^3 v_s} \{ \lambda_1 v_1^4 v_3^2 + \lambda_2 v_2^4 v_3^2 + \lambda_t v_{12}^4 v_3^2 - \lambda_s v_s^2 v_{12}^2 v^2 \\
& + v_1^2 v_2^2 v_3^2 (\lambda_3 + \lambda_4) - (\lambda'_3 + \lambda'_4) v_1^2 v_{12}^2 v_3^2 - (\lambda''_3 + \lambda''_4) v_2^2 v_3^2 v_{12}^2 \} \\
& + \frac{v_3 v_s}{v v_{12}} \{ f_1 v_1^2 + f_2 v_2^2 - f_3 v_{12}^2 \} \\
& - \frac{v_1 v_2}{v_3 v^3 v_{12} v_s \sin \delta_s \sin(\delta + \delta_s)} \{ \lambda_5 v_1 v_2 [v_{12}^2 v^2 (s'cs - s'sc) - 2v_3^4 c'ss] \\
& + \lambda_6 v_1^2 [v_{12}^2 v^2 (scs - ssc) - 4v_3^4 css] + \lambda_7 v_2^2 [v_{12}^2 v^2 (scs - ssc) - 4v_3^4 css] \\
& + (\lambda_8 + \lambda'_8) v_3^2 [v_{12}^2 v^2 (scs - ssc) + 4v_{12}^2 v_3^2 css] + d_{12} v_s^2 [v_{12}^2 v^2 (scs - ssc) - 2v^2 v_3^2 css] \} ;
\end{aligned} \tag{A.9}$$

$$\begin{aligned}
m_{H_3^0 H_4^0}^2 = & \frac{v_3^2}{v^3 v_s} \{ -2\lambda_1 v_1^4 - 2\lambda_2 v_2^4 + 2\lambda_t v_{12}^2 v_3^2 - 2v_1^2 v_2^2 (\lambda_3 + \lambda_4) \\
& (\lambda'_3 + \lambda'_4) v_1^2 (v_{12}^2 - v_3^2) + (\lambda''_3 + \lambda''_4) v_2^2 (v_{12}^2 - v_3^2) \} \\
& - \frac{v_s v^2}{v^3} \{ f_1 v_1^2 + f_2 v_2^2 + f_3 v_3^2 \} \\
& - \frac{v_1 v_2}{v^3 v_s \sin \delta \sin(\delta + \delta_s)} \{ \lambda_5 v_1 v_2 [(s'cs - s'sc) v_{12}^2 + 2v_3^2 c'ss] \\
& + \lambda_6 v_1^2 [(scs - ssc) v^2 + 4v_3^2 css] + \lambda_7 v_2^2 [(scs - ssc) v^2 + 4v_3^2 css] \\
& + (\lambda_8 + \lambda'_8) v_3^2 [(scs - ssc) v^2 - 2(v_{12}^2 - v_3^2) css] + d_{12} v_s^2 v^2 (scs - ssc + 2css) \} ;
\end{aligned} \tag{A.10}$$

$$m_{H_1^0 a_1}^2 = -\sin \delta \{ \lambda_5 (v_1^2 - v_2^2) \cos \delta - v_1 v_2 (\lambda_6 - \lambda_7) \}; \quad (\text{A.11})$$

$$m_{H_2^0 a_1}^2 = -\frac{\sin \delta}{2v_3 v} \{ 2\lambda_5 v_1 v_2 (v_1^2 + v_2^2 + 3v_3^2) \cos \delta + \lambda_6 v_1^2 (v_{12}^2 + 3v_3^2) \\ + \lambda_7 v_2^2 (v_{12}^2 + 3v_3^2) - (\lambda_8 + \lambda'_8) v_3^2 (v_{12}^2 - v_3^2) + d_{12} v_s^2 v^2 \}; \quad (\text{A.12})$$

$$m_{H_3^0 a_1}^2 = \frac{v_{12} \sin \delta}{v} \{ 2\lambda_5 v_1 v_2 \cos \delta + \lambda_6 v_1^2 + \lambda_7 v_2^2 + (\lambda_8 + \lambda'_8) v_3^2 \}; \quad (\text{A.13})$$

$$m_{H_4^0 a_1}^2 = -\frac{v_{12} \sin \delta}{v^2 v_s} \{ 2\lambda_5 v_1 v_2 v_3^2 \cos \delta + (\lambda_6 v_1^2 v_3^2 + \lambda_7 v_2^2 v_3^2 \\ - (\lambda_8 + \lambda'_8) v_{12}^4 + d_{12} v_s^2 v^2) \}; \quad (\text{A.14})$$

$$m_{H_1^0 a_2}^2 = \frac{v \sin \delta}{2v_3} \{ 2\lambda_5 v_1 v_2 \cos \delta + \lambda_6 v_1^2 + \lambda_7 v_2^2 - (\lambda_8 + \lambda'_8) v_3^2 + d_{12} v_s^2 \}; \quad (\text{A.15})$$

$$m_{H_2^0 a_2}^2 = m_{H_3^0 a_2}^2 = m_{H_4^0 a_2}^2 = 0, \quad (\text{A.16})$$

$$m_{a_1 a_1}^2 = -\frac{1}{2v_1 v_2 v_{12}^2 \sin \delta \sin(\delta + \delta_s)} \{ \lambda_5 v_1 v_2 (v_1^4 s' cs - v_2^4 s' sc + 2v_{12}^4 c' ss) \\ + (\lambda_6 v_1^2 + \lambda_7 v_2^2 + (\lambda_8 + \lambda'_8) v_3^2 + d_{12} v_s^2) (v_1^4 scs - v_2^4 ssc + v_{12}^4 css) \}; \quad (\text{A.17})$$

$$m_{a_2 a_2}^2 = -\frac{v_1 v_2 v^2}{2v_{12}^2 v_3^2 \sin \delta \sin(\delta + \delta_s)} \{ \lambda_5 v_1 v_2 (s' cs - s' sc) \\ + (\lambda_6 v_1^2 + \lambda_7 v_2^2 + (\lambda_8 + \lambda'_8) v_3^2 + d_{12} v_s^2) (scs - ssc) \}; \quad (\text{A.18})$$

$$m_{a_1 a_2}^2 = -\frac{v}{2v_{12}^2 v_3 \sin \delta \sin(\delta + \delta_s)} \{ \lambda_5 v_1 v_2 (v_1^2 s' cs + v_2^2 s' sc) \\ + (\lambda_6 v_1^2 + \lambda_7 v_2^2 + (\lambda_8 + \lambda'_8) v_3^2 + d_{12} v_s^2) (v_1^2 scs + v_2^2 ssc) \}. \quad (\text{A.19})$$

The charged mass matrix elements are given by

$$m_{H_1^+ H_1^-}^2 = -\frac{1}{2v_{12}^2} (\lambda_4 v_{12}^4 + \lambda'_4 v_2^2 v_3^2 + \lambda''_4 v_1^2 v_3^2) \\ -\frac{1}{2v_1 v_2 v_{12}^2 \sin \delta_s \sin(\delta + \delta_s)} \{ \lambda_5 v_1 v_2 [v_1^4 s' cs - v_2^4 s' sc + v_{12}^4 c' ss] \\ + (\lambda_6 v_1^2 + \lambda_7 v_2^2 + \lambda_8 v_3^2 + d_{12} v_s^2) [v_1^4 scs - v_2^4 ssc + v_{12}^4 css] \\ + \lambda'_8 v_3^2 [v_1^2 (css + scs) + v_2^2 (css - ssc)] \}; \quad (\text{A.20})$$

$$\begin{aligned}
m_{H_2^+ H_2^-}^2 &= -\frac{v^2}{2v_{12}^2}(\lambda_4' v_1^2 + \lambda_4'' v_2^2) \\
&\quad - \frac{v_1 v_2 v^2}{2v_3^2 v_{12}^2 \sin \delta_s \sin(\delta + \delta_s)} \{ \lambda_5 v_1 v_2 (s' cs - s' sc) \\
&\quad + (\lambda_6 v_1^2 + \lambda_7 v_2^2 + \lambda_8 v_3^2 + d_{12} v_s^2) (scs - ssc) \\
&\quad + \lambda_8' v_3^2 (scs - ssc + 2css) \} ; \tag{A.21}
\end{aligned}$$

$$\begin{aligned}
m_{H_1^+ H_2^-}^2 &= -\frac{v_1 v_2 v_3 v}{2v_{12}^2}(\lambda_4' - \lambda_4'') + \frac{v}{2v_3 v_{12}^2 \sin \delta_s \sin(\delta + \delta_s)} \\
&\quad \{ \lambda_5 v_1 v_2 (v_1^2 s' cs + v_2^2 s' sc + i v_{12}^2 s' ss) \\
&\quad + (\lambda_6 v_1^2 + \lambda_7 v_2^2 + \lambda_8 v_3^2 + d_{12} v_s^2) (v_1^2 scs + v_2^2 ssc + i v_{12}^2 sss) \\
&\quad + \lambda_8' v_3^2 [v_1^2 (css + scs) + v_2^2 (ssc - css)] \} . \tag{A.22}
\end{aligned}$$



Appendix B

Light Neutrino Mass in Seesaw Mechanism

The formalism related to seesaw mechanism with more than one generation heavy neutrinos have been solved very early [78]. We use the notation in Ref. [85] to obtain some relations in type-I seesaw. At the beginning the relation between transformation matrix U and M_{seesaw} is given by

$$\begin{pmatrix} U_{\nu\nu} & U_{\nu N} \\ U_{N\nu} & U_{NN} \end{pmatrix} \begin{pmatrix} \hat{M}_\nu & 0 \\ 0 & \hat{M}_N \end{pmatrix} \begin{pmatrix} U_{\nu\nu}^T & U_{N\nu}^T \\ U_{\nu N}^T & U_{NN}^T \end{pmatrix} = \begin{pmatrix} 0 & M_D \\ M_D^T & \hat{M}_R \end{pmatrix}. \quad (\text{B.1})$$

The above relation leads to the following formulae

$$U_{\nu\nu}\hat{M}_\nu U_{\nu\nu}^T + U_{\nu N}\hat{M}_N U_{\nu N}^T = 0; \quad (\text{B.2})$$

$$U_{\nu\nu}\hat{M}_\nu U_{N\nu}^T + U_{\nu N}\hat{M}_N U_{NN}^T = M_D; \quad (\text{B.3})$$

$$U_{N\nu}\hat{M}_\nu U_{N\nu}^T + U_{NN}\hat{M}_N U_{NN}^T = \hat{M}_R. \quad (\text{B.4})$$

Eq. (B.2) is the usual relation to determine the scale of $U_{\nu N}$ in type-I seesaw. The unitarity property of U provides that $U_{\nu N}$ and $U_{N\nu}$ should be of the same order of magnitude. Eq. (B.4) with the condition that the magnitude of \hat{M}_N is larger than that of \hat{M}_ν gives $U_{NN} \simeq 1$, which leads to

$$U_{\nu N} \simeq M_D \hat{M}_N^{-1} \quad (\text{B.5})$$

from Eq. (B.3). Finally, the unitary condition $U_{N\nu} = -(U_{NN}^\dagger)^{-1}U_{\nu N}^\dagger U_{\nu\nu}$ leads to

$$U_{N\nu} \simeq -\hat{M}_N^{-1} M_D^\dagger U_{\nu\nu}. \quad (\text{B.6})$$

Combining Eq. (B.2) and Eq. (B.5) provides a useful relation

$$U_{\nu\nu} \hat{M}_\nu U_{\nu\nu}^T \simeq -M_D M_N^{-1} M_D^T. \quad (\text{B.7})$$



Appendix C

Large Mixing Matrix

There are a lot of ways to choose the form of such U_0 , and only several cases taken in this thesis are shown below [85]

$$\begin{aligned} U_0^a &= \begin{pmatrix} a & a & i\sqrt{2}a \\ b & b & i\sqrt{2}b \\ c & c & i\sqrt{2}c \end{pmatrix} \mathcal{R}, \quad U_0^d = \begin{pmatrix} 0 & a & ia \\ 0 & b & ib \\ 0 & c & ic \end{pmatrix} \mathcal{R}, \\ U_0^e &= \begin{pmatrix} 0 & 0 & 0 \\ 0 & a & ia \\ 0 & b & ib \end{pmatrix} \mathcal{R}, \quad U_0^f = \begin{pmatrix} 0 & a & ia \\ 0 & 0 & 0 \\ 0 & b & ib \end{pmatrix} \mathcal{R}. \end{aligned} \quad (\text{C.1})$$

Note that for different U_0 the appropriate choices of a and b are also different. The parameters we take from Ref. [85] are given by

$$\begin{aligned} U_0^a &: \quad a = (0.58 - 0.81i)\bar{b}, \quad b = (0.58 + 0.41i)\bar{b}, \quad c = (0.58 + 0.41i)\bar{b}; \\ U_0^d &: \quad a = -0.82\bar{a}, \quad b = (0.41 + 0.66i)\bar{a}, \quad c = (0.41 - 0.66i)\bar{a}; \\ U_0^e &: \quad b = a; \\ U_0^f &: \quad b = (0.013 + 1.03i)a. \end{aligned} \quad (\text{C.2})$$



Appendix D

Overlapped functions in Nucleon

The appendix follows the discussion in Ref. [111]. The electron and bounded muon in a nucleus can be described by wave functions satisfying time independent Dirac equation with a Coulomb potential $V(r)$

$$[-i\alpha \cdot \nabla + m\beta + V(r)]\psi(\mathbf{r}) = E\psi(\mathbf{r}) . \quad (\text{D.1})$$

The general solution of Dirac equation for muon and electron is expressed in the form

$$\psi_{\mu}^{1s} = \begin{pmatrix} g_{\mu}^{-}(r)\chi_{-}(\theta, \phi) \\ if_{\mu}^{-}(r)\chi_{+}(\theta, \phi) \end{pmatrix}, \quad \psi_e^{-} = \begin{pmatrix} g_e^{-}(r)\chi_{-}(\theta, \phi) \\ if_e^{-}(r)\chi_{+}(\theta, \phi) \end{pmatrix}, \quad (\text{D.2})$$

where the symbols $+$ and $-$ correspond to the eigenvalues of K operator in Dirac space. The $1s$ muon bound state is given by [119]

$$\begin{aligned} g_{\mu}^{-}(r) &= \frac{(2mZ\alpha)^{3/2}}{\sqrt{4\pi}} \sqrt{\frac{1+\gamma}{2\Gamma(1+2\gamma)}} (2mZ\alpha r)^{\gamma-1} e^{-mZ\alpha r}, \\ f_{\mu}^{-}(r) &= \frac{(2mZ\alpha)^{3/2}}{\sqrt{4\pi}} \frac{1-\gamma}{Z\alpha} \sqrt{\frac{1+\gamma}{2\Gamma(1+2\gamma)}} (2mZ\alpha r)^{\gamma-1} e^{-mZ\alpha r}, \end{aligned} \quad (\text{D.3})$$

where $\gamma = \sqrt{1 - Z^2\alpha^2}$. The electron wave function with $\kappa = -1$ is given by [121]

$$\begin{aligned} g_e^{-}(r) &= (Er)^{\gamma-1} \frac{2^{\gamma} e^{\pi\alpha Z/2} |\Gamma(\gamma + i\alpha Z)|}{\Gamma(1+2\gamma)} \\ &\quad \text{Re}[(\gamma + i\alpha Z) e^{i\phi} e^{-iEr} F(1 + \gamma + i\alpha Z, 1 + 2\gamma; 2iEr)], \\ f_e^{-}(r) &= -(Er)^{\gamma-1} \frac{2^{\gamma} e^{\pi\alpha Z/2} |\Gamma(\gamma + i\alpha Z)|}{\Gamma(1+2\gamma)} \\ &\quad \text{Im}[(\gamma + i\alpha Z) e^{i\phi} e^{-iEr} F(1 + \gamma + i\alpha Z, 1 + 2\gamma; 2iEr)], \end{aligned} \quad (\text{D.4})$$

where the approximation $m_e \approx 0$ is taken, and $\exp(2i\phi) = -E/(\gamma + i\alpha Z)$, F is the hypergeometric function. To calculate the $\mu - e$ conversion rate, some of the overlapping functions D , $V^{(p)}$, and $V^{(n)}$ are defined as follows

$$\begin{aligned} D &= \frac{4}{\sqrt{2}} m_\mu \int_0^\infty dr r^2 [-E(r)] (g_e^- f_\mu^- + g_\mu^- f_e^-) ; \\ V^{(p)} &= \frac{1}{2\sqrt{2}} \int_0^\infty dr r^2 Z \rho^{(p)} (g_e^- f_\mu^- + g_\mu^- f_e^-) ; \\ V^{(n)} &= \frac{1}{2\sqrt{2}} \int_0^\infty dr r^2 (A - Z) \rho^{(n)} (g_e^- f_\mu^- + g_\mu^- f_e^-) . \end{aligned} \quad (\text{D.5})$$

where $\rho^{(p)}$, $\rho^{(n)}$ are the density distribution for proton and neutron, respectively. $E(r)$ is the electric field with the distance r from the nucleus, which also depends on the proton distribution function. Experiments have determined the $\rho^{(p)}$ for many of the atomic nuclei [120]. We only list two types of the functions to fit the ρ_p [120]

$$\text{Fourier-Bessel expansion: } \rho^{(p)}(r) = \begin{cases} \sum_v a_v j_0(v\pi r/R), & r \leq R, \\ 0, & r > R; \end{cases} \quad (\text{D.6})$$

$$\text{Two parameter Fermi model: } \rho^{(p)}(r) = \frac{\rho_0}{1 + \exp[(r - c_p)/z_p]}, \quad (\text{D.7})$$

where a_v is the coefficient, j_0 is the zeroth order Bessel function, and R is some radius. c_p and z_p are two parameters in the Fermi model, and ρ_0 is used to normalize the density distribution. For neutron distribution function, one of the method in Ref. [111] is to take it simply as the same function as that of proton.

References

- [1] S. L. Chen, N. G. Deshpande, X. G. He, J. Jiang and L. H. Tsai, Eur. Phys. J. C **53**, 607 (2008) [arXiv:0705.0399 [hep-ph]].
- [2] X. -G. He and L. -H. Tsai, Eur. Phys. J. C **71**, 1598 (2011) [arXiv:1010.5204 [hep-ph]].
- [3] L. H. Tsai, *Spontaneous CP violating phase and CKM matrix phase*, Master Thesis (2008), Department of Physics, College of Science, National Taiwan University.
- [4] J. -H. Chen, X. -G. He, J. Tandean and L. -H. Tsai, Phys. Rev. D **81**, 113004 (2010) [arXiv:1001.5215 [hep-ph]].
- [5] N. G. Deshpande, T. Enkhbat, T. Fukuyama, X. -G. He, L. -H. Tsai, K. Tsumura, T. Enkhbat and T. Fukuyama *et al.*, Phys. Lett. B **703**, 562 (2011) [arXiv:1106.5085 [hep-ph]].
- [6] J. Beringer *et al.* [Particle Data Group Collaboration], Phys. Rev. D **86**, 010001 (2012).
- [7] K. Nakamura *et al.* [Particle Data Group Collaboration], J. Phys. G **37**, 075021 (2010).
- [8] C. Amsler *et al.* [Particle Data Group Collaboration], Phys. Lett. B **667**, 1 (2008).
- [9] W. M. Yao *et al.* [Particle Data Group Collaboration], J. Phys. G **33**, 1 (2006).

- [10] S. L. Glashow, Nucl. Phys. **22** (1961) 579; S. Weinberg, Phys. Rev. Lett. **19**, 1264 (1967); A. Salam, in: *proc. 8th Nobel Symposium*, ed. by N. Svartholm(Almquist and Wiskell, Stockholm, 1968).
- [11] Y. Nambu and G. Jona-Lasinio, Phys. Rev. **122**, 345 (1961).
- [12] P. W. Higgs, Phys. Lett. **12**, 132 (1964).
- [13] N. Cabibbo, Phys. Rev. Lett. **10**, 531 (1963).
- [14] M. Kobayashi and T. Maskawa, Prog. Theor. Phys. **49**, 652 (1973).
- [15] D. Hanneke, S. Fogwell and G. Gabrielse, Phys. Rev. Lett. **100**, 120801 (2008) [arXiv:0801.1134 [physics.atom-ph]].
- [16] V. M. Abazov *et al.* [D0 Collaboration], arXiv:1203.0293 [hep-ex].
- [17] L. Reina, hep-ph/0512377.
- [18] [ALEPH and DELPHI and L3 and OPAL and SLD and LEP Electroweak Working Group and SLD Electroweak Group and SLD Heavy Flavour Group Collaborations], Phys. Rept. **427**, 257 (2006) [hep-ex/0509008].
- [19] G. Aad *et al.* [ATLAS Collaboration], arXiv:1112.2577 [hep-ex].
- [20] ATLAS and CMS collaboration, in: 36th International Conference on High Energy Physics, Melbourne, Australia, during 4-11 July, 2012.
- [21] L. -L. Chau and W. -Y. Keung, Phys. Rev. Lett. **53**, 1802 (1984).
- [22] L. Wolfenstein, Phys. Rev. Lett. **51**, 1945 (1983).
- [23] J. H. Christenson, J. W. Cronin, V. L. Fitch and R. Turlay, Phys. Rev. Lett. **13**, 138 (1964).
- [24] E. A. Andriyash, G. G. Ovanesyan and M. I. Vysotsky, Phys. Lett. B **599**, 253 (2004) [arXiv:hep-ph/0310314].

- [25] H. Burkhardt *et al.* [NA31 Collaboration], Phys. Lett. B **206**, 169 (1988).
- [26] The Heavy Flavor Averaging Group (HFAG), E. Barberio *et al.*, arXiv:0808.1297, and Summer 2009 updates at <http://www.slac.stanford.edu/xorg/hfag/>.
- [27] A. Hocker, H. Lacker, S. Laplace and F. Le Diberder, Eur. Phys. J. C **21**, 225 (2001) [hep-ph/0104062]; “Beauty 2009” results in Ref. [28]
- [28] CKMfitter Group (J. Charles *et al.*), Eur. Phys. J. C **41**, 1-131 (2005) [hep-ph/0406184], updated results and plots available at: <http://ckmfitter.in2p3.fr/>.
- [29] B. Pontecorvo, Sov. Phys. JETP **6**, 429 (1957) [Zh. Eksp. Teor. Fiz. **33**, 549 (1957)].
- [30] Z. Maki, M. Nakagawa and S. Sakata, Prog. Theor. Phys. **28**, 870 (1962).
- [31] B. Aharmim *et al.* [SNO Collaboration], Phys. Rev. Lett. **101**, 111301 (2008) [arXiv:0806.0989 [nucl-ex]].
- [32] P. Adamson *et al.* [MINOS Collaboration], Phys. Rev. Lett. **101**, 131802 (2008) [arXiv:0806.2237 [hep-ex]].
- [33] B. Aharmim *et al.* [SNO Collaboration], Phys. Rev. C **81**, 055504 (2010) [arXiv:0910.2984 [nucl-ex]].
- [34] Y. Ashie *et al.* [Super-Kamiokande Collaboration], Phys. Rev. D **71**, 112005 (2005) [hep-ex/0501064].
- [35] K. Abe *et al.* [T2K Collaboration], Phys. Rev. Lett. **107**, 041801 (2011) [arXiv:1106.2822 [hep-ex]].
- [36] F. P. An *et al.* [DAYA-BAY Collaboration], arXiv:1203.1669 [hep-ex].
- [37] <http://hitoshi.berkeley.edu/neutrino>.

- [38] A. G. Cohen, D. B. Kaplan and A. E. Nelson, Ann. Rev. Nucl. Part. Sci. **43**, 27 (1993) [arXiv:hep-ph/9302210].
- [39] S. M. Barr, G. Segre and H. A. Weldon, Phys. Rev. D **20**, 2494 (1979).
- [40] T. D. Lee, Phys. Rev. D **8**, 1226 (1973); T. D. Lee, Phys. Rept. **9**, 143 (1974)
- [41] S. Weinberg, Phys. Rev. Lett. **37**, 657 (1976).
- [42] G. C. Branco, Phys. Rev. Lett. **44**, 504 (1980).
- [43] N. G. Deshpande and E. Ma, Phys. Rev. D **16**, 1583 (1977).
- [44] P. Krawczyk and S. Pokorski, Nucl. Phys. B **364**, 10 (1991). Y. Grossman and Y. Nir, Phys. Lett. B **313**, 126 (1993) [arXiv:hep-ph/9306292].
- [45] D. Chang, X. G. He and B. H. J. McKellar, Phys. Rev. D **63**, 096005 (2001) [arXiv:hep-ph/9909357].
- [46] G. Beall and N. G. Deshpande, Phys. Lett. B **132**, 427 (1983).
- [47] C. A. Baker *et al.*, Phys. Rev. Lett. **97**, 131801 (2006) [arXiv:hep-ex/0602020].
- [48] R. Akhoury and I. I. Y. Bigi, Nucl. Phys. B **234**, 459 (1984).
- [49] I. I. Y. Bigi and A. I. Sanda, Phys. Rev. Lett. **58**, 1604 (1987).
- [50] N. G. Deshpande, G. Eilam and W. L. Spence, Phys. Lett. B **108**, 42 (1982).
- [51] X. G. He, B. H. J. McKellar and S. Pakvasa, Int. J. Mod. Phys. A **4**, 5011 (1989) [Erratum-ibid. A **6**, 1063 (1991)].
- [52] B. H. J. McKellar, S. R. Choudhury, X. G. He and S. Pakvasa, Phys. Lett. B **197**, 556 (1987).
- [53] E. P. Shabalin, Sov. J. Nucl. Phys. **36**, 575 (1982) [Yad. Fiz. **36**, 981 (1982)].
- [54] S. L. Adler, Phys. Rev. **177**, 2426 (1969); J. S. Bell and R. Jackiw, Nuovo Cim. A **60**, 47 (1969).

- [55] R. D. Peccei and H. R. Quinn, Phys. Rev. Lett. **38**, 1440 (1977); R. D. Peccei and H. R. Quinn, Phys. Rev. D **16**, 1791 (1977).
- [56] X. G. He and R. R. Volkas, Phys. Lett. B **208**, 261 (1988) [Erratum-ibid. B **218**, 508 (1989)]. C. Q. Geng, X. D. Jiang and J. N. Ng, Phys. Rev. D **38**, 1628 (1988).
- [57] A. R. Zhitnitsky, Sov. J. Nucl. Phys. **31**, 260 (1980) [Yad. Fiz. **31**, 497 (1980)]; M. Dine, W. Fischler and M. Srednicki, Phys. Lett. B **104**, 199 (1981); J. E. Kim, Phys. Rev. Lett. **43**, 103 (1979); M. A. Shifman, A. I. Vainshtein and V. I. Zakharov, Nucl. Phys. B **166**, 493 (1980).
- [58] H. Fusaoka and Y. Koide, Phys. Rev. D **57**, 3986 (1998) [hep-ph/9712201].
- [59] M. Okamoto, PoS LAT **2005**, 013 (2006) [hep-lat/0510113].
- [60] B. Aubert *et al.* [BABAR Collaboration], Phys. Rev. Lett. **98**, 211802 (2007) [arXiv:hep-ex/0703020]; K. Abe *et al.* [BELLE Collaboration], Phys. Rev. Lett. **99**, 131803 (2007) [arXiv:0704.1000 [hep-ex]]; M. Staric *et al.* [Belle Collaboration], Phys. Rev. Lett. **98**, 211803 (2007) [arXiv:hep-ex/0703036].
- [61] M. Ciuchini, E. Franco, D. Guadagnoli, V. Lubicz, M. Pierini, V. Porretti and L. Silvestrini, Phys. Lett. B **655**, 162 (2007) [arXiv:hep-ph/0703204]; X. -G. He and G. Valencia, Phys. Lett. B **651**, 135 (2007) [hep-ph/0703270]; C. -H. Chen, C. -Q. Geng and T. -C. Yuan, Phys. Lett. B **655**, 50 (2007) [arXiv:0704.0601 [hep-ph]]; Z. -z. Xing and S. Zhou, Phys. Rev. D **75**, 114006 (2007) [arXiv:0704.0971 [hep-ph]]; P. Ball, J. Phys. G **34**, 2199 (2007) [arXiv:0704.0786 [hep-ph]]; K. S. Babu, X. G. He, X. Li and S. Pakvasa, Phys. Lett. B **205**, 540 (1988).
- [62] A. Abulencia *et al.* [CDF Collaboration], Phys. Rev. Lett. **97**, 242003 (2006) [hep-ex/0609040].
- [63] A. Lenz and U. Nierste, JHEP **0706**, 072 (2007) [hep-ph/0612167]; X. -G. He and G. Valencia, Phys. Rev. D **74**, 013011 (2006) [hep-ph/0605202]; K. Cheung,

- C. -W. Chiang, N. G. Deshpande and J. Jiang, Phys. Lett. B **652**, 285 (2007) [hep-ph/0604223].
- [64] S. M. Barr and A. Zee, Phys. Rev. Lett. **65**, 21 (1990) [Erratum-ibid. **65**, 2920 (1990)]; J. F. Gunion and D. Wyler, Phys. Lett. B **248**, 170 (1990).
- [65] S. Weinberg, Phys. Rev. Lett. **63**, 2333 (1989); S. Weinberg, Phys. Rev. D **42**, 860 (1990).
- [66] D. Chang, W. -Y. Keung and T. C. Yuan, Phys. Lett. B **251**, 608 (1990).
D. Chang, X. -G. He, W. -Y. Keung, B. H. J. McKellar and D. Wyler, Phys. Rev. D **46**, 3876 (1992) [hep-ph/9209284].
- [67] E. Braaten, C. -S. Li and T. -C. Yuan, Phys. Rev. Lett. **64**, 1709 (1990).
E. Braaten, C. S. Li and T. C. Yuan, Phys. Rev. D **42**, 276 (1990).
- [68] S. Weinberg, Phys. Rev. Lett. **40**, 223 (1978); F. Wilczek, Phys. Rev. Lett. **49**, 1549 (1982).
- [69] J. Schweppe, A. Gruppe, K. Bethge, H. Bokemeyer, T. Cowan, H. Folger, J. S. Greenberg and H. Grein *et al.*, Phys. Rev. Lett. **51**, 2261 (1983); T. Cowan, H. Backe, M. Begemann, K. Bethge, H. Bokemeyer, H. Folger, J. S. Greenberg and H. Grin *et al.*, Phys. Rev. Lett. **54**, 1761 (1985).
- [70] J. A. Casas and A. Ibarra, Nucl. Phys. B **618**, 171 (2001) [hep-ph/0103065].
- [71] M. C. Gonzalez-Garcia, M. Maltoni and J. Salvado, JHEP **1004**, 056 (2010) [arXiv:1001.4524 [hep-ph]].
- [72] F. De Bernardis, P. Serra, A. Cooray and A. Melchiorri, Phys. Rev. D **78**, 083535 (2008) [arXiv:0809.1095 [astro-ph]]; A. Melchiorri, F. de Bernardis, E. Menegoni, AIP Conf. Proc. **1256**, 96-106 (2010).
- [73] Y. Miyazaki *et al.* [Belle Collaboration], Phys. Lett. B **660**, 154 (2008) [arXiv:0711.2189 [hep-ex]].

- [74] B. Aubert *et al.* [BABAR Collaboration], Phys. Rev. Lett. **99**, 251803 (2007) [arXiv:0708.3650 [hep-ex]].
- [75] U. Bellgardt *et al.* [SINDRUM Collaboration], Nucl. Phys. B **299**, 1 (1988).
- [76] A. Djouadi, Phys. Rept. **457**, 1 (2008) [hep-ph/0503172].
- [77] P. Minkowski, Phys. Lett. B **67**, 421 (1977); T. Yanagida, in *Proceedings of the Workshop on the Unified Theory and the Baryon Number in the Universe*, edited by O. Sawada and A. Sugamoto (KEK, Tsukuba, 1979), p. 95; M. Gell-Mann, P. Ramond, and R. Slansky, in *Supergravity*, edited by P. van Nieuwenhuizen and D. Freedman (North-Holland, Amsterdam, 1979), p. 315; S.L. Glashow, in *Proceedings of the 1979 Cargese Summer Institute on Quarks and Leptons*, edited by M. Levy *et al.* (Plenum Press, New York, 1980), p. 687; R. N. Mohapatra and G. Senjanovic, Phys. Rev. Lett. **44**, 912 (1980).
- [78] J. Schechter and J. W. F. Valle, Phys. Rev. D **25**, 774 (1982); A. S. Joshipura and S. D. Rindani, Phys. Rev. D **46**, 3000 (1992) [hep-ph/9205220].
- [79] G. Belanger, F. Boudjema, D. London and H. Nadeau, Phys. Rev. D **53**, 6292 (1996) [hep-ph/9508317].
- [80] O. Adriani *et al.* [L3 Collaboration], Phys. Lett. B **295**, 371 (1992); P. Abreu *et al.* [DELPHI Collaboration], Z. Phys. C **74**, 57 (1997) [Erratum-ibid. C **75**, 580 (1997)].
- [81] A. Djouadi, J. Kalinowski and M. Spira, Comput. Phys. Commun. **108**, 56 (1998) [hep-ph/9704448].
- [82] W. Buchmuller and D. Wyler, Phys. Lett. B **249**, 458 (1990); W. Buchmuller and C. Greub, Nucl. Phys. B **363**, 345 (1991); J. Gluza, Acta Phys. Polon. B **33**, 1735 (2002) [arXiv:hep-ph/0201002]; G. Ingelman and J. Rathsmann, Z. Phys. C **60**, 243 (1993); A. Pilaftsis, Phys. Rev. Lett. **95**, 081602 (2005) [arXiv:hep-ph/0408103]; A. Pilaftsis and T.E.J. Underwood, Phys. Rev. D **72**,

- 113001 (2005) [arXiv:hep-ph/0506107]; A. de Gouvea, arXiv:0706.1732 [hep-ph]; A. Aranda, O. Blanno and J. Lorenzo Diaz-Cruz, Phys. Lett. B **660**, 62 (2008) [arXiv:0707.3662 [hep-ph]]; S.C. Park, K. Wang, and T.T. Yanagida, arXiv:0909.2937 [hep-ph].
- [83] A. Pilaftsis, Z. Phys. C **55**, 275 (1992) [hep-ph/9901206].
- [84] J. Kersten and A.Y. Smirnov, Phys. Rev. D **76**, 073005 (2007) [arXiv:0705.3221 [hep-ph]]; E. Ma, arXiv:0904.1580 [hep-ph]; Z.Z. Xing, Prog. Theor. Phys. Suppl. **180**, 112 (2010) [arXiv:0905.3903 [hep-ph]]; X.G. He and E. Ma, Phys. Lett. B **683**, 178 (2010) [arXiv:0907.2737 [hep-ph]].
- [85] X. -G. He, S. Oh, J. Tandean and C. -C. Wen, Phys. Rev. D **80**, 073012 (2009) [arXiv:0907.1607 [hep-ph]].
- [86] R. Foot, H. Lew, X.G. He, and G.C. Joshi, Z. Phys. C **44**, 441 (1989).
- [87] F. del Aguila, J. de Blas and M. Perez-Victoria, Phys. Rev. D **78**, 013010 (2008) [arXiv:0803.4008 [hep-ph]]; F. del Aguila, J. A. Aguilar-Saavedra, J. de Blas and M. Perez-Victoria, arXiv:0806.1023 [hep-ph].
- [88] F. del Aguila and J. A. Aguilar-Saavedra, Nucl. Phys. B **813**, 22 (2009) [arXiv:0808.2468 [hep-ph]].
- [89] S. Antusch, C. Biggio, E. Fernandez-Martinez, M. B. Gavela and J. Lopez-Pavon, JHEP **0610**, 084 (2006) [hep-ph/0607020].
- [90] J. Erler, P. Langacker, S. Munir and E. Rojas, JHEP **0908**, 017 (2009) [arXiv:0906.2435 [hep-ph]].
- [91] A. D. Martin, W. J. Stirling, R. S. Thorne and G. Watt, Eur. Phys. J. C **63**, 189 (2009) [arXiv:0901.0002 [hep-ph]].
- [92] G. Abbiendi *et al.* [OPAL Collaboration], Eur. Phys. J. C **52**, 767 (2007) [arXiv:0708.1311 [hep-ex]].

- [93] A. Abada, C. Biggio, F. Bonnet, M. B. Gavela and T. Hambye, Phys. Rev. D **78**, 033007 (2008) [arXiv:0803.0481 [hep-ph]]; X. -G. He and S. Oh, JHEP **0909**, 027 (2009) [arXiv:0902.4082 [hep-ph]]; J. F. Kamenik and M. Nemevsek, JHEP **0911**, 023 (2009) [arXiv:0908.3451 [hep-ph]].
- [94] B. Holdom, W. S. Hou, T. Hurth, M. L. Mangano, S. Sultansoy and G. Unel, PMC Phys. A **3**, 4 (2009) [arXiv:0904.4698 [hep-ph]].
- [95] G. D. Kribs, T. Plehn, M. Spannowsky and T. M. P. Tait, Phys. Rev. D **76**, 075016 (2007) [arXiv:0706.3718 [hep-ph]]; O. Eberhardt, A. Lenz, J. Rohrwild, Phys. Rev. **D82** (2010) 095006. [arXiv:1005.3505 [hep-ph]]; H. -J. He, N. Polonsky and S. -f. Su, Phys. Rev. D **64**, 053004 (2001) [hep-ph/0102144].
- [96] M. S. Chanowitz, M. A. Furman and I. Hinchliffe, Phys. Lett. B **78**, 285 (1978); Nucl. Phys. B **153**, 402 (1979).
- [97] S. Chatrchyan *et al.* [CMS Collaboration], arXiv:1203.5410 [hep-ex].
- [98] S. Chatrchyan *et al.* [CMS Collaboration], JHEP **1205**, 123 (2012) [arXiv:1204.1088 [hep-ex]].
- [99] P. Achard *et al.* [L3 Collaboration], Phys. Lett. B **517**, 75 (2001) [hep-ex/0107015].
- [100] X. G. He and S. Pakvasa, Phys. Lett. **B156**, 236 (1985); K. Kang, M. Shin, Phys. Lett. **B165**, 383 (1985); M. Gronau, J. Schechter, Phys. Rev. **D31**, 1668-1675 (1985); A. A. Anselm, T. A. Zhukovskaya, N. G. Uraltsev and J. L. Chkareuli, JETP Lett. **41**, 269 (1985) [Pisma Zh. Eksp. Teor. Fiz. **41**, 221 (1985)]; X. G. He and S. Pakvasa, Nucl. Phys. B **278**, 905 (1986); T. Hayashi, M. Tanimoto, S. Wakaizumi, Prog. Theor. Phys. **75**, 353 (1986); U. Turke, Phys. Lett. **B168**, 296 (1986); E. A. Paschos, *PROCEEDINGS. Edited by K.R. Schubert and R. Waldi. Hamburg, Germany, DESY, 1987. 493p*; D. -d. Wu, Y. -L. Wu, Chin. Phys. Lett. **4**, 441 (1987); W. S. Hou, A. Soni and H. Steger, Phys. Lett. B **192**, 441 (1987); W. S. Hou and A. Soni, Phys. Lett. B **196**, 92 (1987);

- J. Maalampi, M. Roos, Phys. Lett. **B188**, 487 (1987); K. S. Babu, X. G. He, X. Li and S. Pakvasa, Phys. Lett. B **205**, 540 (1988).
- [101] W. S. Hou, H. n. Li, S. Mishima and M. Nagashima, Phys. Rev. Lett. **98**, 131801 (2007); A. Soni, A. K. Alok, A. Giri, R. Mohanta and S. Nandi, Phys. Lett. B **683**, 302 (2010); A. J. Buras, B. Duling, T. Feldmann, T. Heidsieck, C. Promberger and S. Recksiegel, JHEP **1009**, 106 (2010).
- [102] L. N. Chang, D. Ng and J. N. Ng, Phys. Rev. D **50**, 4589 (1994).
- [103] H. Lacker and A. Menzel, JHEP **1007**, 006 (2010).
- [104] A. J. Buras, B. Duling, T. Feldmann, T. Heidsieck and C. Promberger, JHEP **1009**, 104 (2010).
- [105] A. Lenz, H. Pas, D. Schalla, “Fourth Generation Majorana Neutrinos,” [arXiv:1104.2465 [hep-ph]]. (your ref. 16-18)
- [106] W. H. Bertl *et al.* [SINDRUM II Collaboration], Eur. Phys. J. C **47**, 337 (2006).
- [107] A. Badertscher, K. Borer, G. Czapek, A. Fluckiger, H. Hanni, B. Hahn, E. Hugentobler and H. Kaspar *et al.*, Lett. Nuovo Cim. **28**, 401 (1980); A. Badertscher, K. Borer, G. Czapek, A. Fluckiger, H. Hanni, B. Hahn, E. Hugentobler and A. Markees *et al.*, Nucl. Phys. A **377**, 406 (1982).
- [108] C. Dohmen *et al.* [SINDRUM II. Collaboration], Phys. Lett. B **317**, 631 (1993).
- [109] W. Honecker *et al.* [SINDRUM II Collaboration], Phys. Rev. Lett. **76**, 200 (1996).
- [110] S. Weinberg and G. Feinberg, Phys. Rev. Lett. **3**, 111 (1959); O. U. Shanker, Phys. Rev. D **20**, 1608 (1979); V. Cirigliano, R. Kitano, Y. Okada and P. Tuzon, Phys. Rev. D **80**, 013002 (2009).

- [111] R. Kitano, M. Koike and Y. Okada, Phys. Rev. D **66**, 096002 (2002) [Erratum-
ibid. D **76**, 059902 (2007)] [hep-ph/0203110].
- [112] J. Adam *et al.* [MEG Collaboration], Phys. Rev. Lett. **107**, 171801 (2011)
[arXiv:1107.5547 [hep-ex]].
- [113] M. L. Brooks *et al.* [MEGA Collaboration], Phys. Rev. Lett. **83**, 1521 (1999)
[hep-ex/9905013].
- [114] Research Proposal to INFN, “The MEG experiment: search for the $\mu^+ \rightarrow e^+ \gamma$
decay at PST”, September 2002.
- [115] MUon Science Innovative Commission. Talk given by Y. Kuno in Interna-
tional workshop on FFAG Accelerator, [http://hadron.kek.jp/FFAG/FFAG10_](http://hadron.kek.jp/FFAG/FFAG10_HP/slides/Wed/Wed04Kuno.pdf)
[HP/slides/Wed/Wed04Kuno.pdf](http://hadron.kek.jp/FFAG/FFAG10_HP/slides/Wed/Wed04Kuno.pdf).
- [116] J. P. Miller [Mu2E collaboration], *Proposal to Search for $\mu^- N \rightarrow e^- N$ with a
Single Event Sensitivity Below 10^{-16}* .
- [117] Y. Kuno et.al. [COMET collaboration], *An Experimental Search for lepton
Flavor Violating $\mu - e$ Conversion at Sensitivity of 10^{-16} with a Slow-Extracted
Bunched Beam*.
- [118] Y. Kuno et.al. [PRISM/PRIME Group], Letter of Intent, *An Experimental
Search for a $\mu - e$ Conversion at Sensitivity of the Order of 10^{-18} with a Highly
Intense Muon Source: PRISM*.
- [119] James D. Bjorken and Sidney D. Drell, *Relativistic Quantum Mechanics*,
McGraw-Hill, New York, 1964.
- [120] H. De Vries, C. W. De Jager and C. De Vries, Atom. Data Nucl. Data Tabl. **36**,
495 (1987); G. Fricke, C. Bernhardt, K. Heilig, L. A. Schaller, L. Schellenberg,
E. B. Shera and C. W. de Jager, Atom. Data Nucl. Data Tabl. **60**, 177 (1995).
- [121] A. Aste, C. von Arx and D. Trautmann, Eur. Phys. J. A **26**, 167 (2005)
[nucl-th/0502074].